Cellular localization and function of peptidyl-prolyl *cis-trans* isomerase *h*Par14

Dissertation

zur Erlangung des akademischen Grades
Doktor rerum naturalium (Dr. rer. nat.)

vorgelegt der
Mathematisch-Naturwissenschaftlich-Technischen Fakultät
(mathematisch-naturwissenschaftlicher Bereich)
der Martin-Luther-Universität Halle-Wittenberg

von Frau Dipl.-Biol. Tatiana Reimer
geb. am 2 Juni 1974 in Leszno (Polen)

Verteidigt am 15.05.2003 in Halle/Saale.

Gutachter:

1. Prof. Dr. G. Fischer
2. Prof. Dr. R. Wetzker
3. PD Dr. P. Bayer

urn:nbn:de:gbv:3-000005179
[http://nbn-resolving.de/urn/resolver.pl?urn=nbn%3Ade%3Agbv%3A3-000005179]

Abbreviation

CHUD	Chromatin-unfolding domain
CIP	Calf intestine phosphatase
CK2	Casein kinase 2
CsA	Cyclosporine A
Da	Dalton
DMEM	Dulbecco's Modified Eagle's Medium
DRB	5,6-dichloro-1-b-D-ribofuranosylbenzimidazole
EMSA	Electromobility shift assay
FKBP	FK506 binding protein
FKHRL1	Forkhead transcription factor like 1
GFP	Green fluorescent protein
GST	Glutathione S-transferase
HMG protein	High mobility group protein
IPTG	Isopropyl-β-D-1-thiogalactopyranosid
JNKs	c-Jun N-terminal kinases
LB	Luria-Bertani
NBD	Nucleosomal binding domain
NES	Nuclear export signal
NLS	Nuclear localization signal
NMR	Nuclear magnetic resonance
NPC	Nuclear pore complex
PCR	Polymerase chain reaction
PKA	Protein kinase A
PKB	Protein kinase B
PKC	Protein kinase C
PP2A	Protein phosphatase 2A
PPIase	Peptidyl-prolyl *cis-trans* isomerase
TPR	Tetratricopeptide repeat

Contents

1. Introduction

1.1 Peptidyl-prolyl *cis/trans* isomerases (PPIases)

The specific association of proteins is a fundamental process that plays a critical role in cellular events ranging from the construction of functioning macromolecular complexes to the linking of specific proteins in signal transduction pathways. Interaction between proteins depends on the exact recognition of a peptide sequence or structural motif. A variety of protein domains have, thus, evolved to perform this function. Biological processes are dependent on the action of proteins and their domains, for example, protein folding is assisted by folding helper proteins as disulfide isomerases or peptidyl-prolyl *cis/trans* isomerases (Gothel & Marahiel, 1999; Ferrari & Soling, 1999). These proteins have evolved to recognize specific signatures of protein sequences and supervise *in vivo* protein folding. A significant number of proteins have been identified to contain a peptidyl-prolyl *cis/trans* isomerase domain, a domain that has been suggested to constitute another specific protein recognition unit (Fischer, et al., 1984). The peptidyl prolyl *cis/trans* isomerases (PPIases, EC 5.2.1.8) are enzymes that accelerate the slow *cis/trans* isomerization of peptidyl-prolyl bonds in different folding states of a target protein. PPIase-catalysed protein conformational changes were shown to occur during the refolding of denatured proteins, *de novo* protein synthesis and the formation of biologically active conformations of polypeptides (Schiene-Fischer & Yu, 2001).

PPIases are ubiquitously expressed and highly conserved proteins found in prokaryotic and eukaryotic cells. Based on drug specificity and primary sequence homology, PPIases have been divided into three distinct families: a) the cyclosporin A (CsA)-binding proteins, cyclophilins, b) the FK506 and rapamycin binding proteins, FKBPs, and c) the parvulins, which do not bind immunosuppressant drugs (Fischer, et al., 1989; Schreiber, et al., 1991; Galat, 1993; Rahfeld, et al., 1994a). Even though cyclophilins and FKBPs are known for several decades, the cellular function of these enzymes is not yet completely understood. They are, however, implicated in the folding of newly synthesized proteins, transport and assembly of essential cellular protein complexes (Ivery, 2000). In contrast, the function of a member of the third PPIase family, Pin1 could be uncovered in much more details and an important role in the cell cycle machinery in eukaryotes was proved.

1.2 Parvulins

The parvulin family consists of highly conserved proteins found to be present in both prokaryotic and eukaryotic cells. No parvulin or its homologue has been found in Archaea. The name “parvulin” comes from the Latin word *parvulus*, which means “very small”, a term

given on the basis of its first identified member, Par10, the smallest functional enzyme (Rahfeld, et al., 1994a). The protein members of the parvulin family have no sequence similarity to either cyclophilins or FKBPs. The signature sequence for parvulins contains conserved amino acids like histidine, isoleucine and leucine within PPIase domain, found in all protein members of the family. Generally, prokaryotic parvulins have a chaperon-like activity and eukaryotic parvulins have been linked to several aspects of gene regulation and cell cycle progression (Hanes, et al., 1989; Lu, et al., 1996; Rippmann, et al., 2000; Shaw, 2002).

1.2.1 Prokaryotic parvulins

The first protein member of the parvulin family, Par10 or PPiC, was isolated from *E. coli* (Rahfeld, et al., 1994b; Rudd, et al., 1995). The protein shares no sequence homology with cyclophilins or FKBPs and its enzymatic activity is inhibited neither by cyclosporin A nor by FK-506 or rapamycin. Par10 is a cytoplasmic, single domain protein consisting of 92 residues, and has a molecular mass of 10.1 kDa (Rahfeld et al., 1994b). From investigations of tetrapeptdie model substrates it is known, that Par10 prefers for its PPIase activity prefers hydrophobic amino acids, e.g., leucine or phenylalanine in the position preceding the proline (Rahfeld, et al., 1994b). Based on sequence homology to Par10, other prokaryotic members of parvulins have been identified: PrtM in *Lactococcus lactis* (Vos, et al., 1989, Haandrikman, et al., 1991), NifM in *Azotobacter vinelandii* (Jacobson, et al., 1989), SurA in *E. coli* (Tormo, et al., 1990), PrsA in *Bacillus subtilis* (Kontinen, et al., 1991), PpiD in *E. coli* (Dartigalongue, et al., 1998) and PmpA in *Lactococcus lactis* (Drouault, et al., 2002). SurA and PpiD are both located in the periplasm of *E. coli*. SurA is necessary for bacterial survival during the stationary phase. It assists in the folding of outer membrane proteins (OMP) (Lazar & Kotler, 1996; Rouviere, et al., 1996) and acts as a periplasmic chaperone (Behrens, et al., 2001). PpiD is anchored to the inner membrane via a single transmembrane segment with its catalytic domain exposed to the periplasm. It has a similar function like SurA, involvement in protein folding. In fact, the gene encoding PpiD was isolated as a multicopy suppressor of SurA (Dartigalongue, et al., 1998). PrsA from *Bacillus subtilis* is bound to the outer face of the cytoplasmic membrane. The protein is crucial for efficient secretion of a number of exoproteins. The prsA mutants showed decreased secretion and stability of some exoprotein, while overproduction of PrsA enhanced these processes (Kontinen & Sarvas 1993; Leskelä, et al., 1999). PmpA protein either triggers the folding of secreted lipase or activates its degradation by the cell surface protease HtrA (Drouault, et al., 2002). The protein PrtM from

Lactococcus lactis (Vos, et al., 1989), acts as a folding helper of serine protease SK11 and NifM from *Azotobacter vinelandii* is important for the activation of nifH gene in the nitrogenase pathway (Lei, et al., 1999; Petrova, et al., 2000).

1.2.2 Eukaryotic parvulins

The two parvulin-like PPIases, Ess1/Ptf1 in *Saccharomyces cerevisiae* (hereafter termed Ess1) (Hani, et al., 1995) and *h*Pin1 in human (Lu, et al., 1996), were the first identified eukaryotic members of the parvulin family. Subsequently, *h*Pin1-homologoue proteins have been described for other species like Dodo in *Drosophila melanogaster* (Maleszka, et al., 1998), Ess1 in *Schizosaccharomyces pombe* (Huang, et al., 2001), Pin1 in *Mus musculus.* (MmPin1) (Fujimori et al., 2001), Pin1 in *Arabidopsis thaliana* (AtPin1) (Landrieu, et al., 2000), Pin1 in *Aspergillus nidulans* (Lu, et al., 1996), Pin1 in *Digitalis lanata* (DlPar13) (Metzner, et al., 2000), Ssp1 in *Neurospora crassa* (Kops, et al., 1998), Pin1 in *Xenopus laevis* (xPin1) (Winkler, et al., 2000), Par15 in *Arabidopsis thaliana* (Kamphausen, 2002) and *h*Par14 in human (Uchida, et al., 1999; Rulten, et al., 1999). All these proteins are homologues in their primary amino acids sequence to the PPIase domain of Par10, Ess1 and *h*Pin1. Based on the substrate specificity of PPIase domain, the eukaryotic parvulins can be subdivided into two groups: phospho-specific proteins, preferring negatively-charged residues preceding proline (most eukaryotic parvulins, including *h*Pin1) (Schutkowski, et al., 1998) and nonphospho-specific protein, preferring positively-charged residues preceding proline (Arg-Pro) as *h*Par14 (Uchida, et al., 1999).

1.2.2.1 pSer/pThr-Pro specific parvulin, *h*Pin1

The human Pin1 was identified in a yeast two-hybrid screen as a protein that interacts with NIMA kinase, known to be essential for mitosis in the filamentous fungus *Aspergillus nidulans* (Osmani et al., 1987, Osmani, et al., 1988). The novel protein functionally suppressed the lethal NIMA phenotype in yeast (Lu, et al., 1996). *h*Pin1 is a small, highly conserved 18 kDa protein, localized in the nucleus at nuclear sub-structures variously termed interchromatin granule clusters (IGCs) or speckles (Lu, et al., 1996). Depletion of *h*Pin1 in HeLa cells or the respective homologue in yeast, Ess1 (Hanes, et al., 1989; Lu, et al., 1996), resulted in mitotic arrest, whereas overexpression of *h*Pin1 in HeLa cells caused G2 arrest. The protein has 45 % sequence identity with the *S. cerevisiae* homologue, Ess1, and can functionally substitute the temperature-sensitive Ess1 mutant (Lu, et al., 1996), indicating that function of these two proteins is highly conserved in eukaryotes. Based on the primary sequence

homology, *h*Pin1 is divided into two domains, an amino-terminal WW domain and carboxy-terminal catalytic domain with high homology to the PPIase domain of Par10 from *E. coli* (Lu, et al., 1996). The crystal structure of *h*Pin1 revealed that the WW domain is folded into a 3-stranded β sheet and the PPIase domain consisting of a half β-barrel and four antiparallel strands surrounded by four α-helices (Figure 1.1) (Ranganathan, et al., 1997).

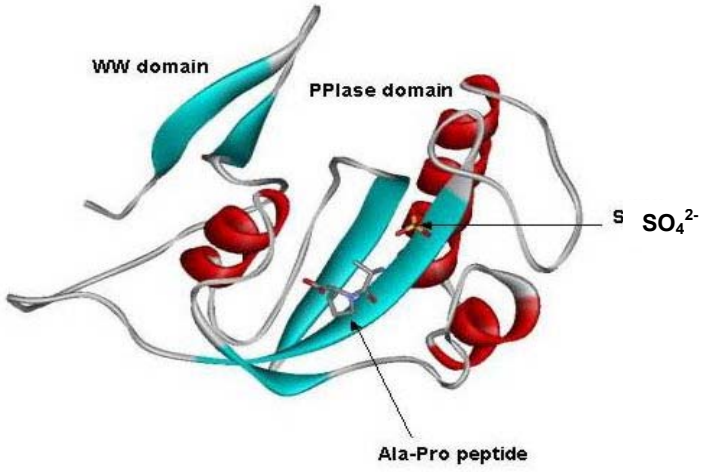

Figure 1.1 The crystal structure of *h*Pin 1 (Ranganathan, et al., 1997; PDB: Pin1). The co-crystallized inhibitory peptide Ala-Pro and a sulphate moiety are shown as sticks. The secondary structure elements are red (α-helices) and blue (β-sheets).

Generally, WW domains contain 38-40 amino acid residues with two invariant Trp residues. WW domains are divided into four classes, three recognizing short proline-rich motifs, and a fourth class recognizing phosphoserine (pSer) or phosphothreonine (pThr)-proline motifs (Sudol, 1996). The WW domain of *h*Pin1 is a member of the fourth group and interacts with phosphorylated Ser/Thr-Pro sequences (Lu, et al., 1999; Verdecia, et al., 2000). In addition to that function, the PPIase domain of *h*Pin1 displays unique phosphorylation-dependent prolyl isomerase activity that specifically catalyses the isomerization of phosphorylated Ser/Thr-Pro bond with up to 1300-fold higher selectivity compared to unphopshorylated substrates.

1.2.2.2 *h*Pin1 interacts with mitotic phosphorylated proteins

Findings show that phosphorylation on Ser/Thr residues immediately preceding proline not only alters the prolyl isomerization rate (Schutkowski, et al., 1998) but also creates a binding site for the WW domain and PPIase domain. This implied that *h*Pin1 binding proteins can be substrates for proline-directed protein kinases such as cyclin-dependent kinases (CDKs) or mitogen-activated protein kinases (MAPKs). Further investigation revealed that indeed *h*Pin1 directly binds a number of proteins in a cell cycle regulated manner. As was reported by Lu and co-workers (Lu, et al., 1999), *h*Pin1-binding activity was low during G1 and S, increased in G2/M, and the highest activity was observed for cells arrested in M phase. The M phase proteins, known to bind to *h*Pin1 are listed in Table 1.1.

Table 1.1 Phosphorylated proteins interacting with *h*Pin1

Protein	Targeted sites	Processes influenced by *h*Pin1 activity	References
NIMA Cdc25 Cdc27, Myt1 Plk1, Wee1	pThr48-Pro pThr67-Pro	Genetic interaction, phosphatase activity, protein dephosphorylation	Shen, et al., 1998 Shen, et al., 1998
Tau	pThr231-Pro	Protein dephosphorylation	Lu, et al., 1999
Rab4		Inhibition of endocytic membrane transport during mitosis	Gerez, et al., 2000
Bcl2		Altering the conformation of Bcl-2 and function	Pathan, et al., 2001
NFAT		Inhibition the calcineurin mediated dephosphorylation of NFAT *in vitro*	Liu, et al., 2001
KRMP1		Pin1 overexpression reverses the G2/M arrest caused by overexpression of KRMP1	Kamimoto, et al., 2001
NHERF-1		Facilitates dephosphorylation of NHERF-1	He, et al., 2001
hSpt5		Transcription regulation, pre-mRNA maturation, protein dynamics	Lavoie, et al., 2001
β-catenin	pSer246-Pro	Regulation of subcellular localization and transcription activity of β-catenin	Ryo, et al., 2001
c-Jun	pSer63-Pro; pSer73-Pro	Transcriptional activity	Wulf, et al., 2001
CTD domain of RNA pol.II	pSer5-Pro (in the repeat)	Regulation of CTD phosphorylation	Albert, et al., 1999 Kops, et al., 2002
CyclinD1		Protein expression, stability and localization	Liou, et al., 2002
CK2		Regulation of topoisomerase II alpha activity, inhibition	Messenger, et al., 2002
Cf-2		Protein stability, transcriptional activity	Hsu, et al., 2001
p53	pSer33-Pro pThr81-Pro pSer315-Pro	Transcriptional activity	Zheng, et al., 2002 Zacchi, et al., 2002 Wulf, et al., 2002

1.2.2.3 Model of action of *h*Pin1

The first evidence that *h*Pin1 binds proteins in a phosphorylation-dependent manner was obtained for Cdc25c and its upstream regulator, polo-like kinase (Plk1) (Crenshow, et al., 1998; Shen, et al., 1998). Cdc25c is a Cdc2-directed phosphatase, a multiple phosphorylated protein during the G2/M transition of the cell cycle. Both, mitotic phosphorylated Cdc25c from Xenopus egg extracts and Plk1 from HeLa cell extract were reported to interact with *h*Pin1. The protein binds to phosphorylated Cdc25c and inhibits its activity to dephosphorylate and activate Cdc2 (Zhou, et al., 2000). Recent work has indicated that *h*Pin1 acts on phosphorylated Cdc25c in a catalytic manner to promote conformational changes in Cdc25c that facilitates its dephosphorylation by protein phosphatase 2A (PP2A) (Zhou, et al., 2000; Stukenberg & Kirschner, 2001). This finding suggests that in a protein with multiple Ser-Pro/Thr-Pro motifs like Cdc25c, an initial phosphorylation event may trigger a succession of alternating phosphorylation-isomerization steps, which leads to conformational changes of Cdc25c. There are two possible models that allow *h*Pin1 to catalyse isomerization of its substrate. One is that every phosphorylated Ser/Thr-Pro motif of *h*Pin1 substrate first binds to the WW domain of *h*Pin1 and is then transferred to and isomerised by the catalytic domain. The other possibility is that the WW domain binds only one or two phosphorylated Ser/Thr-Pro motifs in a *h*Pin1 substrate and the catalytic domain isomerises the rest of the phosphorylated Ser/Thr-Pro bonds in the protein, as described for Cdc25c (Zhou, et al., 2000). Similar model of action of *h*Pin1 has been described for tau protein. Tau is a microtubule-binding protein that is important for the dynamic change in the microtubule structure in mitotic cells. In this case, *h*Pin1 binds to only one phosphorylated Ser/Thr-Pro motif of Alzheimer's disease-associated phosphorylated tau and restores its biological function to promote microtubule assembly (Lu, et al., 1999).

Moreover, *h*Pin1-WW domain regulates subcellular localization (Lu, et al., 2002), nuclear transport (Ryo, et al., 2001), transcription-promoting activity (Komuro, et al., 1999) and pre-mRNA 3'-end formation (Morris, et al., 1999).

1.2.2.4 *h*Pin1 modulates function of transcription factors

The reversible phosphorylation of proteins on serine/threonine residues preceding proline (pSer/pThr-Pro) is a key regulatory mechanism for a control of various cellular processes, including cell division and transcription (Nigg, 1995; Hunter & Karin, 1992). For example, different growth factors and oncoproteins, e.g., Ras, trigger a signalling cascade leading to the activation of c-Jun N-terminal kinases (JNKs). JNKs, which phosphorylate c-Jun on

Ser63-Pro and Ser73-Pro, and enhance their transcriptional activity towards c-Jun target genes, including cyclin D1 (Chang & Karin 2001). It has been demonstrated that overexpression of *h*Pin1 increases the levels of cellular cyclin D1 mRNA and protein. Moreover, *h*Pin1 binds to phosphorylated c-Jun and increases its transcriptional activity towards the AP1 site in cyclin D1 promoter. This action is in cooperation either with activated JNK or oncogenic Ras. The effects of *h*Pin1 on the c-Jun transcriptional activity depend on both the isomerase activity and phosphorylation of c-Jun on Ser63/73-Pro residues (Ryo, et al., 2001). In contrast, inhibition of endogenous *h*Pin1 reduces the transcriptional activity of phosphorylated c-Jun. Another example for *h*Pin1-regulated transcription is described for β-catenin. Regulation of β-catenin is linked to Wnt signalling pathway and involves intracellular localization and protein stability (Hecht & Kemler, 2000). Activation of the Wnt pathway inhibits the phosphorylation of β-catenin by glycogen synthase kinase 3β (GSK-3β) and results in increased β-catenin stability and nuclear accumulation. In the absence of Wnt signals, the APC protein, which is expressed by the tumour suppressor gene and mutated in familial adenomatous polyposis coli (APC), exports β-catenin from the nucleus and recruits into a cytoplasmic complex with GSK-3β (Henderson, 2000). This event promotes β-catenin degradation and downregulates its target genes, i.e., c-myc and fibronectin (Rubinfeld, et al., 1996). Binding of *h*Pin1 to pSer246-Pro motif within the armadillo repeats of β-catenin at a position close to the APC binding site, prevents binding of APC to β-catenin and consequently increases nuclear accumulation of β-catenin and transcriptional activity (Ryo, et al., 2001).

*h*Pin1-regulated transcription has been described for the T cell activation pathway targeted by the immunosuppresant CsA. In quiescent cells, the T-cell specific NFAT transcription factor is phosphorylated and located within the cytoplasm. Following T-cell activation by calcium signalling, NFAT is dephosphorylated by the protein phosphatase, calcineurin, and subsequently translocated to the nucleus (Graef, et al., 2001). Overexpression of *h*Pin1 in Jurkat T-cells prevents NFAT activation by binding to pSer-Pro motifs and thereby blocks dephosphorylation by calcineurin (Liu, et al., 2001). On the other hand, it has been suggested that at physiological level, *h*Pin1 may have an inverted function, which promotes the dephosphorylation of NFAT by calcineurin. This process would then have a possible positive effect on transcription (Liu, et al., 2001).

1.2.2.5 Depletion of Pin1 in different organisms

Functionally, *h*Pin1 is critical for cell proliferation *in vivo* (Lu, et al., 1996). Temperature-sensitive mutations or deletion of Ess1 gene in fission yeast resulted in mitotic arrest and nuclear fragmentation (Lu, et al., 1996). These arrested cells have defective 3' end formation of pre-mRNA, and decreased levels of some mRNAs (Hani, et al., 1998). Inhibition of the *h*Pin1 function in human tumour cells by expression of *h*Pin1 antisense RNA or dominant-negative mutants induces mitotic arrest and apoptosis (Rippman, et al., 2000). Similarly, depletion of *h*Pin1 in Alzheimer's disease brain may also contribute to neuronal death (Lu, et al., 1999). Furthermore, depletion of xPin1 in Xenopus oocytes induces premature mitotic entry and disrupts a DNA replication checkpoint (Winkler, et al., 2000). In contrast, depletion of Pin1 in *Candida albicans* resulted in late mitotic arrest (Devasahayam, et al., 2002). Despite of these findings, the essential role of Pin1 in cell cycle seems to be contradictory. There are reports showing that the depletion of Pin1 did not result in a readily observable phenotype. For example, knockout of *h*Pin1 homologue, Dodo in *D. melanogaster* (Maleszka, et al., 1997), Ess1 in *S. pombe* (Huang, et al., 2001) or Pin1 in *M. musculus* (Fujimori, et al., 1999) did not result in obvious phenotypes. This can be explained by the new finding that Cyp18 and Pin1/Ess1 can act on common targets required for mitosis, and the PPIase activity is linked to their essential function (Wu et al., 2000; Arevalo-Rodriguez et al., 2000; Fujimori, et al., 2001; Huang, et al., 2001). The discovery that *h*Pin1 plays an important role in cyclin D1 signalling pathway and cell proliferation helped to elucidate the phenotype of Pin1-/- mice. The mice displayed a range of cell-proliferative abnormalities, including decreased body weight, testicular and retinal atrophies (Liou, et al., 2001).

1.2.2.6 Parvulin, *h*Par14

The combination of database search and screening of human lung cDNA library lead to the identification of an additional human parvulin homologous gene, *h*Par14. The encoding region of the gene consisted of 1013 bp and encoded a protein of 131 amino acids and had a molecular weight of around 14 kDa (Uchida, et al., 1999). The protein showed primary sequence similarities to Par10 and *h*Pin1, thus, is classified under the parvulin family. The biochemical properties of *h*Par14 were characterized *in vitro* (Uchida, et al., 1999; Roulten et al., 1999). Homology in primary sequence to Par10 allowed *h*Par14 to be divided into two domains, a) an amino-terminal extension of 35 amino acids, which does not show sequence homology to the WW domain of *h*Pin1, and b) a carboxy-terminal domain consisting of 96

amino acid residues with 34.5 % of sequence identity and 73.6 % similarity to Par10 from *E. coli* (Uchida, et al., 1999).

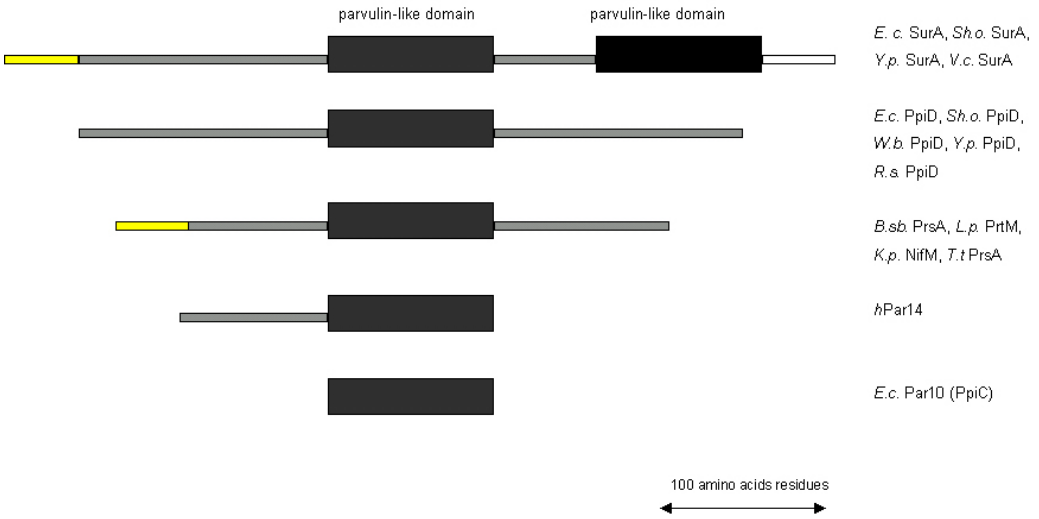

Figure 1.2 Schematic representation of a domain of Par10 compared to selected parvulins. The black colour boxes indicate the parvulin catalytic core; the yellow colour boxes indicate signal peptide sequence. SurA: *E. coli* (accession nr. BAB96621); *Shewanella oneidensis* MR-1(NP-719179); *Yersinia pestis* CO92 (CAC89351); *Vibrio cholerae* (NP-230099); PpiD: *E. coli* (P77241); *Yersinia pestis* CO92 (CAC92388); *Wigglesworthia brevipalpis* (BAC24298); *Shewanella oneidensis* MR-1 (AAN54851); *Ralstonia solanacearum* (CAD15417); PrsA: *Bacillus subtilis* (P24327); *Lactobacillus paracasei* (A44858); *Klebsiella pneumoniae* (S02510); *Thermoanaerobacter tengcongensis* (NP-623647); *h*Par14: *Homo sapiens* (BAA82320); Par10 (PpiC): *E. coli* (P39159). According to Uchida, et al., 1999 with some modifications.

The PPIase domain of *h*Par14 shows high similarity to that of the corresponding domain of *h*Pin1 or Par10 but massive differences in substrate specificity. The relative values of the specificity constant for different substrates showed a general pattern similar to that one found in *E. coli* Par10, with a strong preference for a substrate with basic arginine preceding proline. The specificity constant k_{cat}/K_M obtained for this substrate (Suc-Ala-Arg-Pro-Phe-NH-Np) is 3.95 10^3 M^{-1} s^{-1} (Uchida, et al., 1999). This is lower then the respective value of k_{cat}/K_M for phosphorylated substrates catalysed by Pin1. The low magnitude of the specificity constant of *h*Par14 may indicate that native substrates for this protein are not yet identified.

In contrast to *h*Pin1 but similar to Par10, *h*Par14 does not accelerate *cis* to *trans* interconversion of substrates with phosphorylated amino acid residues preceding proline

(Uchida, et al., 1999). The difference in recognition of phosphorylated substrates underlines the role of a basic cluster in other eukaryotic parvulins. The three amino acid residues Lys63, Arg68 and Arg69 of *h*Pin1 form a positively charged surface groove that can interact with the phosphate moiety (Ranaganthan, et al., 1997). In contrast to *h*Pin1, the positively charged groove is replaced by more negatively charged area of *h*Pa14 including residues Asp74 and Glu46.

The N-terminal extension of *h*Par14 has 40-50 % homology towards glycine-rich sequences of HMGN family of non-histone chromosomal proteins (Uchida, et al., 1999). The nuclear magnetic resonance solution structure of *h*Par14 indicated that the PPIase domain of *h*Par14 folds into $\beta\alpha3\beta\alpha\beta2$ structure (Figure 1.3) that is similar to the structure of *h*Pin1 (Sekerina, et al., 2000; Terada, et al., 2001).

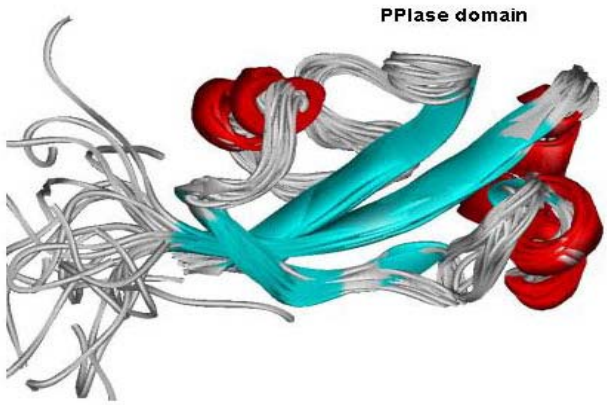

Figure 1.3 NMR solution structure of *h*Par14 (pdb1fjd, residue 28-131). Overlay of 20 lowest energy structures according to Sekerina, et al., 2000. The secondary structure elements are red (α-helices) and blue (β-sheets).

The mRNA of *h*Par14 is detected in many human tissues, including heart, placenta, liver, kidney and pancreas (Uchida, et al., 1999). In addition, the protein was found in Jurkat cells (Sekerina, et al., 2000). Sequence homology analyses indicated that some *h*Par14-like proteins could be found in the database. At least, eight proteins from different species showed high sequence similarity to amino acids sequence of *h*Par14 (Figure 1.4).

```
hPar14              MPPKGKSGSGKAGKGGAASGSDSADKKAQGPKGGGNA----37

M.mus               MPPKGKSGSGKGGKGGAASGSDSADKKSQGPKGGGNA----37
C.ele                    MPPKKTPKGGASGSGKDDGGGQKKEAKGGGTA----32
X.lae                  MPPKGKGGKGAKGGAASGEAADKKAQTPKGGNA----33
D.mel                MPPKKDAKSGKDAGKGGKKPAAEDKSAGKEKKGGNA----36
A.tha          MGKDAKAGGKGKGKQASGSEEAPSKGKGKAGKAADGLGTCTY----42
G.max  VVINIGKDSKPKESGGKGKGKQAASGSDENASKGKGKGGKGGDGLGTCTY----50
L.jap                  KGKGKQAASGSDENASKGKGKGAKGGDGLGTCTY----34
P.tae               KAKESSKGKGKASGGGGSDEKGKGKSGKAADGLGTCTY----38
```

```
hPar14  VKVRHILCEKHGKIMEAMEKLKSGM----------RFNEVAAQYSED-KARQGGDLGWMTRGSMVGPFQEAAFALPVSGMDKPVFTDPPVKTKFGYHIIMVEGRK-------131

M.mus   VKVRHILCEKHGKIMEAMEKLKSGM----------RFSEVATQYSED-KARQGGDLGWMTRGSMVGPFQEAAFALPVSGMDKPVFTDPPVKTKFGYHIIMVEGRK-------131
C.ele   VKVRHILCEKQGKALEAIEKLKSGM----------KFNXVAAQYSED-KARSGGDLGWMTRGSMVGPFQDAAFALSNSSCDKPIYTDPPVKTKFGYHVIMV-GKK-------126
X.lae   VKVRHILCEKHGKVMEAMEKLKSGV----------RFSEVATQYSED-KARQGGDLGWMTRGSMVGPFQDAAFALPAAQWTNLFTLI------------------------109
D.mel   VKVRHILCEKQGKITEAMEKLKAGQ----------KFPEVAAAYSED-KARQGGDLGWQIRGAMVGPFQDAAFALPISTVNNPVYTDPPIKTKFGYHIIMVEGKK-------121
A.tha   VKARHVLCEKQGKINEAYKKLQDGWLSNGDKVPPAEFAKIAAEYSECPSGKKGGDLGWFPRGKMAGPFQDVAFNTPVGVTSAPFKSTH------GYHIILSEGRKN------141
G.max   VKARHILCEKQGKINEAYKKLQDGWLGNGDKVPP-EFAKVAQEYSECPSRKKGGDLGWFPRGKMAGPFQEVAFNTPVRATNAPFK-TH------GYHIILNE----------167
L.jap   VKARHILCEKQGKINEAYKKLQDGWLSNGDKVPPAEFAKIAQEYSECPSGKKGGDLGWFPRGKMAGPFQDVAFNTVVGATSAPFKSTH------GYHIILSEGRKN------134
P.tae   VKARHILCEKQGKVNEAYKKLQDGWLSNGDKVPPAEFAKVAAEY--CPSGKKGGDLGWFPLGKM--PF----FNT------------------------------------105
        **.**:****:**  ** :**:.*          .*  :* :***  ..:.******:.**.*.****:.**    .     . :           :*  **:*
```

Figure 1.4 Multiple sequence alignment of ESTs or proteins homologue to C-terminal *h*Par14. Accession number: *Mus musculus* (XP-177113), *Caenorhabditis elegans* (NP-496824), *Drosophila melanogaster* (NP-651364) and *Arabidopsis thaliana* (AAF98562). *Xenopus laevis* and last three ESTs sequences were supplied by Dr. Rahfeld.

1.2.2.7 *h*Par14 associates with pre-ribosomal ribonucleoproteins (pre-rRNPs)

The cellular function of *h*Par14 remains unknown. However, it was recently reported that *h*Par14 associates with complexes containing pre-rRNA and ribosomal proteins (Fujiyama, et al., 2002). The novel *h*Par14-interacting proteins were identified using GST pull down combined with proteomic analysis. Among the identified proteins, 15 proteins were ribosomal (i.e. L3, L6, L7, L7a) and 23 proteins non-ribosomal including trans-acting factors or proteins expected to be involved in ribosomal biogenesis. Based on these findings, it has been suggested that *h*Par14- associated rRNP complexes represents those formed during postmitotic nucleolar reformation before rDNA transcription or premitotic nucleolar disassembly. Therefore, it has been proposed that *h*Par14 function in events as those occurring in ribosome biogenesis, rDNA transcription, and remodelling of the nucleolus (Fujiyama, et al., 2002).

1.3 Phosphorylation regulates localization and function of PPIases.

The nucleus of eukaryotic cells is a highly dynamic organelle, where protein trafficking into and out of the nucleus occurs through the nuclear pore complex (NPC), a supramolecular structure that spans the nuclear envelope. Small proteins with a molecular weight of up to 40kDa can diffuse through the nuclear pore complex, in contrast to larger proteins, which are transported in a signal and energy dependent manner (for reviews see Jans, 1995). During the past few years, it has become well established that shuttling between nucleus and cytoplasm plays a critical role in the regulation of gene expression and cell cycle progression. It is well known that cargo-specific regulatory mechanisms can control the nucleocytoplasmic transport of certain proteins in different stages of the cell cycle. However, the most common mechanism to regulate protein's cellular localization and function is phosphorylation and dephosphorylation at serine or threonine side chains of target proteins. Reports have shown that the protein members of two PPIases families: parvulins and FKBPs are be phosphorylated by different protein kinases. In the case of cyclophilins, there is no information about possible phosphorylation. Recently published report by Misumi and co-workers (Misumi, et al., 2002) suggested acetylation as a putative posttranslational modification. This work will provide information about phosphorylation regulated cellular localization and function of *h*Par14, member of parvulin family.

1.3.1 Phosphorylation by PKA regulates function of *h*Pin1

The phosphorylation status has been demonstrated to play an important role in regulation of the cellular function of *h*Pin1. The protein is a substrate for PKA (Lu, et al., 2002). The kinase phosphorylates the Ser16 residue within the WW domain of *h*Pin1 and phosphorylation abolishes interactions with phosphorylated proteins. This fact was expected since Ser16 is located at the centre of the binding pocket for pSer/Thr-Pro substrates (Verdecia, et al., 2000). In addition, *in vitro* phosphorylated *h*Pin1 or mutant protein with substituted Ser16 amino acid to Glu, failed to bind mitotic phosphoproteins. Overexpression of mutant protein with substituted Ser16 to Ala resulted in cytoplasmic localization of *h*Pin1, mitotic block and apoptosis (Lu, et al., 2002). Additionally to these observations, phosphorylation at Ser16 appears to be regulated in a cell cycle dependent manner, since the unphosphorylated *h*Pin1 is found in G2/M arrested cells.

1.3.2 Phosphorylation by CK2 regulates function of FKBPs

The CK2 (formally casein kinase 2) is ubiquitously expressed and highly conserved serine/threonine protein kinase (for review see Pinna, 1994). The CK2 is a tetrameric enzyme that is composed of two catalytic (CK2α and/or CK2α') subunits and two regulatory β-subunits (Allende & Allende, 1995). It has been reported that each subunit of CK2 has individual function. CK2β seems to have at least three functions: it confers stability of the holoenzyme, it increases enzyme activity, and it determines substrate specificity (for review see Faust & Montenrach, 2000). The catalytic α subunit is regulated by the β subunit; very little is known about the α' subunit. Analysis of the activity of CK2 revealed that the kinase is present in cytoplasm, nucleus, plasma membrane, mitochondria, endoplasmic reticulum, cytoskeleton, centrosomes, nuclear matrix, nucleolus and nucleosomes (for review see Faust & Montenrach, 2000) of eukaryotic cells. The substrates of CK2 are involved in the regulation of transcription, signal transduction processes, growth control, various steps of development, and the formation of cellular shape and architecture.

Human FKBP25 was the first protein member of FKBP family reported as a substrate for CK2. The phosphorylation of human FKBP25 enhances its nuclear localization and mediates association with nucleolin (Jin & Burakoff, 1993). In the case of human FKBP52, phosphorylation by CK2 within tetratricopeptide repeat (TPR) motif abolished association with Hsp90 (Miyata, et al., 1997). Phosphorylation by CK2 was also reported for insect FKBP46. The phosphorylation had no influence on the binding of FKBP46 to single or double stranded DNA (Steplewski, et al., 2000).

1.4 14-3-3 proteins

Studies have shown that *h*Par14 is phosphorylated at serine residues and detailed analysis of the amino acid sequence revealed a putative 14-3-3 binding motif.

14-3-3 proteins, found in 1967 by Moore and Perez, were described as abundant, acidic, brain proteins. The name of the protein was given on the basis of its fraction number on DEAE-cellulose chromatography and its migration position in starch-gel electrophoresis. Seven mammalian isoforms (β,ε,γ,η,σ,τ,ξ) have been identified with molecular masses of 28-33 kDa. The 14-3-3 family members are dimeric intracellular proteins. The crystal structure of two 14-3-3 proteins revealed that monomers interact with each other at their N-termini to form a dimer (Liu et al., 1995; Xiao et al., 1995). Monomer of 14-3-3 consists of highly conserved amino acid residues including a cluster of the basic residues Lys-49, Arg-56 and Arg-127 (Liu et al., 1995). In contrast, the conservation of residues in the outer part of the 14-3-3 is much

lower. It has been suggested that this less conserved part of the 14-3-3 is responsible for the interaction with target proteins (Atiken, 1996). However, co-crystallization studies of 14-3-3 with a peptide representing a common, phosphorylated 14-3-3 binding motif showed that the peptide is bound to the groove of 14-3-3 proteins (Yaffe et al., 1997). The general consensus sequence found for 14-3-3 using a combinatorial peptide library is R(S/Ar)XpSXP or RX (Ar/S)XpSXP in which pS denotes phospho-serine residue and Ar an aromatic residues. Furthermore, there is an increasing number of 14-3-3 binding ligands whose sequences either differ significantly from this motif or do not require phosphorylation for binding (Fu, et al., 2000).

Intensive studies on 14-3-3 proteins revealed an important role in cells. Early genetic analysis showed that homologues of 14-3-3, BMH1 and BMH2 (Gelperin, et al., 1995) in budding yeast and Rad24 and Rad25 in fission yeast are essential for cell survival (Ford, et al., 1994).

1.4.1 Phosphorylated proteins are ligands for 14-3-3

The 14-3-3 proteins have attracted substantial attention over the past few years because of their pleiotropic biological effects. In particular, 14-3-3 proteins appear to play an important role in the regulation of signal transduction, apoptosis, cell cycle checkpoint control and nutrient-sensing pathways. Over 100 proteins have been found to interact with 14-3-3 (for review see Fu, et al., 2000), including various protein kinases (PKCs, Raf family members, KSR, PCTAIRE, MEKK 1-3, Bcr, PKUα, ASK1), receptor proteins (glucocorticoid receptor, GpIb-IX, α2 adrenergic receptor, GABA receptor, insulin-like growth factor I receptor, IL-3/IL-5/GMCSF receptor βc chain), enzymes (tyrosine and tryptophan hydroxylase, nitrate reductase, serotonin *N*-acetyl transferase, PTPH1 tyrosine phosphatase) structural and cytoskeletal proteins (vimentin, keratins, K8/K18, Tau, Kif1C), small G-proteins and their regulators (rem, Rad, RGS3/7, p190RhoGEF), scaffolding molecules (IRS-1, calmodulin, Grb-2, poloma middle T, p130Cas, Cbl), proteins involved in cell cycle control (Cdc25 phosphatases, Chk1, Wee1, p53), proteins involved in transcriptional control of gene expression (TATA box binding proteins TBP and TFIIB, histone deacetylases 4,5,7, histone acetyl transferase 1, transcription factors NFAT Msn2p and 4p, co-activators TAZ and YAP) and proteins involved in control of apoptosis (BAD, A20, p75NTR-associated cell death executor NADE). The 14-3-3 proteins may participate in different pathways by altering the subcellular localization of their numerous binding partners (Fu, et al., 2000).

1.4.2 Regulation of protein subcellular localization by 14-3-3

The subcellular localization of signalling, apoptotic and cell cycle pathway proteins has attracted considerable interest in recent years. The enzyme localization is often as important as its activation state for the regulation of cell physiology. Much work has been performed on the mechanisms underlying the targeting of proteins to the endoplasmatic reticulum, the Golgi apparatus, the nucleus, the mitochondria, and the plasma membrane (Muslin & Xing, 2000). Relatively little attention has been given to mechanisms promoting the cytoplasmic localization of proteins. 14-3-3s are localized to the cytoplasm of eukaryotic cells (Zhang, et al., 1999). However, there are exceptions to this pattern that describe 14-3-3 isoforms localized in the nuclei of animal and plant cells (Imhof, et al., 1999; Bihn, et al., 1997). Predominant cytoplasmic localization of 14-3-3 proteins has led to the hypothesis that they might be cytoplasmic anchors that block import to the nucleus or to other organelles; or that they promote export from organelles into the cytoplasm (Zhang, et al., 1999). The ability of 14-3-3 proteins to prompt the cytoplasmic localization of binding partners may have dramatic effects on signal transduction cascades, cells cycle progression, regulation of apoptosis pathways, or cytoskeleton organization (Fu, et al., 2000). This model of action is contradicted by the observation that 14-3-3 promotes the nuclear localization of some binding partners. The disparate effects of 14-3-3 proteins on the subcellular localization of binding partners will be discussed below using only three exemplary proteins Cdc25c, TERT and forkhead transcription factor like 1 (FKHRL1).

1.4.3 14-3-3 promotes the cytoplasmic localization of Cdc25c

The protein tyrosine phosphatase Cdc25c is phosphorylated at the Ser216 residue and this modification creates a binding site for 14-3-3 proteins. Interaction between Cdc25c and 14-3-3 results in cytoplasmic accumulation of Cdc25c. The functional significance of this interaction has been demonstrated in several organisms by expressing mutants of Cdc25c that cannot bind to 14-3-3 proteins. Loss of 14-3-3 binding, leads to nuclear accumulation of Cdc25c in fission yeast, Xenopus and human tissue culture cells. Mitotic- and G2 checkpoint control is disrupted in cells overexpressing mutants of Cdc25c (Zeng, et al., 1998).

Two major models have been proposed to explain how 14-3-3 proteins regulate the subcellular localization of Cdc25c. The first model was based on studies of Rad24, one of two 14-3-3 proteins in fission yeast. Rad24 was reported to contain a nuclear export sequence (NES), and it was proposed by Lopez-Girona, et al., (1999) that the protein contributes an “attachable” NES to mediate the nuclear export of Cdc25c in fission yeast. Rad24 dimer was

proposed to interact with both Cdc25c and the nuclear export receptor CRM1. This model was based on the finding that mutations in the putative NES of Rad24 allowed the mutant protein to accumulate in the nuclei of cells, and the mutant protein was not able to deplete Cdc25 from nucleus after DNA damage (Lopez-Girona, et al., 1999). However, later experiments showed that some of the residues comprising the NES of Rad24 are directly involved in substrate binding (Rittinger, et al., 1999) and it is unlikely that these residues regulate the nuclear export of binding partners by functioning as an attachable NES. In contrast to the model presented by Lopez-Girona, a second model has been developed to explain the mode of action of 14-3-3 proteins. It is proposed that 14-3-3 protein inhibits the nuclear import of Cdc25c by interfering with its nuclear localization sequence (NLS) (Kumagai & Dunphy, 1999; Yang, et al., 1999). 14-3-3 protein binds to Ser287 in Xenopus Cdc25c and mutation to alanine completely abrogate 14-3-3 binding and leads to the nuclear accumulation of Cdc25c. A consensus bipartite basic NLS on Cdc25c is located close to the 14-3-3 binding site at amino acid 298-316 (Yang, et al., 1999).

1.4.4 14-3-3 proteins promote the nuclear localization of TERT

The general notion that a primary function of 14-3-3 is to promote the cytoplasmic localization of its binding partners is contradicted by observations with TERT (telomerase). Telomerase is a ribonucleoprotein reverse transcriptase responsible for the maintenance of one strand of the telomere terminal repeats. The key protein subunit of the telomerase complex, known as TERT, possesses reverse transcriptase (RT)-like motifs that directly mediate nucleotide addition. 14-3-3 proteins interact with TERT, and this interaction is not dependent on the presence of phosphoserine (Seimiya, et al., 2000). An amphipatic helix with a characteristic serine/threonine cluster is present in TERT, and mutations at Thr1030, Ser1037 and Ser1041 to Ala in human TERT (hTERT) eliminate its ability to bind 14-3-3. Furthermore, expression of a mutant protein leads to the constitutive cytoplasmic localization of TERT, and this evidence suggests that 14-3-3 promotes the nuclear localization of TERT (Seimiya, et al., 2000).

1.4.5 14-3-3 protein transits to the nucleus and participates in dynamic nucleocytoplasmic transport

The subcellular localization of FKHRL1 is dependent on its phosphorylation by the protein kinase Akt/PKB (here termed PKB). PKB is the cellular homologue of the transforming oncogene of the AKT8 oncovirus (Bellacosa, et al., 1991). The kinase belongs to the AGC

(protein kinase A (PKA)/protein kinase G/protein kinase C-like) class of protein kinases and like other members of this class, requires phosphorylation for activation (Scheid & Woodgett, 2001). In the absence of growth factor, the PKB is inactive and FKHRL1 is present in the nucleus in an unphosphorylated form. Upon growth factor stimulation, PKB is activated, directly phosphorylating FKHRL1 at Thr32 and Ser253, and to a lesser extent at Ser315 (Kops, 1999), and resulting in FKHRL1 relocalization from the nucleus to the cytoplasm (Brunet, et al., 1999). The phosphorylation at Thr32 and Ser253 creates a binding site for 14-3-3, within the nucleus, where ligand free 14-3-3 molecules are located, followed by rapid nuclear export that requires both phosphorylation, 14-3-3 binding and intrinsic NES sequences in FKHRL1. Once FKHRL1 has been exported to the cytoplasm, phosphorylation/14-3-3 binding may play an additional role in preventing nuclear reimport possibly by masking the FKHRL1 NLS (Brunet, et al., 2002).

1.4.6 Possible action of 14-3-3 proteins

14-3-3 dimer is proposed to function through simultaneously engaging multiple phosphorylation sites on a single ligand. A synthetic phosphopeptide with two consensus 14-3-3 motifs binds over 30-fold more tightly than the same peptide containing only a single motif (Yaffe, et al., 1997). The exemplary proteins possessing two 14-3-3 binding sites are serotonin N-acetyl transferase and c-Raf kinase. Serotonin N-acetyl transferase has two sites, located at the N- and C- termini of the protein. These sites allow a single molecule to interact simultaneously with both subunits of dimer 14-3-3 (Obsil, et al., 2001). In the case of c-Raf, the protein contains two 14-3-3 binding sites, one located in the regulatory domain and a second located within the catalytic domain. Binding of 14-3-3 to the regulatory region appears to suppress the basal catalytic activity, but maintains the inactive form in a state that is readily active again (Roy, et al., 1998), that is, when the catalytic domain of c-Raf is displaced from 14-3-3 through dephosphorylation and binding to Ras (Jaumot, et al., 2001). Only dimer 14-3-3 interacting simultaneously with both domains of Raf is capable of facilitate Raf activation (Tzivion, et al., 1998). Moreover, it is suggested that binding of 14-3-3 to both termini of Raf induces a general conformational change to promote Raf interactions with downstream targets or facilitates their subsequent modification by kinases and phosphatases.

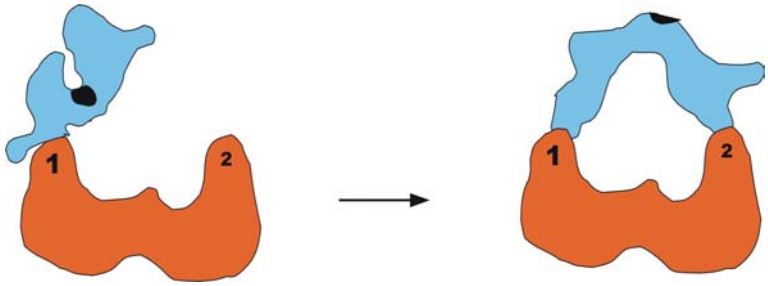

Figure 1.5 A model for 14-3-3 dependent conformational changes upon multi-site binding according to Yaffe, 2002. 14-3-3 binding relies initially upon interaction of a gatekeeper residue with one monomeric subunit (1). Binding of one or more weaker secondary sites (2) facilitates a ligand conformation that is not favourable in the unbound state, exposing one or more regions of the protein (shaded circle) that are inaccessible in a free or monomer bound state.

It seems that for more proteins, there is a single dominant site that functions according to Yaffe's hypothesis as a 'gatekeeper' (Yaffe, 2002). If this site is absent or not phosphorylated, then the secondary site is too weak to promote stable 14-3-3 interactions. In contrast, once the gatekeeper sites are phosphorylated, and bound to one monomer in dimers 14-3-3, the secondary site is able to interact with the other monomeric subunit by virtue of their high local concentration induced by its proximity (Figure 1.3) (Yaffe, 2002).

1.5 The specific aims

In the past few years, there is increasing number of evidence showing an important role of *h*Pin1 in regulation of transcription as well as cell cycle progression. In contrast to *h*Pin1, the cellular function of *h*Par14, a second human member of parvulin family remains unknown. Up to date, only little information concerning subcellular localization or putative interaction with pre-ribosomal protein complex of *h*Par14 has been published. The aims of this work based on the solution of *h*Par14 structure and similarities to HMG proteins are:

- To determine a cellular localization of *h*Par14 in human cells and estimate the amount of protein in nuclear and cytoplasmic compartments
- To determine possible interactions of *h*Par14 with DNA
- To study a possible posttranslational modification of *h*Par14
- To search for novel proteins interacting with *h*Par14

2 Materials and Methods

2.1 Materials

2.1.1 Apparatus

FLA-3000	Fuji-Film
FPLC	Amersham Pharmacia
Heraeus Biofuge Stratos, Centrifuges	Kendro (Honau)
LSM 510	Zeiss
pH-meter	Mettler Toledo GmbH
SLM Aminco French pressure	SLM Aminco
Sorvall RC5B Plus, Centrifuge	Kendro
Thermo-block	Bioblock Scientific
Trio-Thermocycler	Biometra

2.1.2 Chemicals

Acrylamid/Bisacrylamid 37:5:1	Roth, Karlsruhe, Germany
Acrylamid 30%	Roth, Karlsruhe, Germany
Agar	AppliChem, Darmstadt, Germany
Agarose	Serva, Heidelberg, Germany
Ammonium persulphate	Roth, Karlsruhe, Germany
Ampicilin	Roche, Mannheim, Germany
Boric Acid	Sigma, St Loius, MO, USA
Coomassie Brilliant Blue R G25	Serva, Heidelberg, Germany
Dimetylsulphoxide	Sigma, St Loius, MO, USA
EDTA	Serva, Heidelberg, Germany
EGTA	Serva, Heidelberg, Germany
β-Mercaptoethanol	Sigma, St Loius, MO, USA
Paraformaldehyde	Sigma, St Loius, MO, USA
Sodium fluoride	Serva, Heidelberg, Germany
TEMED	Merck, Darmstadt, Germany
Tris	AppliChem, Darmstadt, Germany
Trypsin	Biochrom KG, Berlin, Germany
Tween-20	Sigma, St Loius, MO, USA
Triton X-100	Serva, Heidelberg, Germany

2.1.3 Standards and kits

ECL Western Blotting Reagents	Amersham Pharmacia, Uppsala, Sweden
Coomassie Protein Assay kit	Pierce, Illinois, USA
Qiagen Plasmid Mini Kit	Qiagen, Hilden The Netherlands
Qiagen Plasmid Midi Kit	Qiagen, Hilden, The Netherlands
QIAquick Gel Extraction Kit	Qiagen, Hilden, The Netherlands
QIAquick PCR Extraction Kit	Qiagen, Hilden, The Netherlands
QIAquick Nucleotide Extraction Kit	Qiagen, Hilden, The Netherlands
Qiuck Change Mutagenesis Kit	Stratagene, Amsterdam, The Netherlands
1kb-10kb DNA Marker	New England Biolabs, Beverly, USA
Perfectly Blue Cloning Kit	Novagen, Madison, WI, USA
SeeBlue Plus2 Pre-stained Protein Marker	Invitrogen, Groningen, The Netherlands
TNT Quick Coupled transcription/translation	Promega, Madison, WI, USA

2.1.4 Buffers

1xPBS
8 g/l NaCl, 0.2 g/l KCl, 1.15 g/l Na_2HPO_4, 0.2 g/l KH_2PO_4, pH 7.4

50xTAE

2 M-Tris, 1 M Acidic acid, 100 mM EDTA, pH 8.1

Tris buffer (separating SDS gel)

0.5 M Tris/HCl, pH 6.8

Tris buffer (running SDS gel)

1.5 M Tris/HCl, pH 8.8

Running buffer for SDS-PAGE

50 mM Tris, 380 mM Glycine, 0.1% (w/v) SDS, pH 8.3

Transfer Buffer for Western Blot

SDS-PAGE running buffer plus ¼ volume Methanol

TBT buffer

10 mM Tirs + 150 mM NaCl + 5 % (v/v) Tween-20, pH 7.5

Sample buffer for agarose gels

10 mM Tris, 1 mM EDTA, 50 % (w/v) Glycerol, 0.05 % (w/v) Bromophenol-blue, pH 7.2

10x TBE buffer/EMSA

70 mM Tris, 90 mM boric acid, 1 mM EDTA, pH 7.8

2.1.5 Media for bacterial culture

LB, Luria Broth

10 g/l NaCl, 10 g/l Bacto-Trypton, 5 g/l Yeast extract, pH 7.5

LB-Amp

LB-medium supplemented with Ampicilin (50-100 μg/ml)

LB-Kan

LB-medium supplemented with Kanamycin (10 μg/ml)

2.1.6 Media for eukaryotic cell culture

DMEM medium

DMEM (Dulbecco's Modified Eagle's Medium, Biochrom KG, Berlin), 10 % (v/v) Fetal Bovine Serum, 1 % (v/v) Glutamine

RPMI medium

RPMI 1640 medium (Gibco), 10 % (v/v) Fetal Bovine Serum, 1 % (v/v) Glutamine

Medium for freezing cells

DMEM (Dulbecco's Modified Eagle's Medium, Biochrom, KG, Berlin), 20 % (v/v) Fetal Bovine Serum, 10 % (v/v) DMSO (Sigma)

2.1.7 Bacteria strains

Table 2.1 The bacteria strains of *Escherichia coli* used in this work.

Strain	Reference	Description
XL1 blue	STRATAGENE	Cells used for plasmid propagation and purification
BL21-CodonPlus(DE3)-RP	STRATAGENE	Encodes T7 RNA polymerase under control of the *lacUV5* promoter for easy protein
BL21-CodonPlus(DE3)- RIL	STRATAGENE	Encodes T7 RNA polymerase under control of the *lacUV5* promoter for easy protein
DH5α	STRATAGENE	Cells used for expression of recombinant protein

2.1.8 Human cell lines

Table 2.2 The human cell lines used in this work.

Name	Reference	Description
HeLa	German Collection of Microorganisms Cell Culture, Braunschweig, Germany	Adenocarcinoma; cervix
HEK293	German Collection of Microorganisms Cell Culture, Braunschweig, Germany	Human embryonic kidney
Jurkat	German Collection of Microorganisms Cell Culture, Braunschweig, Germany	T lymphocyte

2.1.9 Plasmids

Table 2.3 The expression plasmids used in this work.

Plasmid	Reference	Description
pEGFP-N1	Clontech	Eukaryotic GFP expression vector
pcDNA4/HisMax C	Invitrogen	Eukaryotic His tagged expression vector
pQE70/His-*h*Par14	Dr. E Bayer (MPI Dortmund)	Prokaryotic expression vector with C-terminal 6xHis
pcDNA3/HA-14-3-3γ	Dr M. Yaffe (MIT, USA)	Eukaryotic 14-3-3γ expression vector
pcDNA3/HA-14-3-3ξ	Dr M. Yaffe (MIT, USA)	Eukaryotic 14-3-3ξ expression vector
pcDNA3/HA-14-3-3θ	Dr M. Yaffe (MIT, USA)	Eukaryotic 14-3-3θ expression vector
pcDNA3/HA-Lys49/Glu 14-3-3	Dr M. Yaffe (MIT, USA)	Eukaryotic 14-3-3 expression vector
pcDNAGS/His14-3-3	GeneStorm (Invitrogene)	Eukaryotic 14-3-3 expression vector
pET/14-3-3 Lys49/Glu	Dr H. Fu (Emory University, USA)	Prokaryotic 14-3-3 expression vector

GST-14-3-3	Dr A.J. Muslin	Prokaryotic 14-3-3 expression vector
GST-*h*Par14	Dr J-U. Rahfeld	Prokaryotic 14-3-3 expression vector
HA-CK2α	Dr D. Litchfield (University of Western Ontario, CA)	Eukaryotic CK2α expression vector
FLAG-CK2β	Dr P. Yew (University of Texas, USA)	Eukaryotic CK2β expression vector

2.1.10 Oligonucleotides

All oligonucleotides used in this work were purchased from MWG Biotech (Germany).

Table 2.4 Oligonucleotides used in this work

Name	Sequence (5' → 3')	Orientation
ΔN6*h*Par14$_{(6-131)}$ -GFP	GAAGATCTGCCACCATGAGTGGTTCTGGAAAAGCGGGG	sense
ΔN14*h*Par1$_{(14-131)}$4-GFP	GAAGATCTGCCACCATGGGGGGAGCAGCCTCTGGGAGT	sense
Reverse-GFP	CGTGGATCCTTTTCTTCCTTCGACCATAATAAT	antisens
His-*h*Par14	ACGGGATCCGCCACCATGCCGCCCAAAGGAAAA	sense
His-*h*Par14	TGGAATTCTTATTTTCTTCCTTCGACCAT	antisens
Ser19/Ala *h*Par14	GGAGCAGCCGCTGGGAGTGAC	sense
Ser19/Ala *h*Par14	GTCACTCCCAGCGGCTGCTCC	antisens
Ser19/Glu *h*Par14	GGAGCAGCCGAAGGGAGTGAC	sense
Ser19/Glu *h*Par14	GTCACTCCCTTCGGCTGCTCC	antisense
Ser7/Ala *h*Par14	CCGCCCAAAGGAAAAGGTGGTTCTGGAAAAGCGGGG	sense
Ser7/Ala *h*Par14	CCCCGCTTTTCCAGAACCACCTTTTCCTTTGGGCGG	antisense
Ser9/Ala *h*Par14	GGAAAAAGTGGTGCTGGAAAAGCGGGGAAAGGG	sense
Ser9/Ala *h*Par14	CCCTTTCCCCGCTTTTCCAGCACCACTTTTTCC	antisense
Ser7,Ser9/Ala *h*Par14	CCCAAAGGAAAAGCTGGTGCTGGAAAAGCGGGGAAAGGG	sense
Ser7,Ser9/Ala *h*Par14	CCCTTTCCCCGCTTTTCCAGCACCAGCTTTTCCTTTGGG	antisense
EMSA	GTAAAAAATGTTTTCATTTTTTAC	

2.1.11 Antibodies

Table 2.5 Antibodies used for Western blotting.

Antigen	Clone	Reference
14-3-3β	C-20	Santa Cruz Biotechnology, Santa Cruz, CA, USA
14-3-3β	H-8	Santa Cruz Biotechnology, Santa Cruz, CA, USA
14-3-3θ	C-17	Santa Cruz Biotechnology, Santa Cruz, CA, USA

14-3-3γ	C-16	Santa Cruz Biotechnology, Santa Cruz, CA, USA
14-3-3ε	T-16	Santa Cruz Biotechnology, Santa Cruz, CA, USA
14-3-3ζ	C-16	Santa Cruz Biotechnology, Santa Cruz, CA, USA
CK2α	C-18	Santa Cruz Biotechnology, Santa Cruz, CA, USA
CK2β	N-20	Santa Cruz Biotechnology, Santa Cruz, CA, USA
c-Myc	9E10	Santa Cruz Biotechnology, Santa Cruz, CA, USA
FLAG-FITC	F 4049	Sigma, St. Louis, MO, USA
GFP	A-6455	Molecular Probes, Eugene, Oregon, USA
HA	Y-11	Santa Cruz Biotechnology, Santa Cruz, CA, USA
His	Penta-His	Qiagen, Heilden, The Netherlands
*h*Par14	-	Pub Production, Herbertshausen, Germany
*h*Pin1	-	Pub Production, Herbertshausen, Germany
α-tubulin	T 5168	Sigma, St Louis, MO, USA

The following secondary antibodies were used: rabbit anti-mouse IgG, mouse anti-rabbit IgG were obtained from Dianova; goat anti-rabbit FITC-coupled IgG, goat anti-mouse TRITC-coupled IgG and goat anti-mouse FITC-coupled IgG were obtained from Molecular Probes.

2.2 Molecular Biology Methods

All procedure of molecular cloning were performed according to standard protocols (Sambrook, et al., 1989). Composition of solution and protocols used during the presented project are provided below only if they differ from available in the references or manufacturer's instructions. Clones were sequenced with Perkin-Elmer ABI 310 automatic sequences.

2.2.1 Competent cells

The competent cells were prepared using calcium chloride method. A single colony of bacterial strain XL1 blue was picked, and inoculated to a starter culture in 5 ml of LB medium without antibiotics. The pre-culture was incubated overnight at 37°C with vigorous shaking at 220 rpm. Next day, the culture was transferred into 50 ml of fresh LB medium and further incubated until cells reached A_{600} equal to 0.6. The cells were centrifuged at 5000 rpm for 15 min. and resuspended in 25 ml of ice cold, sterile 0.1 mM $CaCl_2$ and incubated for 30 min on ice. After second centrifugation for 5 min. at 5000 rpm, cells were resuspended with 5 ml of 0.1 mM $CaCl_2$ supplemented with 30% glycerol, 200 µl samples were aliquot and frozen at –80°C.

2.2.2 Transformation into competent cells

Around 0.2-0.5 μg of plasmid DNA was transferred into 200 μl of competent cells and incubated on ice for 30 min. After that time, the heat shock was performed as followed: 42°C for 1 min. and 2 min. on ice and next 1 ml of LB medium without antibiotics was added. Cells were incubated for 1 hour at 37°C. 100 μl of cell suspension was plated on the LB agar supplemented with required antibiotic and incubated for 17 h. XL1 blue cells were used for cloning purpose and plasmid purification experiments.

2.2.3 Purification and identification of recombinant DNA

The *E. coli* XL1 blue cells transformed with required DNA constructs were used to isolate plasmid-DNA. The DNA preparation for cloning, sequencing and transfection was performed with the following kits: Qiafilter Mini Prep and Qiafilter Midi Prep, according to Qiagen manufacturer's instruction. The concentration and purity of preparation was confirmed on the 0.5-1 % agarose gel supplemented with ethidium bromide (0.5 μg/ml).

2.2.4 Polymerase chain reaction (PCR)

Depending on the purpose the PCR reaction was performed with Taq (Roche) or Pfu DNA polymerase (Stratagene, LaJolla USA). The reaction was carried out in a volume of 100 μl, containing 0.2 mM dNTP mix (dATP, dTTP, dCTP, dGTP), 100 pmol of each primer, 100-200 ng of DNA template, 10 μl of 10x concentrated buffer and 2.5 U of DNA polymerase. The 30 cycles of PCR reaction were performed as followed:

denaturation	5 min	95°C	
denaturation	30 sec	95°C	30 cycles
annealing	30 sec	58°C	
synthesis	2 min/kb	72°C	
end-synthesis	10 min	72°C	

The yield of PCR product and correct size was checked by electrophoresis. The 1/10 volume of PCR product was separated on 1 % agarose supplemented with ethidium bromide (0.5 μg/ml) and electrophoresis for 1h, 80 V. The bands were visualized under UV light.

2.2.5 Plasmid construction

To obtain an amino-terminal His tagged *h*Par14 (in the text abbreviated as His-*h*Par14), the full gene was amplified by PCR with the primers listed in table 2-4. The PCR product was sub-cloned into vector pSTBlue-1 by using cloning kit (Novagen) and digested with BamHI/EcoRI enzymes and the DNA fragment was cloned into mammalian expression vector pcDNA-4C

His/Max (Scheme 2.1). To construct the GFP fusion *h*Par14 and its truncated forms, the full length of *h*Par14$_{(1-131)}$ and the amino-terminal truncated mutants ΔN6*h*Par14$_{(6-131)}$ and ΔN14*h*Par14$_{(14-131)}$ were obtained by PCR amplification with primers listed in table 4-2. The PCR product was sub-cloned into pSTBlue-1 vector and digested with restriction enzymes BglII /BamHI, and the DNA fragment was cloned into the pEGFP-N1 vector (Scheme 2.2).

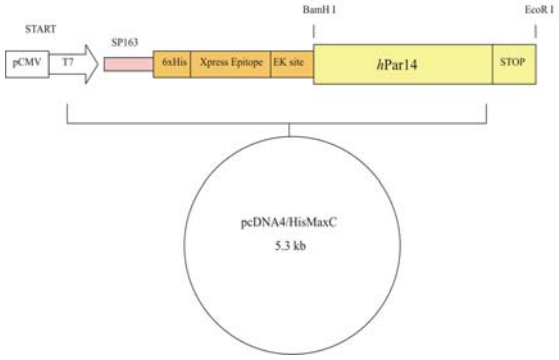

Scheme 2.1 Schematic representation of the *h*Par14 in pcDNA-4C

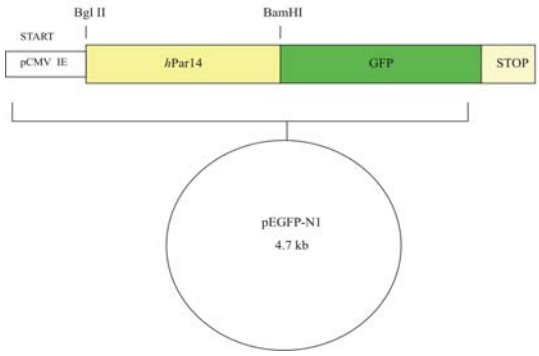

Scheme 2.2 Schematic representation of the *h*Par14 in GFP fusion vector.

The correct position of genes was confirmed by DNA sequencing. The integrity and expression level of the fusion proteins was assessed by Western blot analysis from transfected cells using a polyclonal rabbit antibody against GFP and anti-*h*Par14 rabbit serum.

2.2.6 Mutagenesis

The point mutations in expression plasmid encoding His-*h*Par14 were generated by site-directed mutagenesis using primers listed in Table 2-4 and the Quick Change site-directed mutagenesis kit as described in Stratagene manufacturer's instruction. The position of mutations was confirmed by DNA sequencing.

2.3 Recombinant Protein Methods

2.3.1 Expression and purification of C-terminal His tagged *h*Par14 and its mutants

To obtained carboxy-terminal His tagged recombinant *h*Par14-His/pQE70, Ser19/Ala *h*Par14-His/pQE70, Ser7,Ser9/Ala *h*Par14-His/pQE70, the *E. coli* BL21-CodonPlus(DE3)-RIL was transformed with DNA constructs. The single colony was picked from a freshly streaked selective plate, inoculated in a starter culture 100 ml LB supplemented with 100 μg/ml ampicillin and incubated overnight at 37°C. The pre-culture was transferred to a 6 L of LB medium (100 μg/ml ampicillin, 5 mg/ml tetracycline and 30 μg/ml chloramphenicol) and further incubated until the A_{600} was equal to 0.5. The protein expression was induced by adding isopropyl-β-D-thiogalactoside (IPTG), to a final concentration of 1 mM and incubated for 4-6 h. After that time, cells were harvested by centrifugation at 4°C for 15 min at 5000 rpm. The bacterial pellet from a 6x1 L culture was resuspended in 200 ml of lysis buffer (50 mM Tris pH 8.8, 200 mM NaCl, 0.5 mM PMSF, 0.1% Tween-20, 0.2 % NP-40, 1 mM β-mercaptoethanol, 10% glycerol), French pressed on SLM Aminco (French pressure cells). The obtained supernatant was centrifuged for 30 min at 17000 rpm and next applied to a Ni-NTA column (2.5 x 15 cm) equilibrated with 50 mM Tris-HCl buffer pH 8.8. The column was washed with 1L of washing buffer (50 mM Tris pH 7.8, 1 M NaCl, 0.1 % Tween-20, 25 mM imidazole, 0.5 mM PMSF) and proteins were eluted with 200 ml elution buffer (50 mM Tris pH 7.5, 250 mM imidazole, 0.5 mM PMSF). Fractions of 8 ml were collected and protein purity was analysed on 15 % SDS-PAGE stained with Coomassie Blue. Proteins were dialyzed against buffer 50 mM Tris pH 8.0, 150 mM NaCl and concentrated by using Centricon tubes.

2.3.2 Expression and purification of His tagged 14-3-3 and its mutant

Expression of recombinant His-14-3-3 wild type and His-Lys49/Glu 14-3-3 was performed in *E. coli* BL21-CodonPlus(DE3)-RP. The purification of His-tagged 14-3-3 proteins was performed according to the protocol described for His-tagged *h*Par14 in section 2.3.1.

2.3.3 Expression and purification of GST proteins

Plasmid encoding GST fusion 14-3-3 was kindly provided by Dr. J Muslin and GST-*h*Par14 provided by Dr. J. Rahfeld. GST-14-3-3 and GST-*h*Par14 proteins were expressed in DH5α or BL21-CodonPlus(DE3)-RIL bacteria grown in LB medium supplemented with 100 μg/ml ampicillin at 37°C. After cultures reached an absorbance of greater then 0.4 at 600 nm, IPTG was added to a final concentration of 0.1 mM. After 4h of incubation, cells were pelleted,

washed with PBS, and then resuspended in PBS containing 1.5 μg/ml aprotinin, 10 μg/ml leupeptin, 1mM DTT and 100 μM phenylmethylsulfonyl fluoride (PMSF). Triton X-100 was added to bacterial suspension to a final concentration of 1 %, and the solution was incubated with continual mixing for 30 min. at 4°C. Cells were lysed using a French press. Cell debris were pelleted by centrifugation for 30 min. at 17000 rpm. The supernatant was applied to GSH column (2 x 10 cm) packed with glutathione immobilized on agarose beads (Amersham Pharmacia). After extensive washing with PBS, the proteins were eluted using free glutathione (10 mM reduced glutathione, 50 mM Tris-HCl, pH 8.0, 1 mM DTT). Eluted protein was dialyzed against 50 mM Tris-HCl, pH 8.0, 150 mM NaCl, without DTT and subjected to gel filtration.

2.3.4 Determination of protein concentration

The total cellular protein concentration was determined using the Coomassie Blue Protein Assay. The assay method is based on the absorbance shift from 465 to 595 nm that occurs when dye Coomassie brilliant blue G-250 binds to proteins in an acidic solution. Upon addition of sample, the dye will bind protein, resulting in a colour change from greenish brown to blue. In our experiment, 10-20 μl of the protein solution was mixed with 1 ml of Coomassie Blue reagent (Pierce) and the absorbance at 595 nm was measured. The protein concentration was calculated using a standard curve prepared for bovine serum albumin.

The concentration of purified, recombinant proteins was estimated using spectrophotometry method. The calculation of concentration was done using Beer-Lambert law

$$A = \varepsilon \times c \times d$$

where ε is extinction coefficiency in $M^{-1} \times cm^{-1}$; c is concentration in M; d is cuvette in cm. The extinction coefficiency of His-*h*Par14 is 8290 (M^{-1} cm^{-1}) and His-14-3-3 is 25580 (M^{-1} cm^{-1}). The concentration was measured with wavelength from 240 nm to 320 nm.

2.4 Electromobility shift assay (EMSA)

The shift assay was performed with a 24-mer oligonucleotide (5'-GTAAAAAATGTT TTCATTTTTTAC-3') selected and optimised by fluorescence titration experiments (Surmacz et al., 2002). An aliquot (50 pmol) of the single stranded oligonucleotides were 5' end-labelled with [γ^{32}P] ATP (ICN Pharmaceuticals, Inc.) and T_4 polynucleotide kinase (Promega) and purified using QIAquick nucleotide removal kit. 50 pmol of labelled oligonucleotide were annealed (94°C, 5 min; 58°C, 5 min) in 100 μl of TE buffer and then slowly cooled. The 5' and

3' ends of oligonucleotide are complementary and formed double-stranded DNA. DNA - protein binding reaction was performed using 0.5 μg or 1 μg of *h*Par14 or *h*Par14 phosphorylated with CK2, incubated with 4 μl of the radiolabelled probe (2 pmol, 50.000-80.000 cpm) in 40 μl of 1x binding buffer (10 mM Hepes pH 7.5, 40 mM NaCl, 10 % glycerol and 0.1 mM EDTA) for 1 hour at 12°C. In a competition experiment, the same amount of unlabelled specific or nonspecific oligonucleotides were incubated for 30 min. prior adding the specific radioactive probe. The reaction was incubated for the next 30 min. The labelled probe was separated from DNA-protein complexes by electrophoresis on 6 % nondenaturing polyacrylamide gels in 0.5 x Tris-borate/EDTA buffer pH 7.8 at 12°C. Autoradiography was carried out by exposure of the gel to intensifying screen (FujiFilm) for 14 h at room temperature.

2.5 Cell Biology Methods

2.5.1 Eukaryotic cell culture

The eukaryotic cells HeLa and HEK293 were maintained in Dulbecco's modified Eagle's medium (DMEM) supplemented with 10 % fetal bovine serum (FBS), supplemented with glutamine. Jurkat cells were cultured in RPMI-1640 medium also supplemented with 10 % FBS and glutamine. Cells were incubated at 37°C in a 5 % CO_2 atmosphere. The passage was performed when cells reached confluence of 70-80 %.

2.5.2 Transient transfection

HeLa cells were grown in 6-well plates or 10 cm plates until they reached confluence of 80-90%. At that time, cells were transfected with 1 μg or 5 μg of following plasmids: His-*h*Par14 vector His-Ser19/Ala-*h*Par14, His-Ser19/Glu-*h*Par14, His-Ser7,Ser9/Ala-*h*Par14, HA-14-3-3 (ζ,θ,γ), HA-Lys49/Glu-14-3-3, HA-CK2α, FLAG-CK2β; using 8-15 μl of Lipofectamine 2000 according to manufacturer's instruction. After 30 h incubation, cells were lysed and extract subjected to immunoprecipitation or resolved on 15 % SDS-PAGE, transferred to nitrocellulose and immunoblotted with antibody against proteins.

2.5.3 Cell fractionation and Western blotting

Cell fractionation was done according to Schreiber et al., 1989 with some modifications. Briefly, $1x10^6$ HeLa cells were washed in cold PBS and collected by centrifugation and resuspended in 400 μl ice cold hypotonic buffer (10 mM Hepes pH 7.5, 10 mM KCl, 2 mM $MgCl_2$, 0.1 mM EDTA, 0.1 mM EGTA, 10 mM NaF, 1 mM DTT, 0.1 mM Na_3VO_4, 1 μM ocadaic acid, 1 x Pharmingen-Protease-Inhibitor Cocktail). The cells were allowed to swell on ice for 15 min,

then 25 µl of a 10% NP-40 was added and immediately cells were vigorously vortex 2 x10 sec. The cytoplasmic fraction was obtained as a supernatant after centrifugation at 13000 rpm for 30 sec. The pellet was washed in hypotonic buffer and proteins extracted with hypertonic buffer (25 mM Hepes pH 7.5, 0.5 mM NaCl, 5 mM $MgCl_2$, 1 mM EDTA, 10 mM NaF, 10% glycerol, 0.5 % NP-40, 0.1 mM Na_3VO_4, 1µM ocadaic acid, 1 x Pharmingen-Protease-Inhibitor Cocktail), yielding nuclear fraction. The total protein concentration was estimated using Coomassie Protein Assay Reagent Kit. The purity of fraction preparation was analysed by Western Blotting using antibody against two markers protein c-myc (nuclear fraction) and tubulin (cytoplasmic faction). To detect endogenous *h*Par14, equal amount of total cellular proteins were resolved on 15 % SDS-PAGE and transferred to nitrocellulose. Blots were blocked in TBS/5 % milk and incubated with rabbit-*h*Par14 antibodies (1:2000) overnight. After washing, blots were incubated with HRP-conjugated goat anti-rabbit antibody (2 h, 22°C), washed and visualized using enhanced chemiluminescence ECL reagent (Amersham Pharmacia Biotech). Antibodies to *h*Par14 were obtained by immunizing rabbits with 500 µg of highly purified recombinant protein, done by PAB productions, Herbertshausen, Germany.

2.5.4 Labelling *in vivo*

Thirty hours after transfection with wild type (WT) His-*h*Par14 and His-Ser19/Ala *h*Par14, HeLa cells were labelled with [^{32}P] orthophosphate in a phosphate free DMEM medium. Cells were pre-incubated with 3 ml of phosphate free medium containing dialyzed 10 % (v/v) FCS for 3 h at 37°C. The medium was then replaced with the same volume of DMEM phosphate free medium, containing 2 mCi of [^{32}P] orthophosphate. After 6 h of labelling, the cells were washed twice with 6 ml of ice-cold PBS and lysed for 30 min in 1 ml of cold lysis buffer (50 mM Tris pH 7.5, 150 mM NaCl, 2 mM EGTA, 50 mM NaF, 10 mM EDTA, 10 mM Na_3VO_4, 1 µM ocadaic acid, 1 mM DTT, 1 % Triton X-100, 10 % glycerol and 1 x Protease Inhibitor Cocktail). The extracts were cleared by centrifugation at 13000 rpm for 15 min. His tagged proteins were precipitated using Ni-NTA agarose beads for 1 h at 4°C. The Ni-NTA beads were washed three times with 1ml of ice-cold lyses buffer (supplemented with 10 mom imidazole) and proteins eluted with buffer 50mM Tris-HCl pH 7.5, 100 mM imidazole. The eluted proteins were precipitated with TCA and subjected to 12 % SDS-PAGE, transferred to nitrocellulose and detected by autoradiography. The same membrane was subjected to Western analysis with anti-*h*Par14 serum. Followed the incubation with secondary antibody, the proteins were visualized by chemiluminescence using ECL reagent.

2.5.6 Co-immunoprecipitation

Co-immunoprecipitation assay was performed using whole cell extract obtained from HeLa cells co-transfected with His-*h*Par14/HA-CK2α, His-*h*Par14/FLAG-CK2β, His-*h*Par14/HA 14-3-3γ, His-*h*Par14/HA 14-3-3θ, His-*h*Par14/HA 14-3-3ζ or His-*h*Par14/V5 14-3-3(ζ/δ). Cells were homogenized in lyses buffer (10 mM Hepes pH 7.5, 130 mM NaCl, 10 mM KCl, 1 mM EDTA, 1 mM EGTA, 10 mM NaF, 0.5 % NP-40, 5 % glycerol, 10 mM Na_3VO_4, 1 μM ocadaic acid, 1 mM DTT, 1x Protease Inhibitor Cocktail). The total amount of cellular proteins was estimated using Coomassie Protein Assay Reagent Kit. Equal amounts of proteins were subjected to immunoprecipitation using anti-HA (10μg), anti-CK2β or anti-V5 antibodies and incubated for 2-3 h at 4°C on the over-end-shaker. As a control, the same amount of proteins was precipitated using mouse or rabbit control IgG. The immuno-complexes were bound to protein A/G sepharose (Oncogene) for 2 h at 4°C on the over-end-shaker, washed three times with buffer A (50 mM Tris pH 7.5, 150 mM NaCl, 1 mM EDTA, 1 % NP-40, 5 % glycerol) and incubated with 2 x NuPAGE LDS sample buffer (Invitrogen) for 10 min at 37°C. Eluted proteins were analysed by 4-12% BT SDS-PAGE (Invitrogen) in 1x MES running buffer (pH 7.3) (0.05 M 2-(N-morpholino) ethane sulfonic acid, 0.05 M Tris 3.465 mM SDS and 1.025 mM EDTA). Proteins were transferred onto nitrocellulose and immunoblotted with either anti-CK2α, anti-*h*Par14, anti-His or anti-14-3-3 antibodies. Detection was done with HRP-labelled anti-rabbit or anti-goat secondary antibody and enhanced chemiluminescence using ECL reagent.

2.5.7 The principle of GST pull-down assay

The assay is an *in vitro* technique that consists of a GST (from *Schistosoma japonicum*) tagged bait protein (the protein of interest) that can be used to identify putative binding partner(s) (the prey). The bait protein, purified from an appropriate expression system (e.g., *Escherichia coli*), is immobilized on a glutathione affinity gel. The bait serves as the secondary affinity support for identifying new protein partners or for confirming a previously suspected protein partner to the bait. Prey protein can be obtained from multiple sources including recombinant purified proteins, cell lysate or *in vitro* transcription/translation reactions. Protein-protein interactions can be visualized by SDS-PAGE and associated detection methods depending on the sensitivity requirements of the interacting proteins. These methods include Coomassie or silver staining, Western blotting and [^{35}S] radioisotopic detection.

2.5.8 GST pull down assay with HEK293 cell extract

HEK293 extract was prepared with lyses buffer. Cells were sonicated 3 x 10 s and centrifuged at 13000 rpm for 15 min at 4°C. The protein extract obtained from cells was incubated with 5 μg of recombinant glutathione *S*-transferase (GST) *h*Par14 fusion protein or GST alone for 6 h at 4°C on the over-end-shaker. Next 20 μl of glutathione sepharose beads were added and further incubated for 2 h at 4°C on the over-end-shaker. After extensive washes, protein sample buffer was added to retained fractions, boiled, and then analysed by 15 % SDS-PAGE and immunoblotting with anti-14-3-3 antibody. Proteins were visualized by enhanced chemiluminescence.

2.5.9 GST pull down with *in vitro* translated *h*Par14

In vitro pull-down assays were carried out by incubating GST fusion 14-3-3 with ^{35}S-labelled *h*Par14 or its mutant. ^{35}S-labelled proteins were generated using T7-coupled *in vitro* transcription/translation kit. The proteins were incubated in binding buffer (50 mM Tris-HCl pH 7.5, 150 mM NaCl, 1% NP-40, 1 mM EDTA, 5 % glycerol, 1 μM ocadaic acid, 1 mM DTT, 5 % glycerol and 1x Protease Inhibitor Cocktail) for 1 h at 4°C on the over-end-shaker. Next 20-30 μl of GSH beads were added and further incubated for 1 h at 4°C. After extensive wash, protein sample buffer was added to retained fractions, boiled, separated on 15 % SDS-PAGE and transferred to nitrocellulose membrane. Bound proteins were visualized by autoradiography.

2.5.10 DNA cellulose binding assay

The assay was carried out as described by MacCallum and Hall, 2000 with some modification. In principle, 50 μl of HEK 293 nuclear extract was diluted with 250 μl of dilution buffer to give a final concentration of 10 mM Tris-HCl pH 7.5, 150 mM NaCl, 10 % glycerol, 1 mM EDTA, 10 mM NaF, 1 mM DTT, 100 μg/μl bovine serum albumin (BSA), 0.5 % NP-40, protease inhibitors. 100μl of native double stranded DNA cellulose (50 % slurry) (Amersham Pharmacia Biotech Inc.) was pre-incubated for 30 min. at 4°C with DNA binding buffer (20 mM Tris-HCl pH 7.5, 100 mM KCl, 10 % glycerol, 1 mM EDTA, 10 mM NaF, 100 μg/ml BSA, 0.5 % NP-40) and protease inhibitors. After centrifugation the supernatant was removed and incubated with diluted nuclear extract for 1 h at 4ºC. The DNA cellulose-protein complexes were washed four times in 1 ml of washing buffer (20 mM Tris pH 7.5, 1 mM EDTA, 10 % glycerol, 100 μg/ml BSA, 0.5 % NP-40) and eluted with increasing concentration of NaCl. Eluted proteins were

precipitated with TCA, analysed by 15 % SDS-PAGE and immunoblotted with anti-*h*Par14 antibody. The similar procedure was applied for GST-pull down with recombinant *h*Par14.

2.6 Assays for posttranslational protein modification

2.6.1 Recombinant kinase assay

The recombinant kinase assays were performed with recombinant human CK1 (1000 U), CK2 (500 U), PKA (2500 U), PKB and PKC (2000 U) (all enzymes from New England Biolabs) incubated with 3 μg of recombinant *h*Par14-His in the presence of 200 μM [γ-^{32}P] ATP (8 μCi/mmol) for 1 h at 30°C. The reaction was terminated by boiling samples in 4× Laemmli sample buffer, followed by separation on 17.5 % SDS-PAGE, Coomassie Blue staining and autoradiography with an intensifying screen (Fuji Film) for 14 h at room temperature. The phosphorylation was analysed by Fuji film FLA-3000. Signal was quantified using Advanced Image Data Analyzer AIDA 2.0 (Raytest Isotopenmessgerate GmbH).

2.6.2 Kinetic measurement

The activity test sample had a total volume of 4 μl and contained 1.7 μM of recombinant CK2. Further components of the reaction mixture were various concentration of *h*Par14 from 1.1 to 44 μM, CK2 buffer (20 mM Tris-HCl (pH 7.5), 50 mM KCl, 10 mM $MgCl_2$) and 200 μM [γ-^{32}P] ATP. After incubation for three different times at 30°C, the reaction was terminated by addition of 4×Laemmli sample buffer. Subsequently, samples were boiled for 3 min and subjected to a 17.5 % gel electrophoresis. To ensure initial kinetics phosphorylation was followed only 5 % toward completion. SDS-PAGE gels were submitted to autoradiography with an intensifying screen. Signals were quantified using a Fuji BAS reader.

Kinetic parameters K_M and V_{max} of phosphorylation were determined using 1.1 to 44.0 μM and were calculated by nonlinear regression analysis of the initial velocities.

2.6.3 Endogenous kinase assay

For endogenous kinase assays 50 μg of nuclear or cytosolic extracts obtained from HeLa cells were incubated with 0.5 or 3 μg of recombinant *h*Par14-His in the presence of 200 μM [γ-^{32}P] ATP for 1 h at 30°C. His tagged *h*Par14 was precipitated using Ni-NTA agarose beads, extensively washed and analysed by 15 % SDS-PAGE. Protein's phosphorylation was detected by autoradiography. For inhibition studies 300 μM of 5,6-dichloro-1-β-D-ribofuranosylbenzimidazole (DRB) (Sigma) or heparin (Sigma) (100 μg/ml) was added to the kinase reaction.

2.7 MALDI-TOF analysis

The molecular mass of the phosphorylated protein was determined by MALDI-TOF mass spectrometry on a Bruker REFLEX mass spectrometer, upgraded with a gridless delayed extraction ion source (Bruker-Daltonik, Bremen, Germany). Sinapinic acid was used as matrix. The non-tagged *h*Par14 (3-131 aa) was in vitro phosphorylated by CK2. The truncation of first two amino acids (Met and Pro) was identified after purification. The phosphorylated protein could not easily be separated from the unmodified *h*Par14, so the mixture of hPar14/phosphorylated hPar14 was digested with trypsin (Roche Diagnostics, Mannheim, Germany) in 50mM ammonium bicarbonate buffer at 37°C overnight. The resulting tryptic peptides were separated by HPLC (Shimadzu LC-10A, Kyoto, Japan) first on a Nucleosil 500-C3 PPN column (125 x 2 mm) and second on a Nucleosil 500-C18 PPN column (125 x 2 mm) (Machery-Nagel, Düren, Germany). The gradient of 1-40 % B (B: acetonitrile/ 0.08 % trifluoroacetic acid, A: 0.1 % aqueous trifluoroacetic acid) in 60 min at a flow rate of 0.2ml/min was used. The HPLC fractions were collected and the masses of each peptide determined by MALDI-TOF mass spectrometry. A saturated solution of α-cyano-4-hydroxycinnamic acid in acetone was used as matrix. The fraction with retention time 14.1 min in the second HPLC run (C18-column) contained the phosphorylated peptide. To determine the phosphorylated amino acid a MS/MS experiment was performed on an ESI-Q-TOF mass spectrometer (Micromass, Manchester, UK) equipped with a nanospray source. The determination of the peptide masses was also performed with nano-ESI-MS on the same instrument.

2.8 Microscopy techniques

2.8.1 Indirect immunofluorescence

HeLa cells grown on cover slips (20 mm x 20 mm) in 6-well plates were transfected at confluence of 80 % with 1 μg of wild type His-*h*Par14 or its mutants as well as HA-14-3-3 and its mutant using Lipofectamine 2000 according to manufacturer's suggestions. The transiently transfected cells were washed three times with PBS and fixed with 3 % paraformaldehyde (PA) in PBS for 10 min. Following three times washing with PBS, cells were permeabilized in 0.25 % Triton X-100 (PBS) for 5 min. and blocked for 2 h with filtered 5 % skim milk in PBS. Next, cells were incubated with anti-His (1:30), anti-HA (1:40) and FLAG M2 coupled to FITC antibody (1:40) in the presence of 10 % normal goat serum overnight at 4°C. After 3 times washing with PBS for 30 min., cells were incubated with fluorescein (FITC)-conjugated goat anti-mouse, fluorescein (FITC)-conjugated goat anti-rabbit IgG or tetramethyl rhodamine isocyanate phalloidin (TRITC)-conjugated goat anti-mouse IgG as the secondary antibody (1:200) for 2 h

at room temperature. Cells were washed three times with PBS for 30 min., slides mounted in Vectashield Mounting Medium (Vector, Burlingame, CA, USA) on a microscope glass and visualized using Laser Scanning Confocal 510 LSM microscope. The LSM microscope equipped with filters for fluorescein or rhodamine. Both 488 nm and 543 nm (krypton/argon) laser lines were used for excitations, and 505-530 nm -band-pass and 560 nm -long pass filters were used for emission. The cells were analysed using a Zeiss Plan-Apochromat (1.3 NA) x 40 objective or C-Apochromat W corr x 63 objective. Image processing was performed using the standard system operating software provided with the Zeiss 510 microscope (version 2.5). The nuclei were stained with propidium iodide (Molecular Probes).

2.8.2 Green fluorescence analysis

To perform the GFP fluorescence experiment, HeLa cells were grown on cover slips in 6-well plate in DMEM medium. The cells were transfected with 1 μg of a *h*Par14-GFP, ΔN6*h*Par14$_{(6-131)}$-GFP and ΔN14*h*Par14$_{(14-131)}$-GFP DNA construct using Lipofectin (LifeTechnologies, Inc) according to manufacturer's instruction. Twenty-four hours after transfection cells were fixed with 1.5 % PA in PBS for 15 min. at room temperature and mounted on a microscopy glass in Vectashield Mounting Medium. GFP images were analysed using a Zeiss C-Apochromat W Korr x 63 objective, with a 488 nm laser line for excitation and 505 nm long-pass filter for emission. Images were collected using a Zeiss LSM 510 laser-scanning microscope and analysed with standard system operating software provided with the Zeiss LSM 510 microscope.

3. Results

3.1 *h*Par14 is localized in the cytoplasm and the nucleus

Since *h*Par14 was discovered, there is no direct information about the subcellular localization of this protein in cells and its putative function. To gather information about the intracellular localization of endogenous *h*Par14, HeLa cells were fractionated according to the protocol described in Materials and Methods. The total cellular protein concentration was estimated using Coomassie Protein Assay. Equal amount of cytoplasmic and nuclear fractions were subjected to 15 % SDS-PAGE, transferred to nitrocellulose and immunoblotted with anti-*h*Par14 rabbit serum, anti-α tubulin (control for cytoplasmic preparation) and anti-c-myc (control for nuclear preparation) (Figure 3.1).

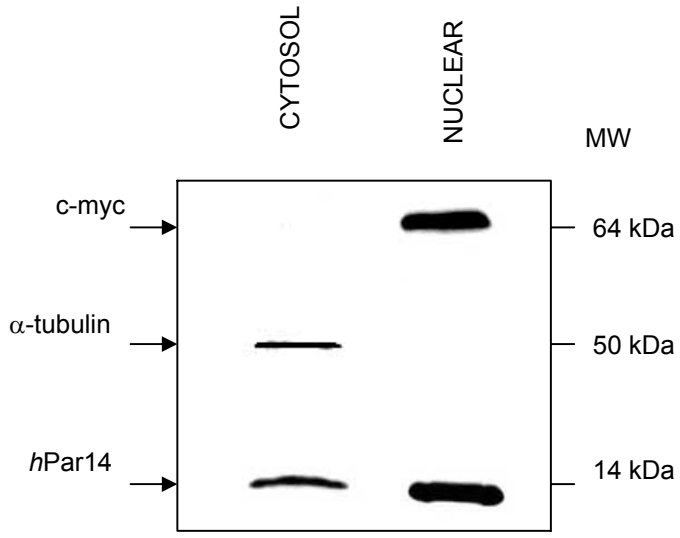

Figure 3.1 Localization of *h*Par14 in HeLa cells detected by Western blot. HeLa cells were fractionated and equal amount of cytosolic and nuclear fractions were separated by SDS-PAGE and analysed by Western blot using anti- c-myc (1:100), anti-α-tubulin (1:500) and anti-*h*Par14 rabbit serum (1:1000) antibodies.

The fractionation of the HeLa cells revealed that *h*Par14 is present in both cellular fractions: cytosolic and nuclear, with higher abundance in the nucleus as detected by Western blot analysis. This is in agreement with previous observations where a relatively high level of endogenous *h*Par14 was demonstrated in the nucleus compared to cytoplasm using electron microscopy (Thorpe, et al., 1999). To estimate the difference in amount of *h*Par14 between cytosolic and nuclear fractions, a densitometry analysis of the Western blot data was

performed (Figure 3.1), using Advanced Image Data Analyser AIDA 2.0. This analysis revealed that the amount of *h*Par14 is two-fold higher in the nucleus than in the cytoplasm (Figure 3.2).

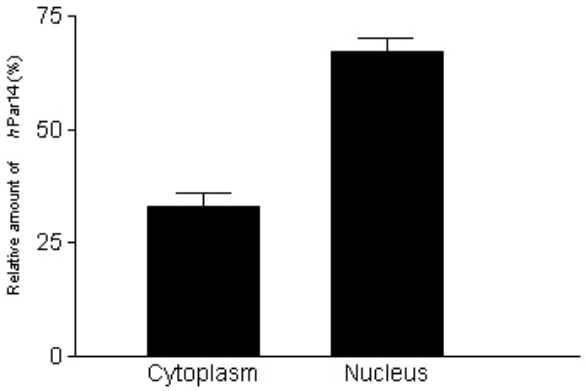

Figure 3.2 Relative amount of *h*Par14 in cytosolic and nuclear fraction obtained from HeLa cells. Black line indicates mean error.

To test whether the *in vivo* distribution of *h*Par14 is similar to that observed *in vitro*, a DNA construct encoding *h*Par14 fused on its carboxy terminus to the green fluorescent protein (GFP) of the jellyfish *Aequorea victoria* was developed and expressed in HeLa cells. Figure 3.3 shows fluorescence image of HeLa cells transfected with the *h*Par14-GFP construct and analysed by fluorescence microscopy. The most intensive green light emission comes from the nucleus but the protein is also detected in the cytoplasm.

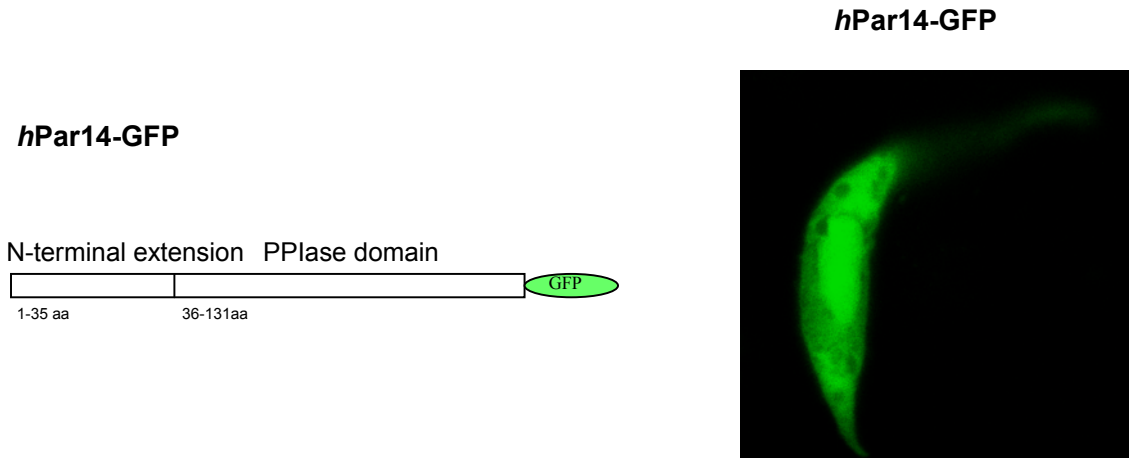

Figure 3.3 Fluorescence image of HeLa cells transfected with *h*Par14-GFP. *The right pa*nel, *h*Par14-GFP expressed in HeLa cells. Cells transfected with DNA construct encoding *h*Par14-GFP, were fixed

and analysed by fluorescence microscopy. GFP images were collected using confocal fluorescence microscope at 60x water immersion C Apochromat objective. The picture shows green fluorescence of transfected cells. Three independent experiments showed the same results. *The left panel*, scheme of *h*Par14 fused to GFP.

To eliminate potential artefacts that might result from expression of the recombinant protein, we examined the endogenous *h*Par14 protein using affinity purified anti-*h*Par14 serum. The immunofluorescence analysis confirmed nuclear localization of endogenous *h*Par14 (Figure 3.4) but low cytoplasmic staining of *h*Par14 is also detected. As an additional control, the localization of *h*Pin1 that is known to be an exclusive nuclear protein was tested. The localization pattern of *h*Pin1 is very similar to that of *h*Par14. The protein is mainly detected in the nucleus. Some cytoplasmic staining is also observed.

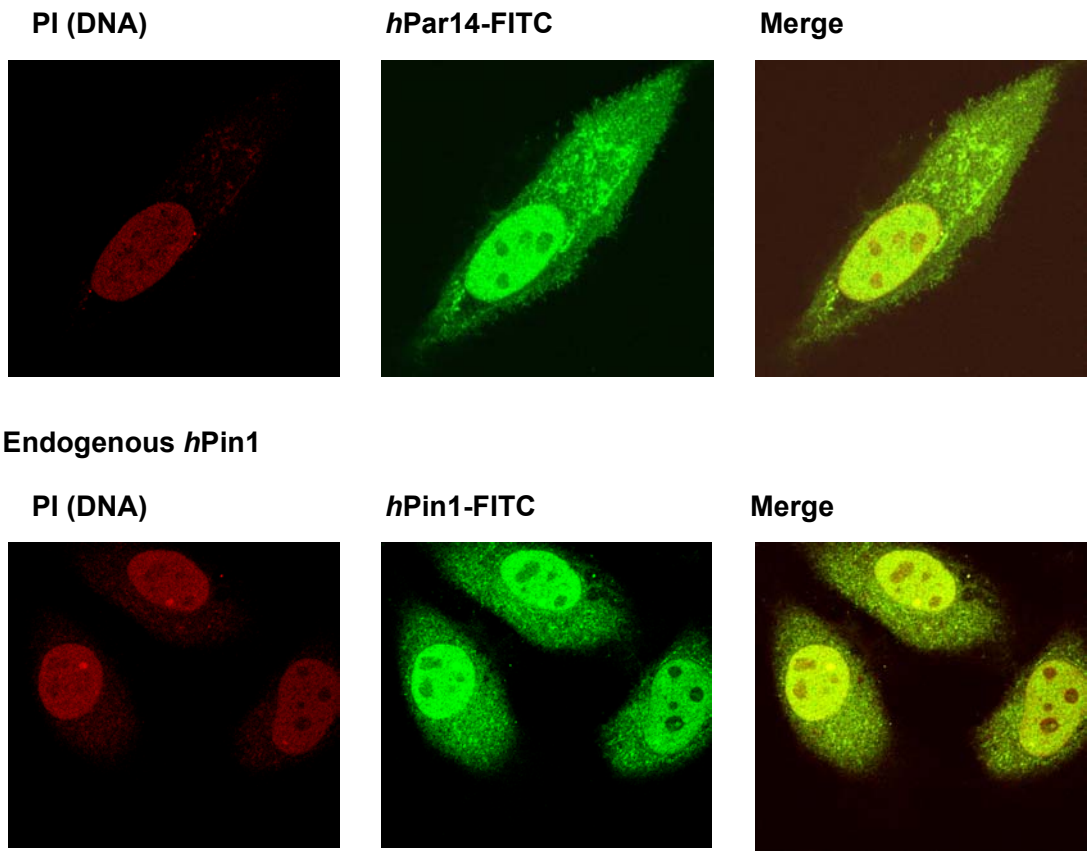

Figure 3.4 Immunofluorescence localization of endogenous *h*Par14 and endogenous *h*Pin1. HeLa cells were fixed, blocked, permeabilized and stained overnight with affinity purified anti-*h*Par14 or anti-*h*Pin1

serum. Followed staining with anti-rabbit secondary antibody coupled to FITC and propidium iodide (PI) in the presence of RNAse, cells were analysed using confocal fluorescence microscopy with objective C-Apochromat 63x/1.2 W corr.

3.1.1 The 14 amino acids of *h*Par14 N-terminal are necessary for nuclear localization

Shuttling of proteins between the cytoplasm and the nucleus can be achieved in two different ways. Relatively small proteins of molecular weight 14 kDa, e.g. parvulin, may be able to diffuse freely into the nucleus on a minute time scale (for review see Gama-Carvalho & Carmo-Fonseca, 2001). The influx occurs through the nuclear pore complexes, which are supramolecular assemblies, embedded in the nuclear envelope. Selective entry into the nucleus would require a specific nuclear localisation signal (NLS), which induces gating of the pore complex and rapid passage into the compartment. Such signals are either short basic stretches of up to eight amino acids or bipartite sequences consisting of two basic segments separated by about ten less-conserved amino acids. Many of these targeting sequences are found in the C- or N-termini of their corresponding molecules.

The unstructured N-terminal domain of *h*Par14 exhibits a basic stretch of residues. Rulten and co-workers suggested that the extension might target the protein to the nucleus (Rulten, et. al 1999). Therefore, a study on the influence of N-terminal truncation of *h*Par14 on its cellular localization was conducted. Figure 3.5 A shows fluorescence images of HeLa cells transfected with *h*Par14-GFP constructs, wherein the first six ΔN6*h*Par14$_{(6\text{-}131)}$-GFP and the first fourteen ΔN14*h*Par14$_{(14\text{-}131)}$-GFP N-terminal residues were deleted. ΔN6*h*Par14$_{(6\text{-}131)}$-GFP which lacks the first six amino acids is equally distributed through the nuclear matrix. The intracellular localization of ΔN14*h*Par14$_{(14\text{-}131)}$-GFP is different from those observed for WT-protein and ΔN6*h*Par14$_{(6\text{-}131)}$-GFP. The fluorescence image of ΔN14*h*Par14$_{(14\text{-}131)}$-GFP shows a cytoplasmic localization of the recombinant protein. The molecules seem to accumulate in the nuclear envelope and the entry to the matrix is disturbed (Figure 3.5 B). In addition, we tested the expression of full-length and truncated forms of *h*Par14 fused to GFP by using Western blot with anti-GFP antibody. As is shown in Figure 3.5 B, all indicated proteins are expressed and have the expected molecular mass.

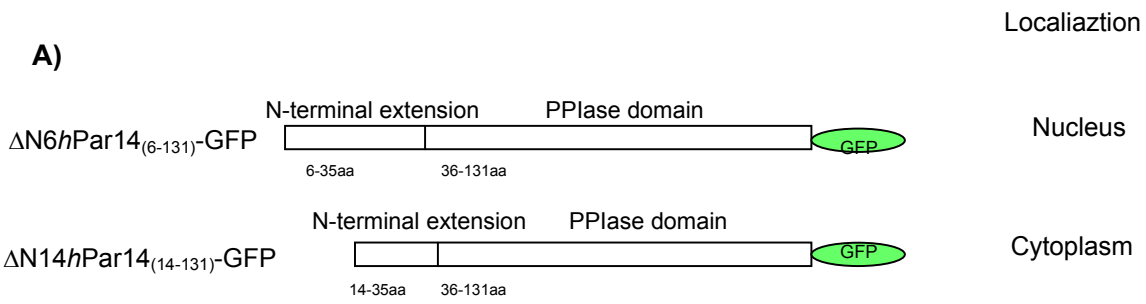

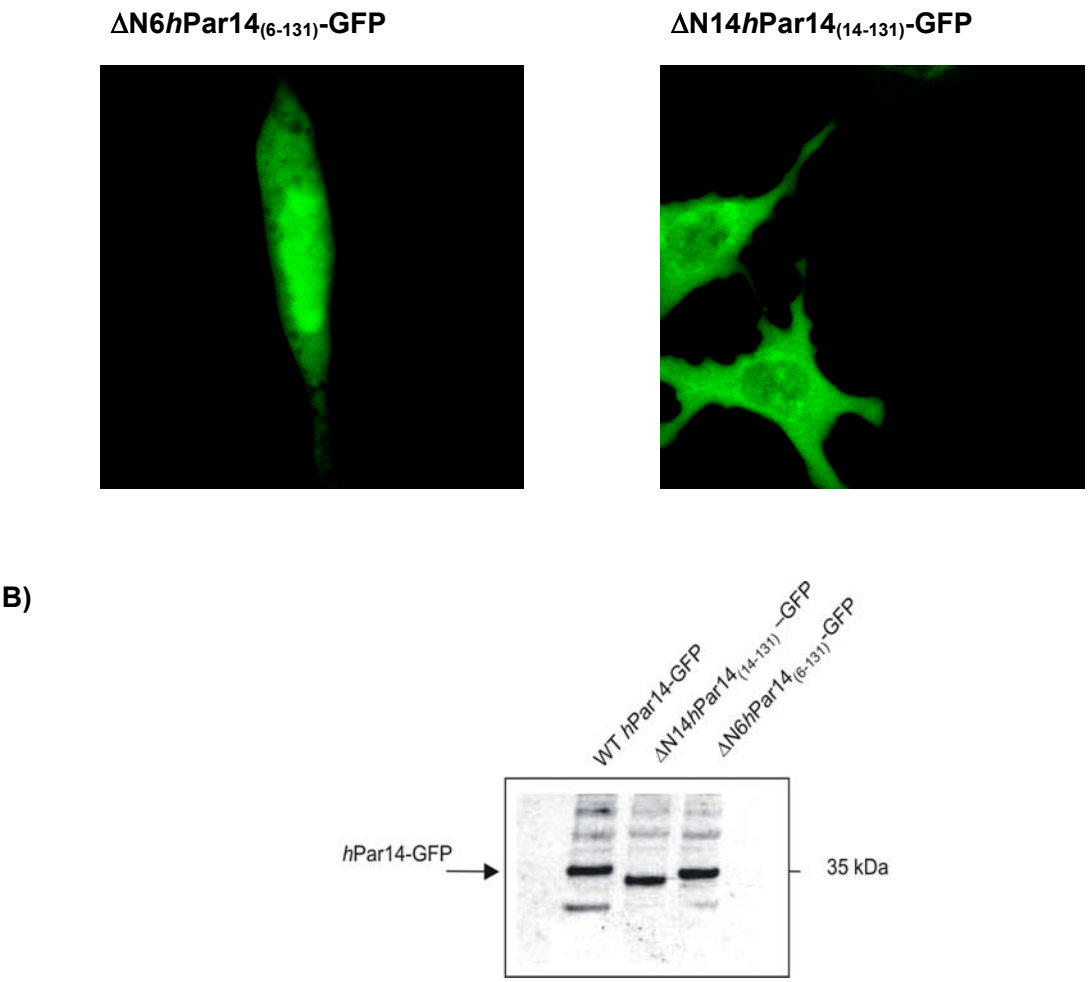

Figure 3.5 The subcellular localization of truncated *h*Par14-GFP in HeLa cells. **A)** Schematic representation of the ΔN6*h*Par14$_{(6-131)}$-GFP and ΔN14*h*Par14$_{(14-131)}$ -GFP. *Middle panel*, the fluorescence image of HeLa cells transfected with *h*Par14-GFP constructs, fixed and analysed by confocal fluorescence microscopy at C-Apochromat 63x/1.2 W corr objective. Three independent experiments showed identical results. **B)** Expression of *h*Par14 and its truncated form fused to GFP analysed by Western blot.

Thus, the signal for proper nuclear distribution of *h*Par14 is restricted to amino acids Ser7 to Lys14, which does not contain a classical NLS sequence. Despite the fact, that residues Ser7 to Lys14 are responsible for the entry to the nucleus, *h*Par14 would be able to diffuse freely from the nucleus back to the cytoplasm. Retention of the protein could be due to binding to large, non-diffusible elements, e.g. the chromatin structure, which would explain the higher content of *h*Par14 in the nuclear fraction when compared to the cytoplasmic fraction.

3.2 Binding of *h*Par14 to DNA

Note: The investigation on binding of *h*Par14 to DNA was done in collaboration with the research group of Dr. Bayer at the Max Planck Institute for Molecular Physiology in Dortmund. The presented results were published in *Journal of Molecular Biology* (2002) **321**, 235-247. The fluorescence titration and NMR data were obtained by Dr. Bayer and will be cited in the text.

3.2.1 Similarities between *h*Par14 and HMGN2 proteins

Remarkable homologies of the *h*Par14 N-terminal extension to the HMG17 were found after a pattern search against sequences in the Swissprot data bank (Uchida, et al., 1999). HMGN proteins contain three major functional motifs, namely, a bipartite nuclear localization signal (NLS), a nucleosomal-binding domain (NBD) and a chromatin-unfolding domain (CHUD) (Trieschmann, et al., 1995). The binding of HMGN to nucleosomes decreases the compactness of the chromatin fiber, increases the accessibility of the nucleosomal DNA and thereby facilitates transcription and replication from chromatin templates (Bustin, 2001). Figure 3.6 shows the alignment of the 37 residues along the N-terminal sequence of *h*Par14 with HMG17 sequences from various species. A detailed comparison reveals 45 % identity of the N-terminus of *h*Par14 to the CHUD domain and the flanking sequences of HMGN2.

```
hPar14(1-37)        MPPKGKSGSGKAGKGGA..ASGSDSADKKAQGPKGGGNA
                      .:::: :   ::: :   :   :     ::   : :.:
BOVIN(48-89)      GEKVPKGKKGKADAGKBGBBPAZBGBAKTBZAZKAEGAGDA
CHICK(48-89)      SEKVPKGKKGKADAGKEGNNPAENGDAKTDQAQKAEGAGDA
HUMAN(48-89)      GEKVPKGKKGKADAGKEGNNPAENGDAKTDQAQKAEGAGDA
MOUSE(48-89)      GEKVPKGKKGKADAGKDGNNPAENGDAKTDQAQKAEGAGDA
PIG(48-89)        GEKVPKGKKGKADAGKDGNNPAENGDAKTDQAQKAEGAGDA
RAT(48-89)        GEKVPKGKKGKADAGKDGNNPAEDGDAKTDQAQKADGAGDA
EST(48-90)        GEKLPKGRKGKADAGKDGNNPAKNRDASTLQSQKAEGTGDA
                        NLS              CHUD
```

Figure 3.6 Multiple sequence alignment of the N-terminal (1-37 amino acids) domain of *h*Par14 and various HMGN2 (HMG17) domains. Identical residues are shown in red, similar residues in blue. Abbreviations: NLS- Nuclear Localization Signal and CHUD- Chromatin-Unfolding Domain.

3.2.2 *h*Par14 binds at physiological salt concentrations to native double stranded DNA

The studies on cellular localization of *h*Par14 and solution of the NMR structure of the protein suggested a potential DNA-binding capability of *h*Par14 (Sekerina, et al., 2000). Therefore, we decided to test whether *h*Par14 binds to double-stranded DNA. A DNA-cellulose affinity assay was performed, using a double stranded native DNA immobilized on cellulose, incubated with recombinant non-tagged *h*Par14 or diluted nuclear extract from HEK293 cells. As shown in Figure 3.7, endogenous *h*Par14 from nuclear extract as well as recombinant protein binds to double-stranded DNA-cellulose at salt concentrations of 100-200 mM NaCl. As a control for the DNA assay with nuclear extract, the presence of the non-related protein *h*Pin1 was monitored (Figure 3.7 B). The control protein was not detected in eluted fractions.

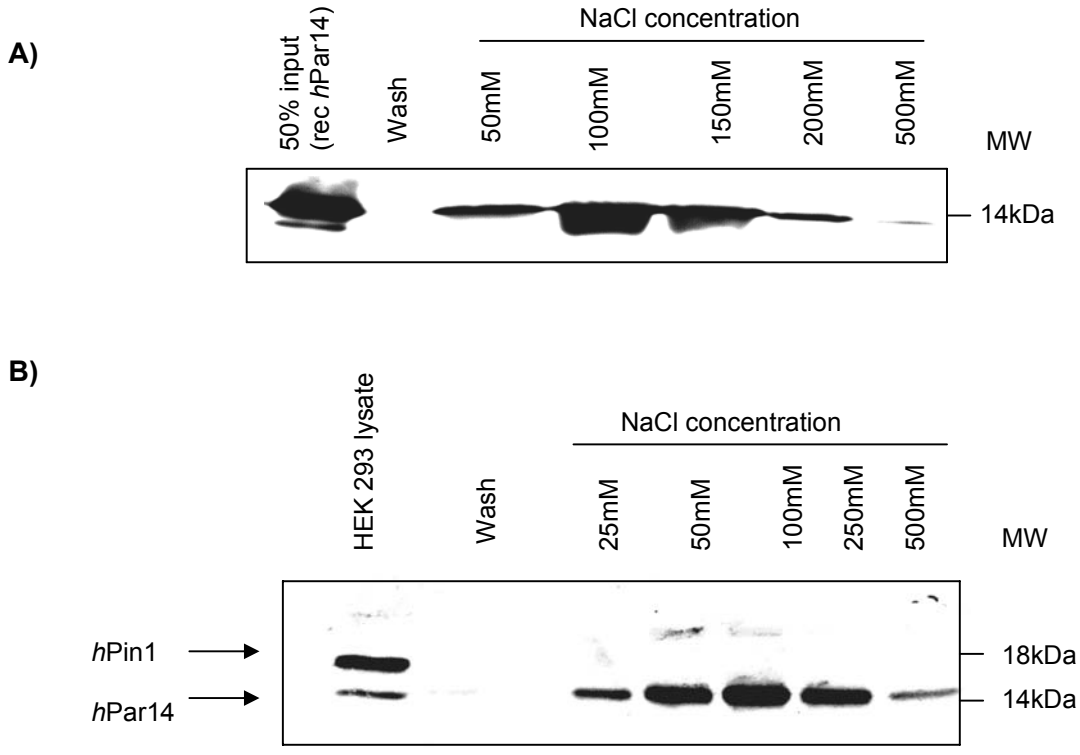

Figure 3.7 Recombinant *h*Par14 and endogenous protein from HEK 293 cells binds to double stranded DNA. **A)** Recombinant *h*Par14 (5μg) or **B)** the diluted nuclear extract from HEK 293 was incubated with double stranded (ds) DNA coupled to cellulose. Followed washing, bound protein was eluted with increasing concentration of NaCl from 50 mM up to 500 mM. The proteins were separated by SDS-PAGE and analysed by Western blot using anti-*h*Par14 serum or anti-*h*Pin1 antibody (used as a non-related protein marker).

To examine whether *h*Par14 fused to GFP possesses a DNA-binding ability or not, a DNA-cellulose assay was performed using GFP tagged proteins expressed in HeLa cells. The difference in cellular distribution of *h*Par14-GFP and ΔN14*h*Par14$_{(14-131)}$–GFP led us to investigate the role of truncation on binding to DNA. As studies with green fluorescent protein hybrid indicated that both, *h*Par14-GFP and ΔN6*h*Par14$_{(6-131)}$-GFP are localized to the nucleus, so we decided to include in our experiment the full length *h*Par14-GFP. Therefore, it was incubated with DNA immobilized on cellulose. Elution with increasing concentration of NaCl revealed that similar to previous observation, *h*Par14-GFP binds to double-stranded DNA-cellulose at salt concentrations of 100-200 mM NaCl. In contrast ΔN14*h*Par14-GFP is present in flow through fraction and does not bind to double stranded DNA (Figure 3.8).

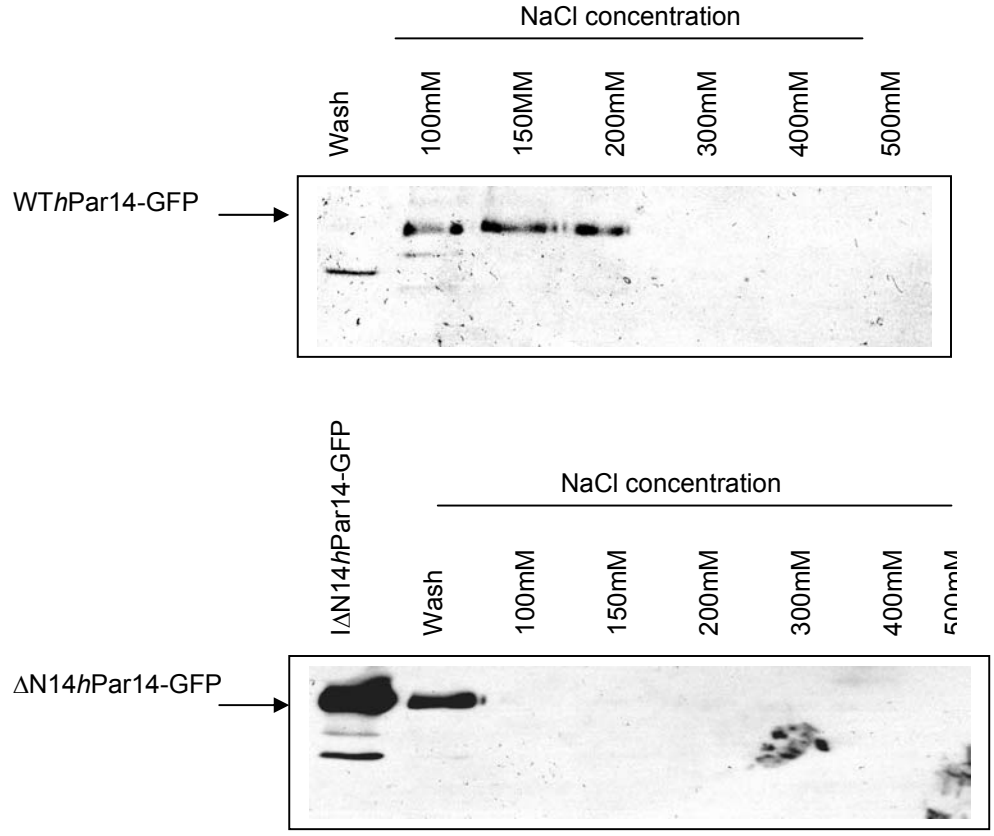

Figure 3.8 The full length *h*Par14-GFP and not mutant ΔN14*h*Par14$_{(14-131)}$-GFP binds to DNA cellulose. Transfected HeLa cells with WT *h*Par14-GFP or ΔN14*h*Par14$_{(14-131)}$ -GFP were homogenized and incubated with DNA cellulose. Followed washing, bound proteins were eluted with increasing concentration of NaCl (from 100 mM up to 500 mM), separated by SDS-PAGE and analyzed by Western blot using anti-GFP antibody.

3.2.3 Monitoring binding of *h*Par14 to DNA

On the bases of the striking sequence similarities of *h*Par14 to members of the high mobility group proteins, we intended to develop DNA constructs and test them for complex formation with *h*Par14 *in vitro*. HMGN proteins bind in a non-specific manner to tightly bent DNA of nucleosomes (Widom, 2001). Particular sequences that cause DNA to have net directional bends are known to exist. The best studied are A-tract bending motifs found in kinetoplasts (Marini et al., 1982) which comprise repeating stretches of five to six dA bases. A recent NMR structural study of A-tract bending (MacDonald, et al., 2001) suggests that each repeating unit is bent by ~19° in the direction of the minor groove. Hence, we decided to choose the sequence 5-GATAAAAATC-3 as a starting nucleosomal DNA model. The two complementary oligonucleotide strands were connected through a stabilizing tetra loop element (Nelson, et al., 1996), thus, increasing the probability for monomeric double-strand formation (Figure 3.9).

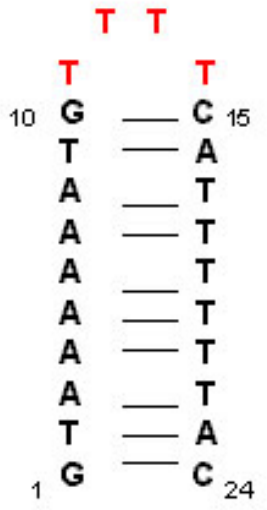

Figure 3.9. Schematic representation of a model oligonucleotide (construct 1) used in DNA binding studies. A tetra loop element consisting of thymin bases is marked in red.

Changes in the position of adenine were performed to obtain DNA model compounds, 1 to 11. The fluorescence titration experiments of these compounds with *h*Par14 yielded binding constants in the range 100 nM to 1000 nM as shown in Figure 3-10 (Surmacz, et al., 2002).

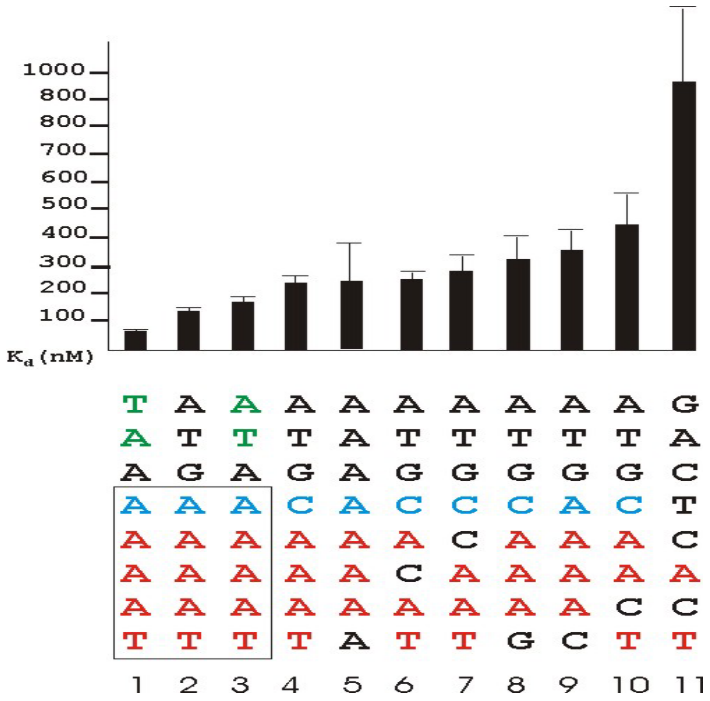

Figure 3.10 K_d values for *h*Par14/DNA-binding derived from fluorescence titration experiments. K_d values are represented by black bars, black lines indicate mean errors. Below the bars are the sequences of the corresponding oligonucleotides (from bases 2 to 9, top (5') to bottom (3')). Surmacz, et al., (2002)

DNA constructs that exhibit the sequence $dA_{4\text{-}6}dT$ bound with highest affinity to *h*Par14 (constructs 1-3; K_d <190 nM). Alterations in one or two base-pairs in the minimal dA_4dT element led to slightly increased K_d values (constructs 4-10; K_d> 200 nM) depending on the position of exchange. Compound 11 (Figure 3-10) with three alterations in the dA_4dT box bound to *h*Par14 with K_d values in the micromolar range (Surmacz, et al., 2002).

The compounds, 1 to 3, which showed the highest affinity to *h*Par14, carry A-motifs within their sequences. Such A-tracts are known to exhibit pronounced macroscopic curvature. The program bend.it was used to calculate the bend angles of the compounds and plotted the angles against their experimentally determined K_d values (Surmacz, et al., 2002). Figure 3-11 shows that *h*Par14 binds preferentially to DNA double strands with high local curvature per helix turn.

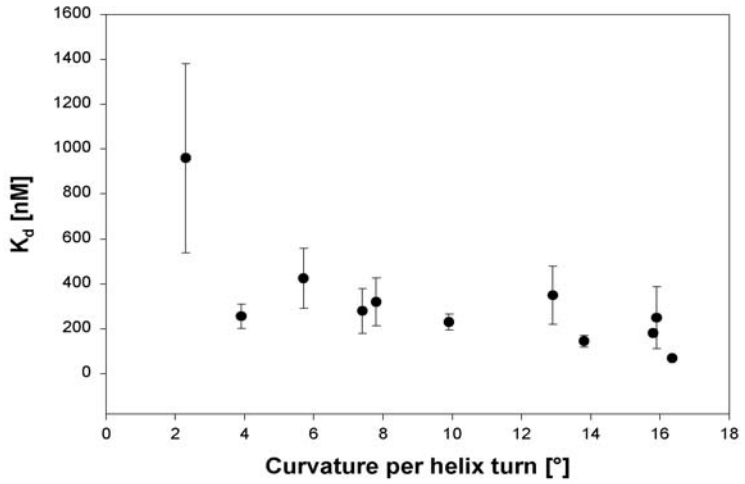

Figure 3.11 Correlation between the K_d values of *h*Par14/DNA-binding and DNA bend angles. K_d values were derived from fluorescence titration experiments. Curvature was predicted using the web-engine bend.it. Filled circles represent data points, black lines indicate mean errors. Surmacz, et al., (2002)

To confirm binding of *h*Par14 to double-stranded DNA by an alternative method, an electro-mobility shift assay was carried out using a 5'-end [γ^{32}P] labelled Construct 1. The DNA-protein binding reaction was performed in the presence of unlabelled specific competitor DNA - construct 1 or in the presence of unlabelled unspecific competitor DNA- (Control) construct 2. Figure 3-12 shows the autoradiogram after exposing the gel to an intensifying screen. The free oligonucleotide is found as an intensive band at the bottom of the gel. Upon binding, *h*Par14 induces a band-shift (Figure 3.12, lane 3-5) that corresponds to the DNA-protein complex and can be seen just below the middle of the gel. Pre-incubation with specific competitor (Construct 1) decreased DNA-protein complex formation (Figure 3.12, lane 6-8). Upon addition of a 100-fold excess of unspecific competitor DNA – (Control) construct 2 (K_d~10^{-5}) (lanes 10-12), a 50 % decrease in the intensity of the bands (as expected from stoichiometry) was observed due to the complex formation of the specific binder (K_d~10^{-7}) and *h*Par14.

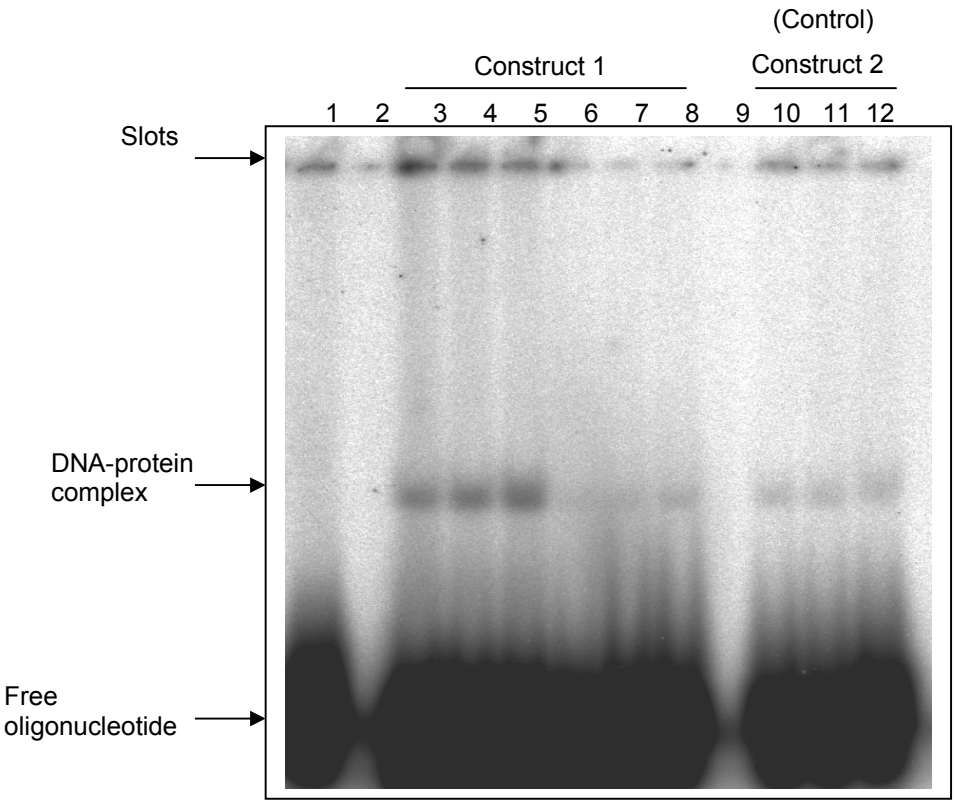

Figure 3.12 Electromobility shift assay (EMSA) with *h*Par14. DNA-Construct 1 was used for complex formation. Lanes 3-5, the radiolabelled specific oligonucleotide was incubated with increasing amounts (0.5, 1, 2 μg) of *h*Par14. Lanes 6-8, 100-fold molar excess of unlabeled specific probe was used for competition with labelled oligonucleotide. Lanes 10-12, 100-fold molar excess of unlabeled non-specific probe (Control) Construct 2 in competition with labelled specific DNA. As a control (1), free oligonucleotide was used.

To test whether *h*Par14 binds to unspecific (Control) construct 2 as indicated by the experiment shown in Figure 3-12 (lanes 10-12), an additional band shift analysis using unspecific, labeled (Control) construct 2 was performed. Figure 3-13 shows the autoradiogram after exposing the gel to an intensifying screen. *h*Par14 induces a slight band-shift (Figure 3.13, lane 1-2) that corresponds to the DNA-protein complex and is located just below the middle of the gel. The complex protein-DNA disappeared after addition of a 100-fold excess of unspecific DNA competitor –(Control) construct 2.

There is no change in enzymatic activity of *h*Par14 in the presence of DNA construct (Dr. Rahfeld, personal communication).

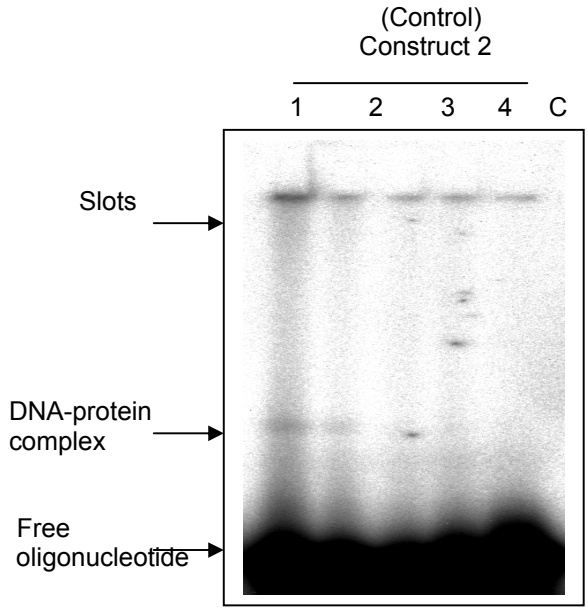

Figure 3.13 *h*Par14 has a low affinity to the non-specific DNA-Construct 2. The double-stranded non-specific binder 5'-ATTCGATCGGGGCGGGGCGACC-3 (Construct 2 (Control)) was used for complex formation. Lane 1 and lane 2 represent the radiolabelled non-specific oligonucleotide incubated with two different concentration (1μg or 2 μg) of *h*Par14. Lane 3 and lane 4 represent the unlabeled non-specific oligonucleotide incubated with *h*Par14 (1μg or 2μg) prior to the radiolabelled non-specific DNA. C - free DNA-Construct 2 used as control.

NMR investigations showed that the model compound 1 (specific *h*Par14 binder) binds with sufficient high affinity to produce numerous distinct chemical shift changes in the ^{15}N-HSQC NMR spectrum (Surmacz, et al., 2002). Spectral chemical shift changes reveal that the DNA binding site localizes to amino acids Gly35, Gly49, Ile51, Met52, Met55, Ala76, Met85, Gly88, Val91, Phe94, and Phe120 forming a hydrophobic patch at the surface of the PPIase domain of *h*Par14, flanked by several polar residues (Asn36, His48, Gln95, Thr118) (Figure 3.13). Seven residues of the N-terminal region of *h*Par14 were reported to interact with DNA. Among those are three glycine residues (probably Gly8, Gly10 and Gly15), one lysine (probably Lys11 or Lys14) as well as Ala17 and Ala18. The NMR analysis also revealed that the unfolded N-terminal extension of *h*Par14 is necessary for high affinity DNA binding.

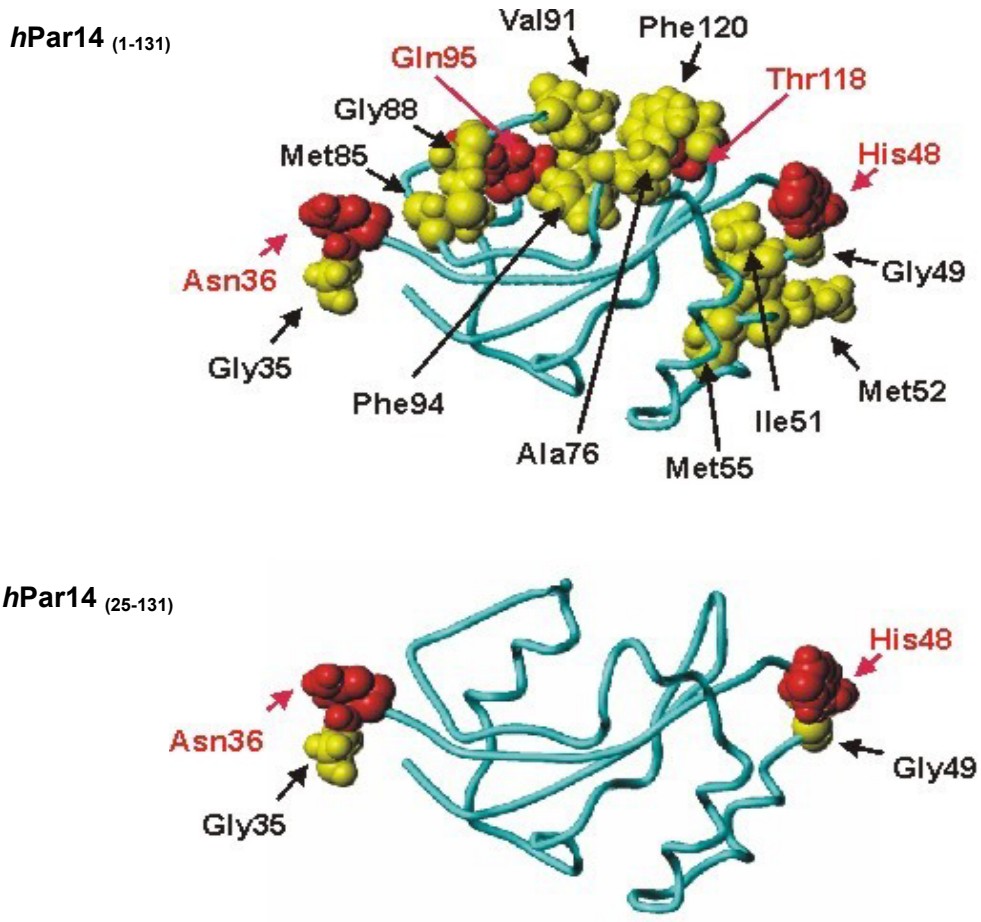

Figure 3.14 A van der Waals representation of amino acid residues affected by binding to DNA. Hydrophobic residues are labeled with yellow, polar residues with red. Amino acid residues of the PPIase domain with K_d values <50μM are show. *The upper picture*, *h*Par14 $_{(1\text{-}131)}$ and *the lower picture*, *h*Par14 $_{(25\text{-}131)}$. According to Surmacz, et al., (2002) *J. Mol. Biol.* **321**, 235-241

3.3 Posttranslational modification of *h*Par14

Phosphorylation and dephosphorylation events in various proteins that are often sequestered in the cytoplasm have been shown to activate their nuclear import or export signals (Jans, 1995). Additionally, phosphorylation of DNA binding proteins may negatively regulate their interaction with DNA. The unequal distribution of *h*Par14 in cells prompted us to investigate a putative role of phosphorylation in subcellular distribution and DNA binding of *h*Par14.

3.3.1 *h*Par14 is phosphorylated *in vitro* by endogenous kinase from HeLa extract and recombinant kinases

To examine if recombinant *h*Par14 is phosphorylated, an *in vitro* endogenous kinase assay was performed in the presence of [γ-^{32}P] ATP, recombinant *h*Par14-His, cytosolic and nuclear extracts from HeLa cells. Following the kinase reaction, *h*Par14-His was isolated from the mixture using Ni-NTA agarose beads and analysed by SDS-PAGE. From Figure 3.15, one can see that *h*Par14-His is phosphorylated *in vitro* by a cellular protein kinase, which can utilize ATP as a phosphate donor and is present in both cytosolic and nuclear fractions.

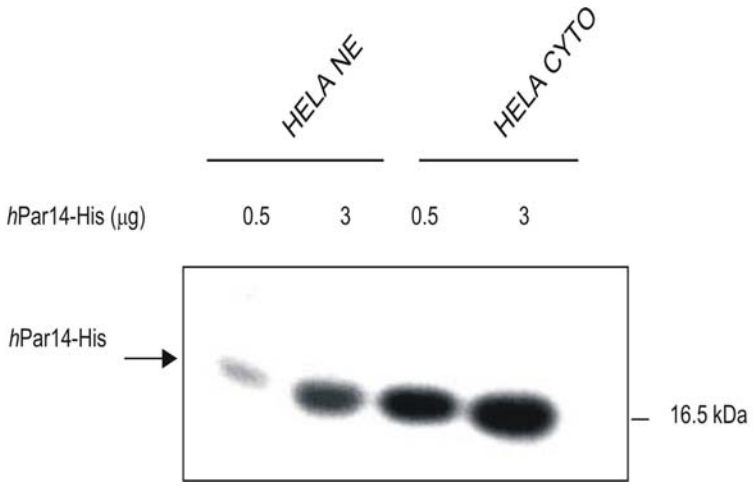

Figure 3.15 *h*Par14 is phosphorylated by a kinase from nuclear and cytosolic extracts. HeLa cells were homogenized and fractionated as described in Materials and Methods. The cytosol (HELA CYTO) and nuclear (HELA NE) extracts were incubated with 0.5 or 3μg of recombinant carboxy-terminal His tagged *h*Par14 (*h*Par14-His) in the presence radioactive ATP. *h*Par14-His was isolated from the mixture by binding to Ni^{2+}-NTA beads. Beads were washed and boiled in Laemmli sample buffer. Eluted proteins

were resolved by SDS-PAGE and protein phosphorylation was detected by autoradiography. The *arrow* indicates the phosphorylated *h*Par14-His

To identify the protein kinase that phosphorylates *h*Par14, we performed a search for predicted phosphorylation sites using the NetPhos 2.0 Prediction Server, a sequence analysis program at ExPASy, Switzerland (www.expasy.ch). Analysis of the primary amino acid sequence of *h*Par14 revealed one potential phosphorylation site for casein kinase 1 (CK1) and PKA, two for casein kinase 2 (CK2), PKB and PKC, respectively (Figure 3.16).

***h*Par14**

MPPKGKSGSGKAGKGGAASGSDSADKKAQGPKGGGNAVKVRHILCEKHGKIMEAMEKLKSGMRFN

EVAAQYSEDKARQGGDLGWMTRGSMVGPFQEAAFALPVSGMDKPVFTDPPVKTKFGYHIIMVEGR

K-131

Phosphorylation site	Motif	Putative kinase
• S-23	SGSD**S**ADK	CK1
• S-19	A**S**GSDSAD	CK2
• S-104	LPV**S**GMDK	CK2
• S-89	RG**S**MVGGP	PKA
• S-7	K**S**GSGKAG	PKB, PKC
• S-9	KSG**S**GKAG	PKB, PKC

Figure 3.16 Predicted phosphorylation sites for *h*Par14 identified with NetPhos 2.0 Prediction software.

Each of these kinases was tested for phosphorylation of *h*Par14 *in vitro* using recombinant kinase assay. An effective phosphorylation was found for CK2 as shown from the intensity of the radioactive band (Figure 3.17 A, B). The phosphorylation is also detected for three other kinases PKA, PKB and PKC (Figure 3.17 A). Protein bands corresponding to the CK2α and CK2β subunits were observed to be phosphorylated in every sample due to the autophosphorylation activity exhibited by CK2 (Meggio, et al., 1994). The same autophosphorylation activity was observed for the three other tested kinases (Figure 3.17 C).

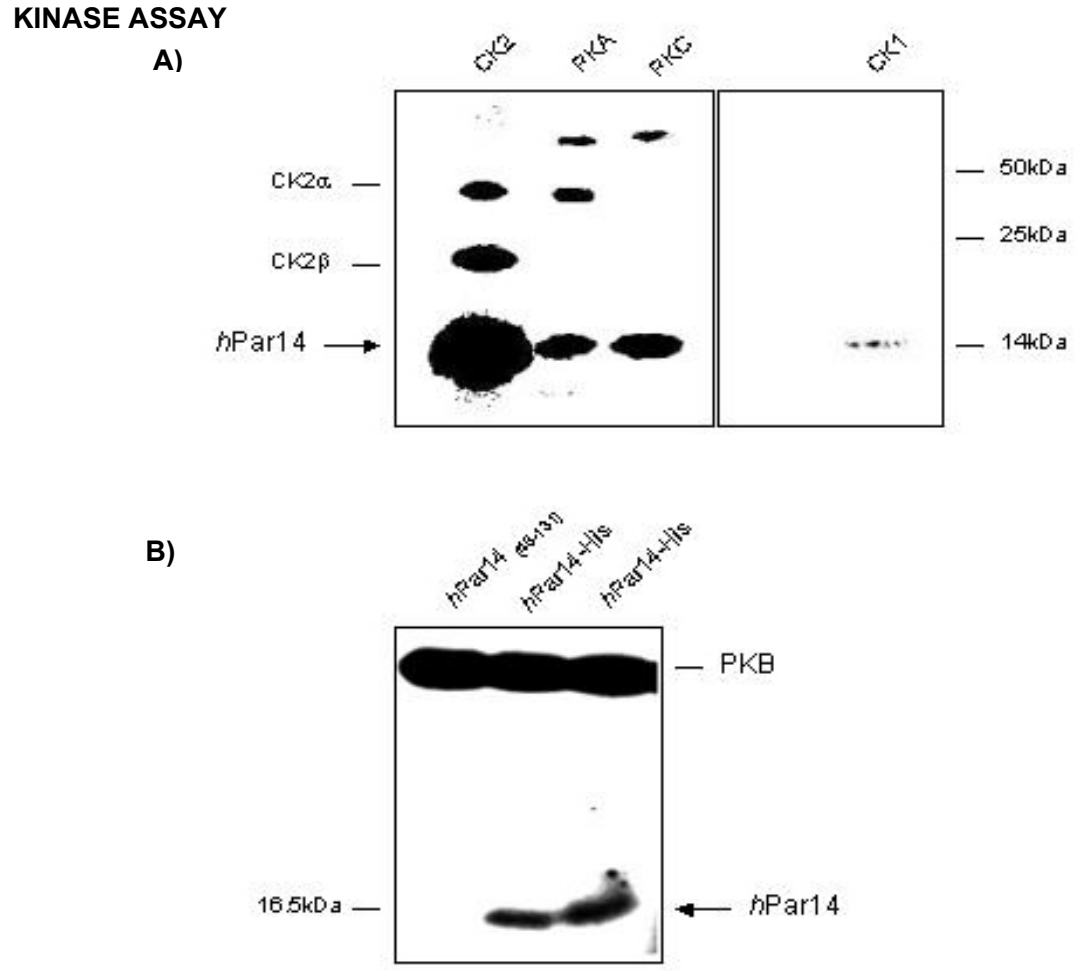

Figure 3.17 *h*Par14 is phosphorylated by the CK1, CK2, PKA, PKB and PKC kinases *in vitro*. Recombinant *h*Par14 was used as a substrate for *in vitro* phosphorylation and incubated with **A)** recombinant CK2 (500U), PKA (2500U), PKC (2000), CK1 (1000) and **B)** recombinant PKB (200U) kinases. The protein was resolved by SDS-PAGE and phosphorylation detected by autoradiography. The two *upper* bands indicate autophosphorylated CK2α and CK2β subunits and *lower* band shows autophosphorylated PKB.

The results from GFP studies and DNA binding analysis suggest that N-terminal extension of *h*Par14 plays an important role in elucidating the function and localization of *h*Par14. From *in vitro* kinase assay, one can see that phosphorylation of *h*Par14 by CK2 is higher than compared to other kinases. One of the predicted sites for CK2 is closely located to the putative NLS signal within *h*Par14 and apparently in a close neighbourhood to amino acids Ala17 and Ala18 which are involved in DNA binding. Therefore, it was necessary to look for a possible role of CK2 mediated phosphorylation on *h*Par14 localization and binding to DNA.

3.3.2 *h*Par14 is specific substrate for casein kinase 2

CK2 kinase activity is detected in the nucleus and cytoplasm. The data from *in vitro* endogenous (Figure 3.15) and recombinant kinase assays (Figure 3.17) suggest that CK2 is a potential kinase that phosphorylates *h*Par14 *in vivo*. Taking advantage that CK2 activity is characterized by its sensitivity to low concentration of heparin (Hathaway, et al., 1980; O'Farrell, et al., 1999) and DRB (Zandomeni & Weinmann, 1984), the endogenous kinase assay was performed with cell lysate in the presence of recombinant *h*Par14-His, [γ-^{32}P] ATP, heparin or DRB. As shown in Figure 3.18 phosphorylation of *h*Par14 is not inhibited by control-ethanol (lane 1) and not by heparin (lane 2) but effectively inhibited by the addition of DRB (lane 3) (Figure 3.18). It is surprising that heparin, reported, as a potent CK2 inhibitor did not decrease kinase activity. More interestingly, phosphorylation of *h*Par14 was clearly increased as shown in Figure 3.18, lane 2. To confirm that the observed effect is not due to unequal protein concentrations, the same protein concentration used for the assay, was subjected to SDS-PAGE and stained Coomassie blue staining. The gel shows comparable protein concentration.

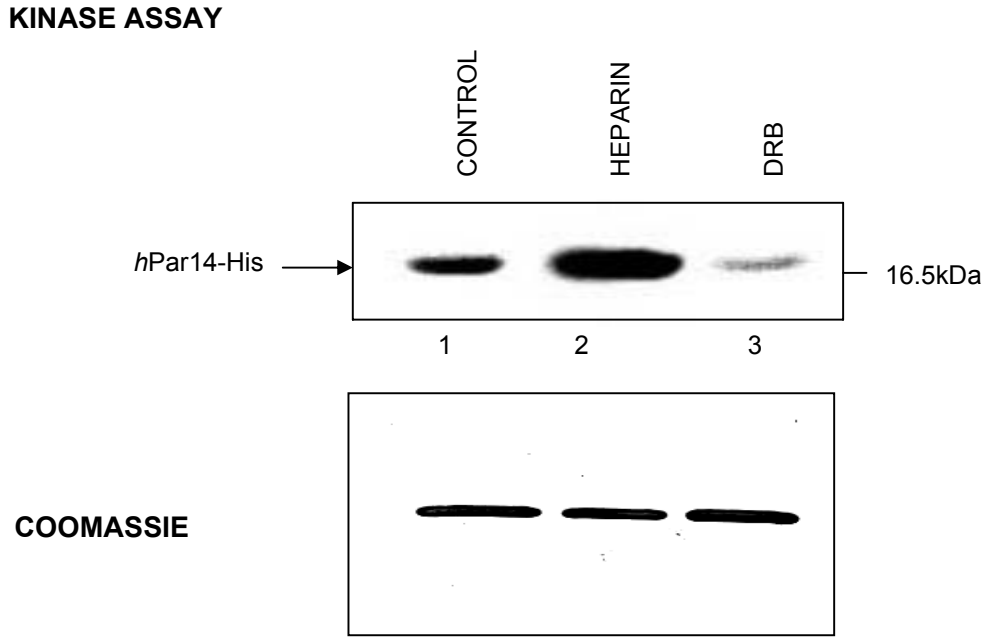

Figure 3.18 DRB inhibits phosphorylation of *h*Par14 by an endogenous kinase from cell extract. Recombinant *h*Par14-His (3μg) was incubated with cell lysated obtained from HeLa cells in a presence of [γ-^{32}P] ATP, no inhibitor (lane 1), CK2-inhibitor, heparin (100 μg/ml) (lane 2) or CK2-inhibitor, DRB (300 μM) (lane 3). The protein was incubated with Ni-NTA beads. Beads were washed and boiled in

Laemmli sample buffer. Eluted protein was separated by SDS-PAGE and phosphorylation detected by autoradiography. *Bottom panel*, Coomassie blue staining.

To demonstrate that the similar unexpected effect of inhibition is also observed in the kinase assay with recombinant CK2, the phosphorylation of *h*Par14 by bacterially expressed CK2 in the presence of heparin or DRB was performed. Comparable results were obtained whereby the phosphorylation of *h*Par14 was inhibited by DRB (lane 3) and not by heparin (lane 2) (Figure 3.19 A). Heparin again enhances the phosphorylation of *h*Par14. As a control, the inhibition of autophosphorylation of CK2α and CK2β subunits by DRB and heparin was monitored. To determine CK2 kinase activity, the intensity of radioactive bands of *h*Par14 was quantified using AIDA 2.0 software. As shown in Figure 3.19 B the kinase activity was inhibited by DRB. However, in the presence of *h*Par14 and heparin the activity was two-fold higher when compared to the control (lane 1).

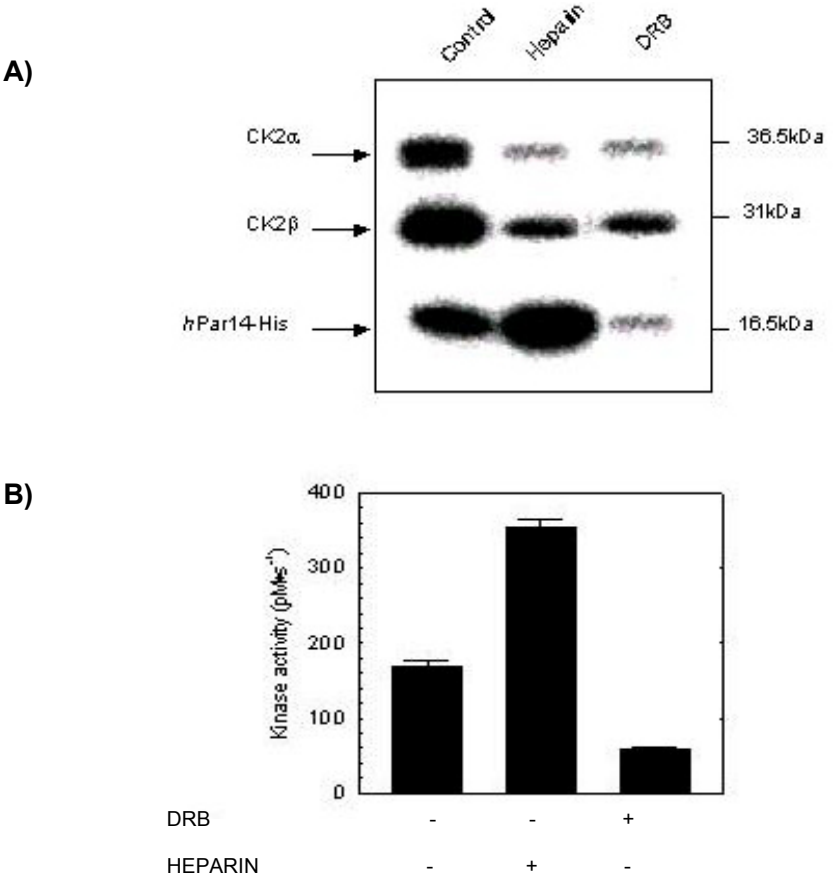

Figure 3.19 DRB inhibits phosphorylation of *h*Par14 by recombinant CK2. **A)** Recombinant *h*Par14-His was incubated with [γ-^{32}P] ATP, CK2 in absence of inhibitor or presence of heparin (100μg/ml) or DRB (300μM). *h*Par14-His was bound to Ni-NTA beads. Beads were washed, analysed by SDS-PAGE and

phosphorylation was detected by autoradiography. The two upper arrows indicate autophosphorylation of CK2 subunits. **B)** The activity of CK2 in the absence or presence of inhibitors was analysed by AIDA 2.0 software.

The kinetic constant of CK2 with hPar14 as a substrate was determined. The obtained initial rates for the CK2 reaction were plotted against different concentration of the kinase substrate, hPar14. We determined a K_m value of 20.1 μM and a V_{max} of 8.6 nM s^{-1}. The enzymatic activity ($k_{cat}/K_{m)}$ of CK2 is 253 M^{-1} s^{-1}. The graph in Figure 3.20 represents the Michaelis-Menten behaviour of the phosphate transfer reaction.

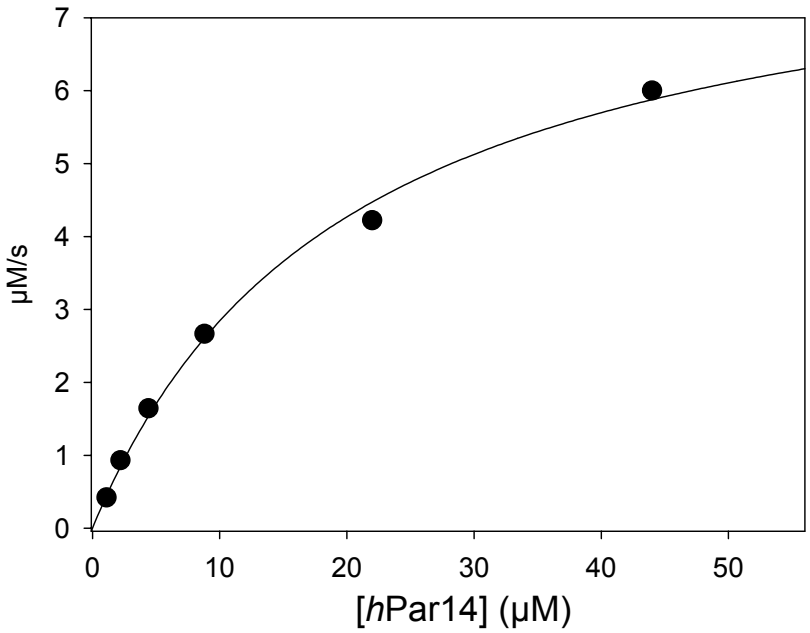

Figure 3.20 Enzyme kinetics of CK2 in the presence of *h*Par14, in Michaelis-Menten representation. Each point represents the various concentration of *h*Par14 incubated with 1.7 μM of CK2 at 30 °C in a CK2 buffer. Kinetic parameters K_M and V_{max} of phosphorylation were calculated by nonlinear regression analysis of the initial velocities.

3.3.3 Serine 19 in *h*Par14 is phosphorylated by CK2 *in vitro*

CK2 preferentially phosphorylates substrates containing the acidic amino acid residues glutamate or aspartate immediately downstream (+1 to +3) from the phosphoacceptor site (Meggio, et al., 1994). The CK2 consensus site has been described as Ser/Thr-X-X-Glu/Asp where Ser/Thr are phosphoacceptor residues and X represents any non-basic amino acid. To determine *in vitro* CK2 phosphorylation site within *h*Par14, a MALDI-TOF mass spectrum

analysis was performed. Recombinant non-tagged *h*Par14 was phosphorylated by CK2. The mass of the phosphorylated protein was 13662 in the MALDI-TOF mass spectrum (Figure 3.21).

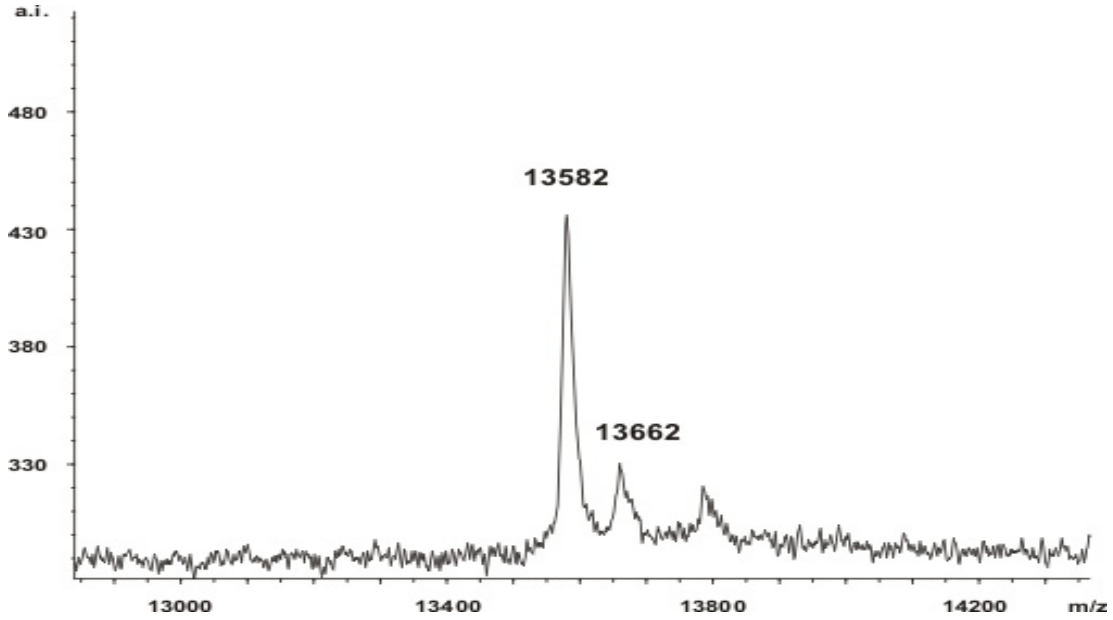

Figure 3.21 MALDI mass spectrum of the mixture non-phosphorylated and phosphorylated *h*Par14. The peak without labelling is the matrix adduct.

A difference of 80 Da to the unmodified protein indicated introduction of one phosphate group. As the phosphorylated protein (less than 10 %) could not easily be separated from the predominant unmodified protein, the mixture (phosphorylated/non-phosphorylated *h*Par14) was digested with trypsin. The digested peptides were separated by RP-HPLC and their masses determined by MALDI-TOF mass spectrometry. The RP-HPLC chromatogram was compared with the RP-HPLC chromatogram of a tryptic digest of unmodified *h*Par14. There were no differences in both chromatograms and also no mass differences in the fractions, so re-chromatography of the fraction from 0-10 min retention time was done with a C18 HPLC column to analyse the hydrophilic peptides. The HPLC peak at 14.1 min retention time showed a higher intensity as compared to the same peak in the chromatogram of the unmodified protein digest mixture (Figure 3.22).

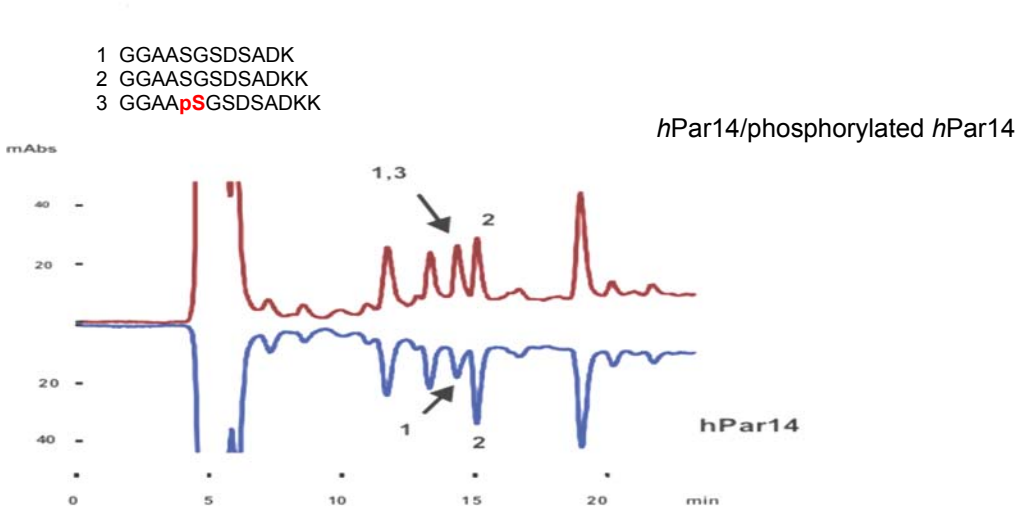

Figure 3.22 Comparison of the HPLC chromatograms of the tryptic digests of *h*Par14 and the mixture *h*Par14/phosphorylated *h*Par14.

Fractions 15-26 and 15-27 obtained from HPLC contained the nonphosphorylated peptide (GGAASGSDSADK) and the single-phosphorylated peptide (GGAASGSDSADKK), respectively. MALDI-TOF and ESI mass spectra of these fractions demonstrated single-phosphorylation. The peptide 15-27 was sequenced using MS/MS fragmentation spectrum and Ser19 was unambiguously identified as the phosphorylated amino acid residue (Figure 3.23). There was no detected phosphorylation by CK2 in a second predicted site (LPVSGMD) within *h*Par14.

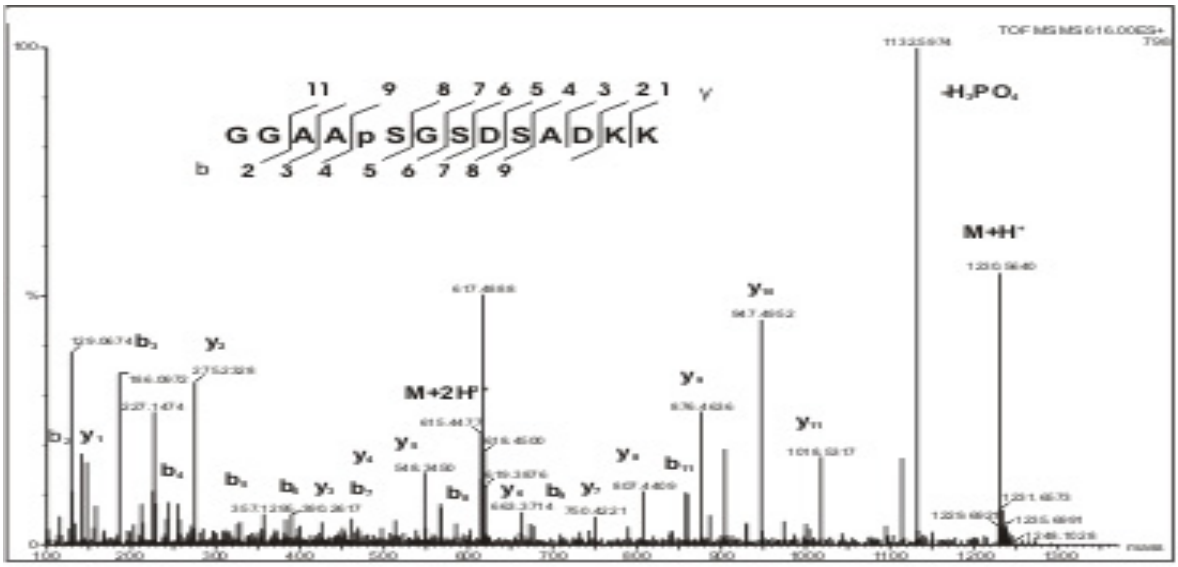

Figure 3.23 Nano-ESI-MS/MS spectrum of the phosphorylated peptide 15-27. The fragment ion nomenclature suggested by Biemann for peptides was used.

3.3.4 Phosphorylation of *h*Par14 in HeLa cells *in vivo*

To determine whether *h*Par14 is phosphorylated *in vivo* in mammalian cells at the site identified by mass analysis, we transfected HeLa cells with DNA constructs encoding His-*h*Par14 WT and mutant protein His-Ser19/Ala *h*Par14. The transfected cells were metabolically labelled for 5h in the presence of [^{32}P] orthophosphate. The expressed His-tagged proteins were extracted from cells, analysed by SDS-PAGE and transferred to nitrocellulose. Protein phosphorylation was detected by autoradiography. The band in the range of 16.5 kDa was identified as a His-*h*Par14 WT (Figure 3.24 A) (lane 1 and lane 3), whereas the second band in the same range of molecular mass corresponding to mutant His-Ser19/Ala *h*Par14 was greatly reduced (lane 2 and 4) (Figure 3.24 A).

A)

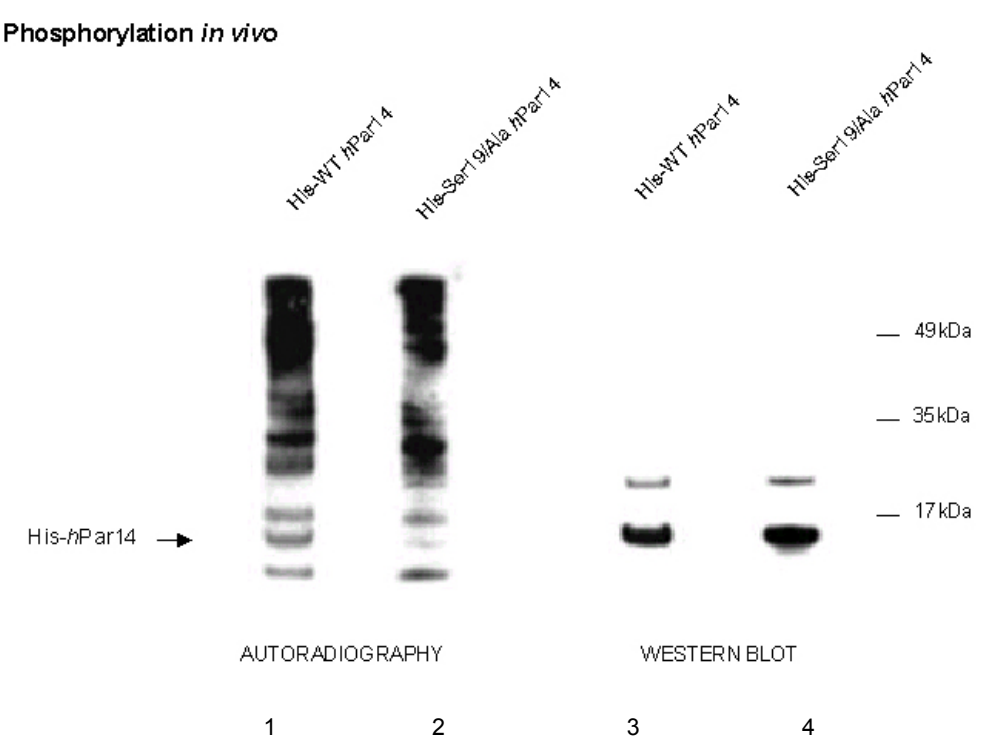

B)

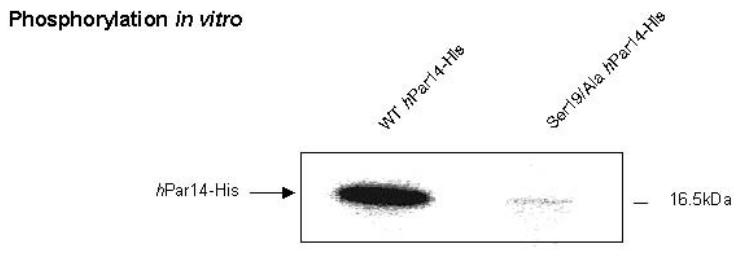

Figure 3.24 Phosphorylation of wild type and mutant Ser19/Ala *h*Par14 *in vivo* and *in vitro*. **A)** Transiently transfected HeLa cells with His-WT and His-Ser19/Ala *h*Par14 were metabolically labelled and homogenized. Cell extract was incubated with Ni-NTA beads. Beads were washed and proteins eluted with 100 mM imidazole. Eluted proteins were precipitated with TCA and separated by SDS-PAGE and electroblotted onto nitrocellulose membrane. Protein phosphorylation was detected by autoradiography. The same membrane was subjected to Western blot analysis using anti-*h*Par14 serum. **B)** Recombinant WT and Ser19/Ala *h*Par14-His was incubated with recombinant CK2 in the presence of [γ-^{32}P] ATP. His tagged *h*Par14 was incubated with Ni-NTA beads. Beads were washed and boiled in Laemmli sample buffer. Eluted proteins were separated by SDS-PAGE and phosphorylation was detected by autoradiography.

To exclude the possibility of an artefact, the same membrane was probed with anti-*h*Par14 serum. The radioactive signal and signal from western blot were overlapped. Bands 1and 3 correspond to the wild type while bands 2 and 4 to mutant *h*Par14. The data showed that *h*Par14 is indeed phosphorylated *in vivo*. Moreover, decrease in phosphorylation of mutant protein indicates that Ser19 residue is a potential phosphorylation site. To confirm that Ser19 of *h*Par14 is the CK2 phosphorylation site *in vitro*, we performed kinase assay with recombinant WT *h*Par14-His and mutant Ser19/Ala *h*Par14-His. As shown in Figure 3.24 B, only WT *h*Par14-His and not mutant *h*Par14 is efficiently phosphorylated by CK2 *in vitro*.

3.3.5 *h*Par14 interacts with CK2

To examine, whether His-*h*Par14 can interact with HA-CK2α and FLAG-CK2β co-transfection and co-immunoprecipitation experiments were performed. HeLa cells, transfected with DNA constructs, were lysed and overexpressed proteins were co-immunoprecipitated using anti-HA or anti-CK2β. The immunocomplexes were resolved on SDS-PAGE followed Western blot analysis with anti-*h*Par14 serum, anti-CK2α and anti-CK2β antibodies. The His-*h*Par14 is co-precipitating with HA tagged CK2α (Figure 3.25 A) and the CK2α is also detected in co-immunoprecipitation with anti-HA antibody (Figure 3.25 A). Additionally, His-*h*Par14 is found in co-immunoprecipitation with CK2β antibody (Figure 3.25 B). In this case, the reciprocal experiment with CK2β was not possible. An electrophorretic migration of endogenous CK2β is similar with migration of the immunoglobulin light chain.

A)

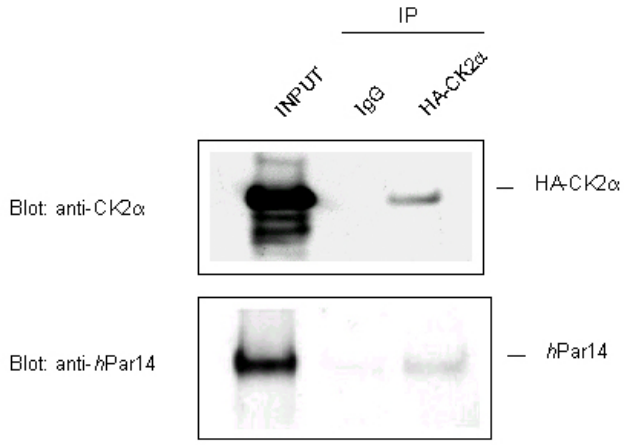

B)

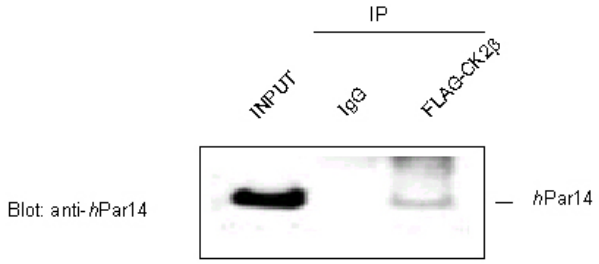

Figure 3.25 *h*Par14 interacts with CK2α and CK2β subunits. Transfected HeLa cells with *h*Par14/HA-CK2α and His-*h*Par14/FLAG-CK2β were homogenized and incubated with either anti-HA or anti-CK2β antibodies. The immuno-complexes were bound to protein A/G sepharose. Beads were washed three times with ice cold washing buffer and 2x sample buffer was added. Eluted proteins were separated by SDS-PAGE and analysed by Western blot using anti-HA or anti-*h*Par14 antibody. Each picture represents separate experiment.

Findings that CK2 subunits interact with *h*Par14 *in vivo* prompted to study the co-localization of both proteins. First, the subcellular distribution of individual subunits of CK2 was tested. HeLa cells were transfected with a DNA construct encoding CK2α subunit tagged with the influenza hemagglutinin (HA) epitope and CK2β subunit tagged with FLAG epitope. Transfected cells were fixed and incubated with antibody against the individual tagged subunits of CK2. As shown in Figure 3.26, both CK2 subunits are localized in the nucleus with a little cytoplasmic detection for CK2β.

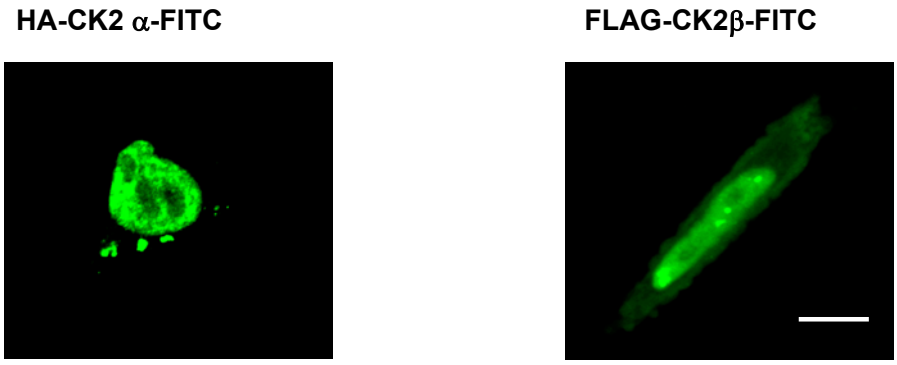

Figure 3.26 Subcellular localization of CK2α and CK2β subunits. Transfected HeLa cells with HA-CK2α and FLAG-CK2β were fixed, permeabilized and incubated with anti-HA and FLAG-FITC conjugated antibodies. For detection of HA-CK2α, the FITC-conjugated anti-rabbit secondary antibody was used. The cells were analysed by confocal fluorescence microscopy at objective 40x Plan apochromat. Scale bar, 10μm

The observed subcellular distribution of CK2 subunits in HeLa cells is similar to distribution of *h*Par14, suggesting that both proteins may localize in the same compartment *in vivo*. A double transfection and labelling experiment was performed to test the co-localization of CK2 and *h*Par14 in HeLa cells. Cells were co-transfected with His-*h*Par14, CK2α-HA and CK2β-FLAG subunits, fixed and incubated with antibodies. As shown in Figure 3.27, both proteins co-localized to the nuclear membrane. The co-localization of catalytic subunit of CK2 with *h*Par14 suggests that phosphorylation may play important role in the nuclear targeting of substrate protein.

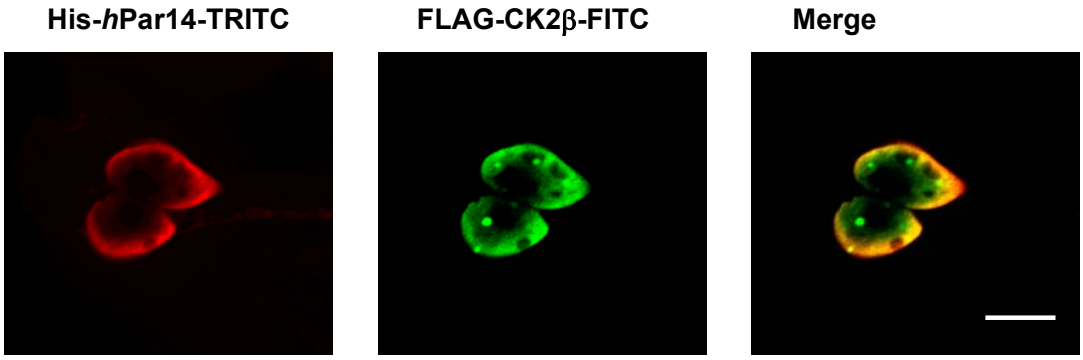

Figure 3.27 Co-localization of *h*Par14 with CK2α and CK2β subunits. Transfected cells with DNA constructs encoding His-*h*Par14, HA-CK2α and FLAG-CK2β were fixed, permeabilized and incubated with anti-His, anti-HA and anti-FLAG-FITC antibodies. Detection was done using FITC or TRITC coupled goat anti-mouse or anti-rabbit secondary antibodies. Cells were analysed by confocal fluorescence microscope at objective 40x Plan apochromat. Scale bars, 10μm.

3.3.6 Expression of mutant Ser19/Ala *h*Par14 results in cytoplasmic localization

It has been reported that CK2-mediated phosphorylation plays a role in regulating the subcellular localization of its substrates (Jans, 1995). The phosphorylation of large T antigen of SV-40 at Ser111 and Ser112 residues by CK2 results in a significantly faster rate of nuclear uptake of a large T antigen (Rihs, et al., 1991). The immunolocalization studies showed that *h*Par14 and CK2 localized to the nuclear membrane. Based on this information, the question whether posttranslational modification of *h*Par14 is important for its nuclear localization was addressed. In order to understand the biological significance of phosphorylation of *h*Par14, we introduced mutations at serine 19 of *h*Par14. The residue was mutated to alanine (His-Ser19/Ala *h*Par14, non-phosphorylated form) or glutamic acid (His-Ser19/Glu *h*Par14, mimics the phosphorylation) and such DNA constructs were transiently transfected in HeLa cells. The protein expression level of WT and mutants was assayed by Western blot analysis. As shown in Figure 3.28 A both mutant proteins were expressed in a similar level. Then the cellular localization of the His-*h*Par14 WT, His-Ser19/Ala *h*Par14 and His-Ser19/Glu *h*Par14 expressed in HeLa cells was examined. As expected, wild type *h*Par14 was located in the nucleus whereas mutant His-Ser19/Ala *h*Par14 showed significantly cytoplasmic localization (Figure 3.28 B). The phospho-mimetic His-Ser19/Glu *h*Par14 showed an interesting pattern. The protein was dispersed in the nucleus with strong staining around the nuclear membrane as shown in Figure 3.28 B.

The localization of WT *h*Par14 was observed to be nuclear in majority of the transfected cells. In contrast, the cells transfected with His-Ser19/Ala *h*Par14 exhibit strictly cytoplasmic localization. Taken together, our results clearly indicate that phosphorylation of *h*Par14 at Ser19 residue is important for nuclear localization.

A)

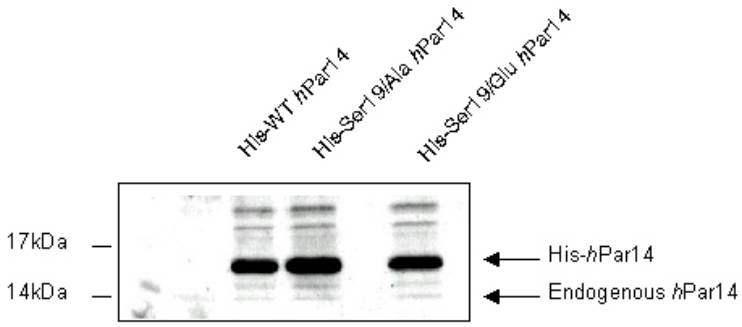

B)

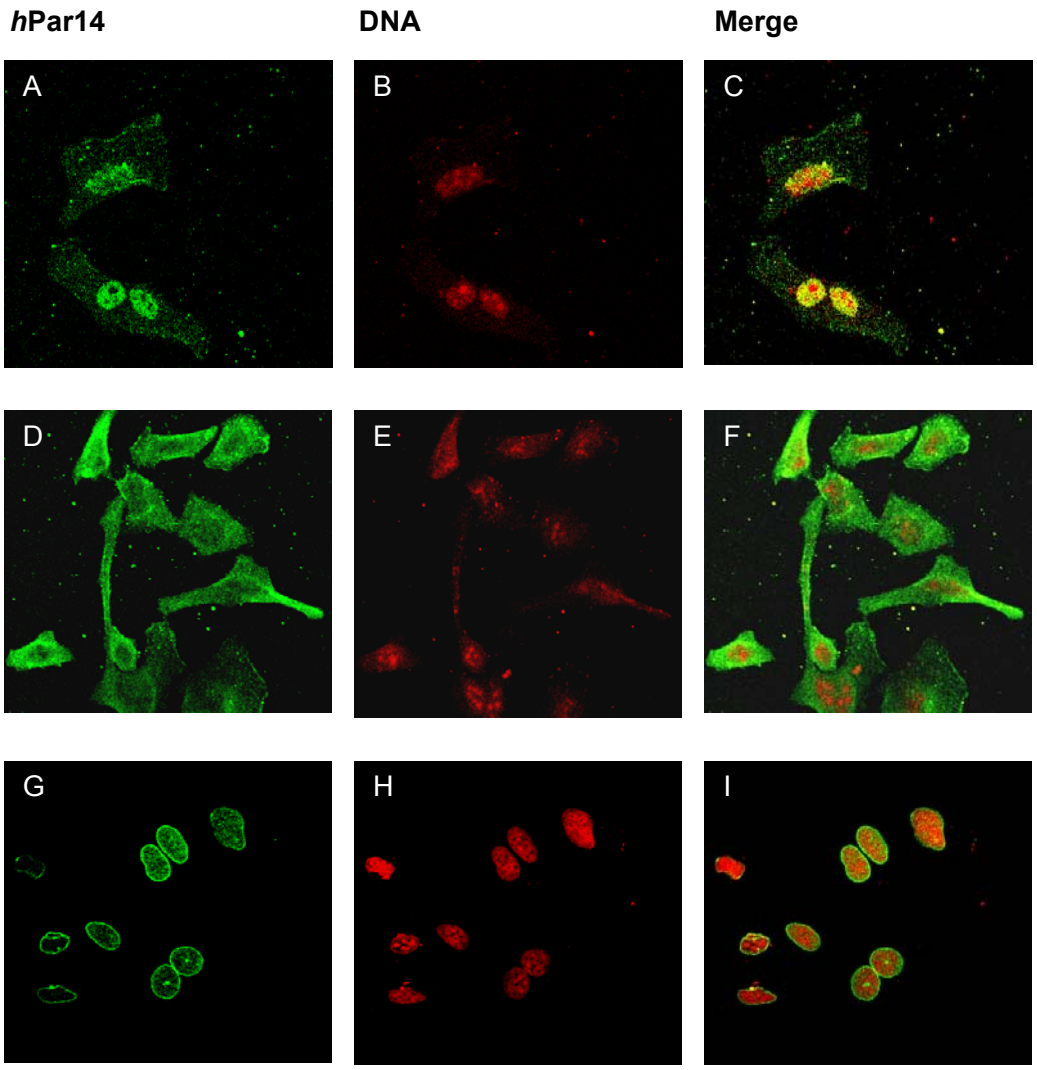

Figure 3.28 Mutation at Ser19 residue of *h*Par14 results in its cytoplasmic localization. **A)** Transfected cells with WT or mutants *h*Par14 were homogenized. Equal amount of total cellular protein was separated by SDS-PAGE and analysed by Western blot using anti-*h*Par14 antibody. C- non-transfected HeLa cells (control). **B)** Immunofluorescence analysis of HeLa cells transiently transfected with His-hPar14 WT, His-Ser19/Ala *h*Par14 and His-Ser19/Glu *h*Par14. Cells were fixed and incubated with anti-His antibody. Detection was done with a goat anti-mouse FITC antibody. Protein localization was analysed by confocal fluorescence microscopy. PI indicates propidium iodide, DNA staining. The letters indicate: A,B,C-His-*h*Par14 WT, D,E,F-His-Ser19/Ala *h*Par14 and G,H,I-His-Ser19/Glu *h*Par14.

3.3.7 Phosphorylation of *h*Par14 by CK2 alters interaction with DNA

To test whether phosphorylation of *h*Par14 influences the DNA binding properties of the protein the non-phosphorylated and non-radioactive CK2-phosphorylated *h*Par14 with 5'-end [γ^{32}P] labelled specific construct 1 (Figure 3.9) was incubated. The formation of complexes was monitored by electrophoretic mobility shift assay. Phosphorylation of *h*Par14 results in a slightly reduced binding affinity to the double-stranded construct 1 as shown by the decreased intensity of the DNA-protein complex (lane 3 and lane 4) (Figure 3.29).

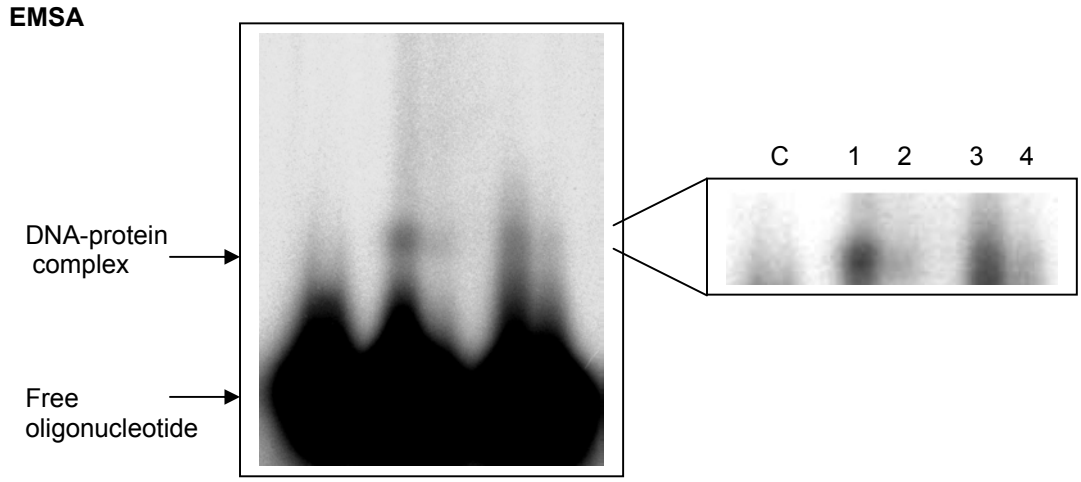

Figure 3.29 Phosphorylation of *h*Par14 by CK2 influences DNA binding. Electromobility shift assay (EMSA) of non-phosphorylated *h*Par14 (0.5 μg and 1 μg) (lane 1 and lane 3) and CK2 phosphorylated *h*Par14 (0.5 μg and 1 μg) (lane 2 and lane 4). Letter C indicates free oligonucleotide.

To test whether binding of DNA to *h*Par14 compete with phosphorylation, we performed kinase assay. Recombinant *h*Par14 was pre-incubated with non-labelled construct 1 and then subjected to phosphorylation with CK2. Incubation of *h*Par14 with DNA significantly decreases

phosphorylation by CK2 as compared to the control DNA poly dI/dC that did not affect the phosphorylation level (Figure 3.30). There were no detectable changes in a PPIase activity of *h*Par14 after phosphorylation by CK2 (Dr. Rahfeld, personal communication).

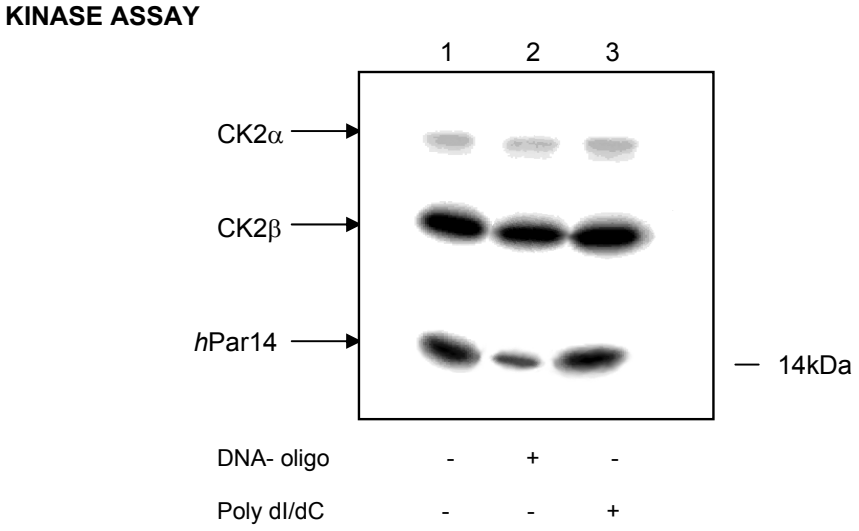

Figure 3.30 Decreased phosphorylation of hPar14 in the presence of DNA construct. Binding of specific DNA-oligo to *h*Par14 decrease phosphorylation by CK2 *in vitro*. Recombinant *h*Par14 (3 μg) was incubated with specific DNA-oligo prior phosphorylation with recombinant kinase. The bottom *arrow* indicates phosphorylated *h*Par14 in an absence of Construct 1 (lane 1), presence of Construct 1 (lane 2) and control non-specific DNA poly dI/dC (lane 3).

3.4 *h*Par14 interacts with 14-3-3 proteins

Preliminary phosphorylation experiments suggest a possible interaction between *h*Par14 and 14-3-3 proteins. Firstly, phosphorylation within N terminal extension of *h*Par14 by PKB and analysis of *h*Par14 primary amino acid sequence suggest the presence of a potential 14-3-3 binding motif. Secondly, unequal distribution of *h*Par14 between the cytoplasm and the nucleus suggests the existence of a slow protein export from the nucleus via binding to shuttling protein. Thirdly, at the time of our investigation interactions between *h*Par14 and 14-3-3 was also found by Dr. M. Yaffe (MIT, USA) (personal communication).

3.4.1 Expression and purification of recombinant GST-*h*Par14 and GST-14-3-3

The recombinant GST proteins were expressed and purified using glutathione affinity column. The purified protein fractions were analysed on SDS-PAGE and stained with Coomassie blue as shown in Figure 3.31.

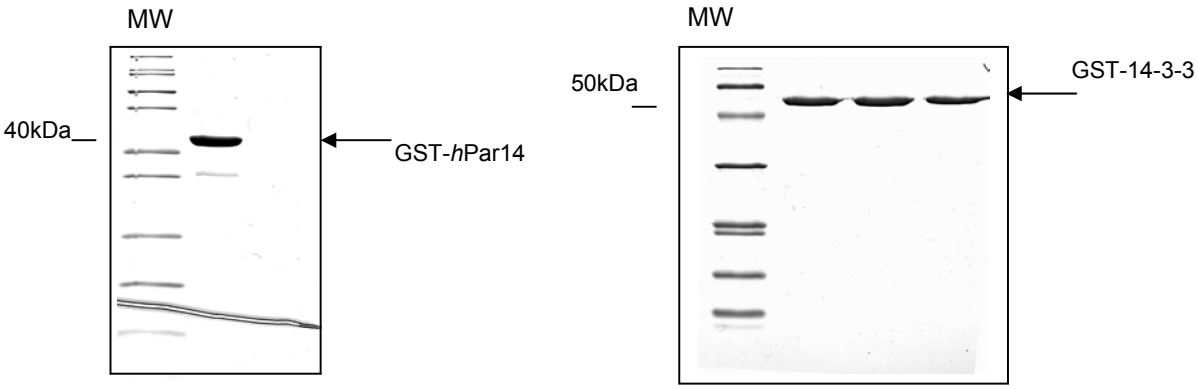

Figure 3.31 Expression of recombinant GST-*h*Par14 and GST-14-3-3. *Right panel*, GST-14-3-3 and *left panel*, purified GST-*h*Par14. Recombinant protein was expressed in *E.coli* and purified using affinity (GSH column), DEAE and gel filtration purification. Pure fractions were resolved onto SDS-PAGE and stained with Coomassie blue.

3.4.2 Detection of *h*Par14 and 14-3-3 interactions by GST pull down and immunoprecipitation

The interaction between *h*Par14 and 14-3-3 proteins was monitored by GST pull down assay. The equal amount of cellular proteins obtained from HEK293 extract were incubated with

glutathione agarose tagged with GST or with the GST-*h*Par14. Bound proteins were resolved on SDS-PAGE and immunoblotted with anti-14-3-3 antibody (recognizing all seven isoforms of 14-3-3 proteins). Western analysis verified that endogenous 14-3-3 from HEK293 was bound to the GST-*h*Par14 and not to GST alone as shown in Figure 3.32 A.

The same assay was used to confirm further the specificity of *h*Par14 and 14-3-3 interactions. The recombinant GST and GST-14-3-3 were incubated with ^{35}S-labelled *h*Par14 synthesized *in vitro*. Bound proteins were detected by autoradiography. Consistent with previous observation, *h*Par14 binds only to the GST-14-3-3 protein and not GST alone (Figure 3.32 B).

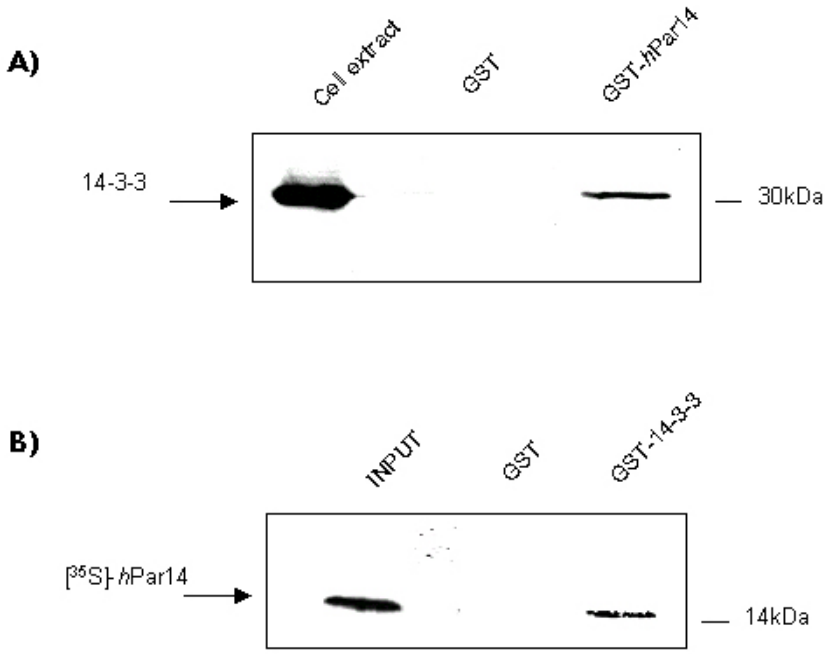

Figure 3.32 Both endogenous *h*Par14 from HEK 293 extract and *in vitro* translated *h*Par14 bind to 14-3-3 *in vitro*. **A)** Equal amount of HEK 293 cell extract was incubated with 5 μg of GST or GST-*h*Par14 and GSH beads. Bound proteins were separated by SDS-PAGE and analysed by Western blot using anti-14-3-3 antibody. **B)** [S^{35}] methionine-labelled *h*Par14, translated *in vitro* was incubated with GST or GST-14-3-3. Bound proteins were resolved by SDS-PAGE and detected by autoradiography.

GST pull-down studies indicate the *in vitro* interaction between *h*Par14 and 14-3-3 proteins and it was necessary to investigate whether the same interaction can be observed in HeLa cells. Therefore, immunoprecipitation analysis using HeLa cells co-transfected with tagged DNA constructs encoding His-*h*Par14, HA-14-3-3γ, HA-14-3-3θ and HA-14-3-3ξ proteins, was

performed. Cells were lysed and incubated with anti-His antibody to separate the tagged *h*Par14 associated proteins from cell extract. The Western analysis with antibodies specific to tag revealed that HA 14-3-3θ (lane 3), HA 14-3-3γ (lane 6) and HA 14-3-3ξ (lane 9) co-precipitated along with anti-His antibody (Figure 3.33). In a parallel experiment, the same blot was incubated with anti-His and 14-3-3 antibodies. As shown in Figure 3-33, His-*h*Par14 as well as 14-3-3 is present in all co-precipitated samples (Figure 3.33).

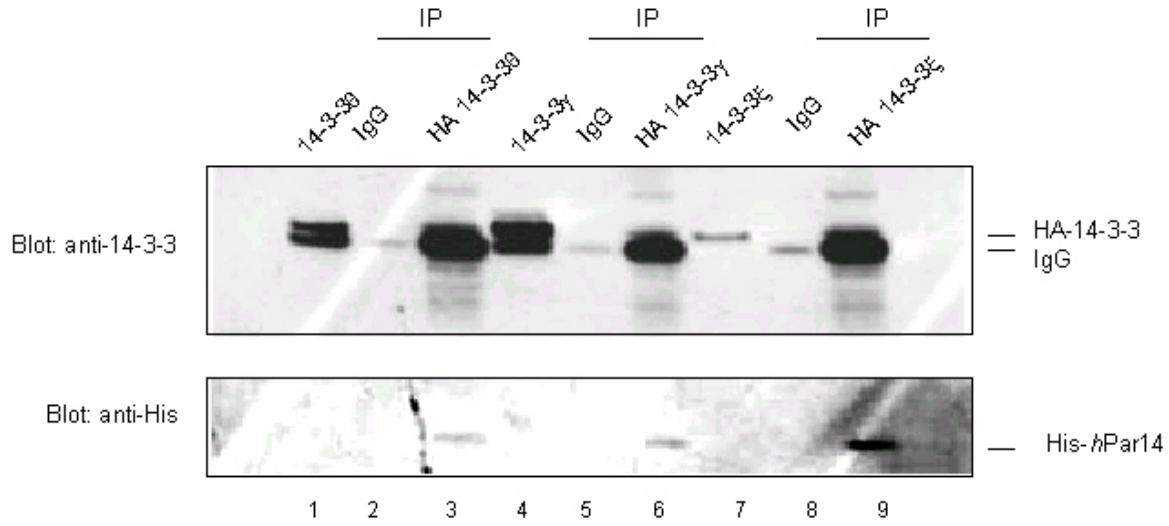

Figure 3.33 Co-immunoprecipitation of *h*Par14 with 14-3-3 proteins. Transiently transfected HeLa cells with either 14-3-3 isoforms alone or His-*h*Par14/HA-14-3-3γ, His-*h*Par14/HA-14-3-3θ, His-*h*Par14/HA-14-3-3ξ were homogenized and subjected to immunoprecipitation using anti-HA antibody. The immuno-complexes were incubated with protein A/G sepharose. Beads were washed and 2x LDS sample buffer was added. Eluted proteins were separated by SDS-PAGE and analysed by Western blot using anti-His antibody for His-*h*Par14 and anti- 14-3-3. Lanes indicate: 1,4, 7, control cells transfected only with 14-3-3 isoforms; lanes 2, 5, 8, IP with IgG from cells expressing His-*h*Par14/HA-14-3-3 isoforms; lanes 3, 6, 9 IP with anti-HA from cells expressing His-*h*Par14/HA-14-3-3 isoforms. IP-immunoprecipitation; WB-Western blot.

The previous data showed the interaction between *h*Par14 and 14-3-3 homodimer. The 14-3-3 proteins exist either as a homodimer or heterodimer (Zhang, et al., 1997). To determine whether the *h*Par14 interacts with 14-3-3 heterodimer, a co-immunoprecipitation was performed. HeLa cells transfected with DNA constructs encoding His-*h*Par14 and V5-14-3-3δ/ζ

proteins were subjected to immunoprecipitation using anti-His and anti-V5 antibodies. Bound proteins were resolved on SDS-PAGE and detected by Western blotting. As shown in Figure 3.34, His-*h*Par14 binds to 14-3-3δ/ζ heterodimer.

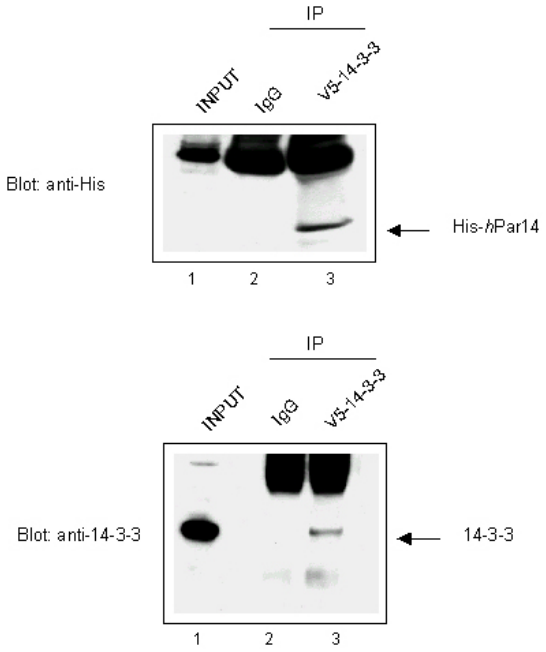

Figure 3.34 *h*Par14 interacts with heterodimer 14-3-3δ/ζ. Transfected HeLa cells with His-*h*Par14/V5-14-3-3 δ/ζ were homogenized and proteins from cell extract immunoprecipitated using V5 antibody. The immuno-complexes were incubated with protein A/G sepharose. Bound proteins were washed and 2x LDS sample buffer was added. Eluted proteins were separated by SDS-PAGE and analysed by Western blot using anti-14-3-3 or anti-*h*Par14 antibodies. *Upper picture,* lane 1-cells transfected with V5-14-3-3 alone, lane 2- IP anti-IgG mouse (control), lane 3- IP anti-V5. *Lower picture*, lane 1- cells transfected with V5-14-3-3 alone, lane 2- IP anti-IgG mouse (control), lane 3-IP anti-V5. IP-immunoprecipitation; WB- Western blot.

3.4.3 Binding of *h*Par14 to 14-3-3 is phosphorylation dependent

The phosphorylated serine residues of the 14-3-3 ligands are believed to play an important role in the interaction between the two proteins. The earlier findings that *h*Par14 prepared by *in vitro* translation binds to 14-3-3 suggested that either the interaction is phosphorylation-independent or *h*Par14 is phosphorylated by an endogenous kinase present in the reticulocyte lysate. To test whether phosphorylation is required for the interaction of *h*Par14 with 14-3-3, ^{35}S labeled-*h*Par14 was incubated with a broad-spectrum calf intestine phosphatase (CIP), prior to a pull down assay with GST-14-3-3. As a control, the same amount of labeled protein

was incubated with CIP in the presence of a phosphatase inhibitor cocktail. Intact *h*Par14 binds to GST-14-3-3 (lane 1) as well as protein incubated with the phosphatase inhibitor (lane 2). The incubation of protein with phosphatases (CIP) decreases binding to GST-14-3-3 (lane 3) (Figure 3.35 A) indicating that phosphorylation of *h*Par14 by a protein kinase (s) within the reticulocyte lysate is required for *h*Par14 to interact with 14-3-3. To test, whether the endogenous *h*Par14 from cell lysate binds to 14-3-3 in a similar phosphorylation dependent manner, HEK293 lysate was pre-incubated with CIP alone or CIP in the presence of phosphatase inhibitors prior to a pull down assay with GST-14-3-3. Consistent with previous data, intact *h*Par14 (lane 1) or protein incubated with CIP in the presence of phosphatase inhibitors (lane 2) binds to GST-14-3-3. Dephosphorylation of *h*Par14 with CIP decreases binding to GST-14-3-3 (lane 2) (Figure 3.35 B).

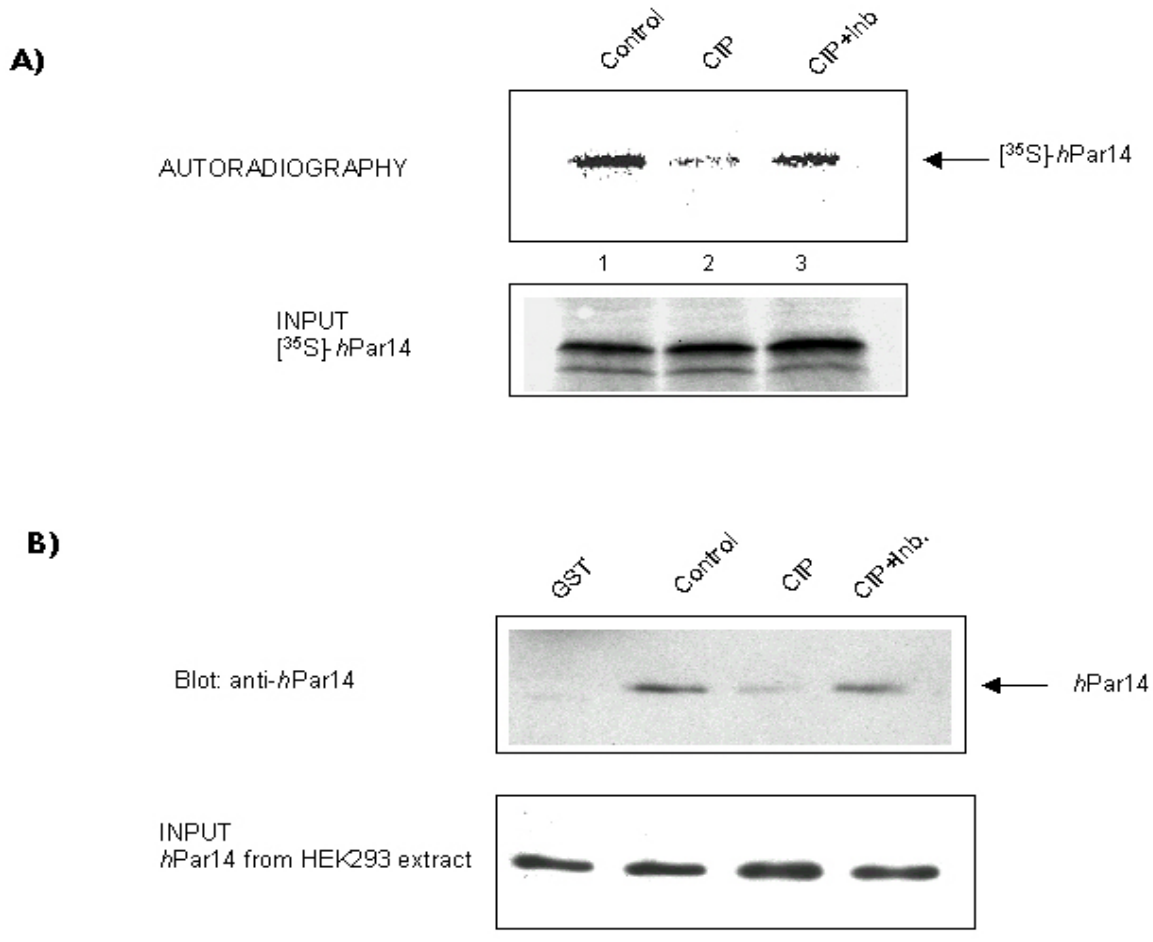

Figure 3.35 Phosphorylation of *h*Par14 is required for binding to 14-3-3 proteins. **A)** [^{35}S] methionine-labelled *h*Par14 was synthesized using *in vitro* translation kit. The protein was dephosphorylated with alkaline calf phosphatase (CIP) (200U) or phosphatase supplied with inhibitors and incubated with GST

alone or GST-14-3-3 in the presence of GSH beads. Beads were washed and boiled in Laemmli sample buffer. Eluted proteins were separated by SDS-PAGE and detected by autoradiography. As a control, *h*Par14 non-treated with phosphatase was used. **B)** HEK293 cell extract was incubated with CIP in the absence or presence of inhibitors of phosphatases, added to GST or GST-14-3-3. Bound proteins were resolved by SDS-PAGE and analysed by Western blot using anti-*h*Par14 serum. The lower picture indicates input of HEK293 extract used in the experiment.

3.4.4 Identification of 14-3-3 binding site within *h*Par14

Analysis of *h*Par14 amino acid sequence using NetPhos 2.0 identified two residues Ser7 and Ser9 as putative phosphorylation sites for PKB and PKC (Figure 3.16). Moreover, the phosphorylation of *h*Par14 within N terminal extension by PKB and PKC was identified (Figure 3.17). To test whether Ser7 and Ser9 residues are indeed phosphorylated *in vitro*, both residues were mutated to alanine. The mutant, recombinant protein was subjected to kinase assay. As shown in Figure 3.36 only wild type *h*Par14-His is phosphorylated by both PKB and PKC (lane 1, lane 2). The mutation at both Ser7 and Ser9 residues in *h*Par14 completely abolished phosphorylation by PKB (lane 3) and PKC (lane 4) (Figure 3.36).

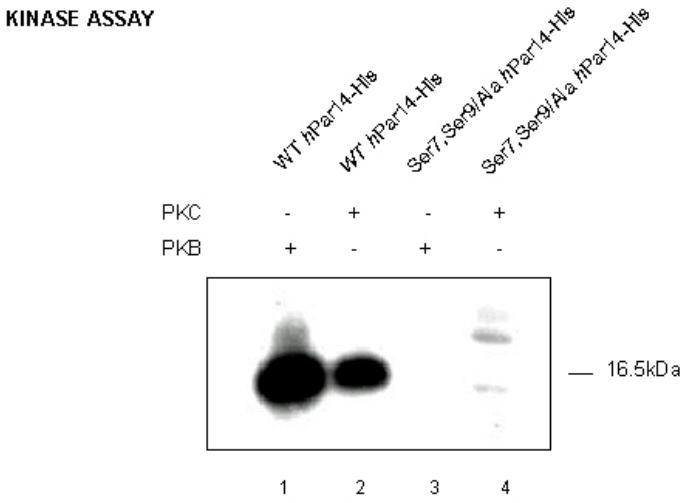

Figure 3.36 The wild type *h*Par14 and not mutant Ser7,Ser9/Ala *h*Par14-His is phosphorylated by PKB and PKC. The recombinant proteins were expressed in *E. coli*, purified and subjected to a kinase assay with either recombinant PKB or PKC. The protein mixture was incubated with Ni-NTA beads. Beads were washed and boiled in Laemmli sample buffer. Eluted proteins were separated by SDS-PAGE and protein phosphorylation was analysed by autoradiography. Lanes indicate: 1, 2- wild type *h*Par14-His 3,4-mutant Ser7,Ser9/Ala *h*Par14-His.

Since it has been demonstrated that *h*Par14 is phosphorylated at Ser7 and Ser9 by either PKB or PKC within motif KGKSGSGK and the fact that the substrates for PKB bind to 14-3-3 (Fu, et al., 2000), it was necessary to look for sequence similarities to known 14-3-3-binding motifs. The sequence surrounding the phosphorylated Ser7 and Ser9 residues in KGKSGSGK of *h*Par14 corresponds to the canonical R(K)x_{1-2}Sx_{1-3}S (so called Type I) recognition motifs of 14-3-3 proteins as shown in Figure 3.37.

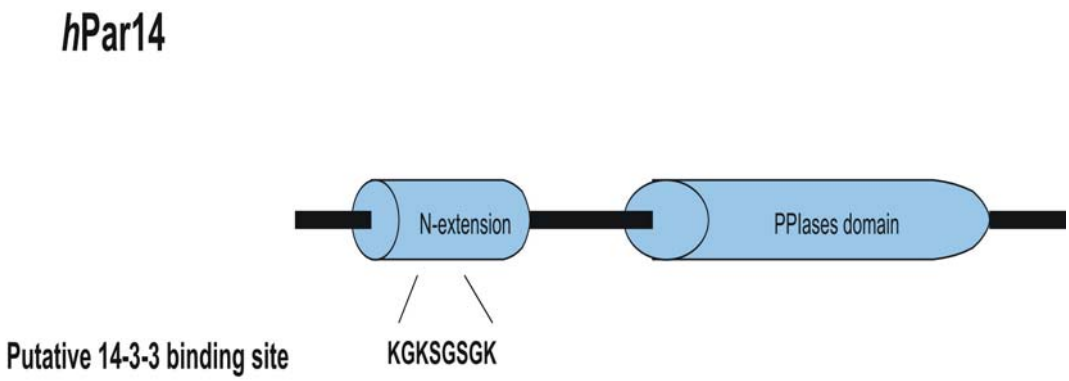

Figure 3.37 Schematic representation of putative 14-3-3 binding site within *h*Par14.

To verify that these sites were responsible for the phosphorylation-dependent binding of *h*Par14 to 14-3-3, Ser7 and Ser9 residues in *h*Par14 were mutated to alanine and binding to 14-3-3 was examined following the *in vitro* translation. The recombinant [^{35}S] labeled proteins were incubated with GST or GST-14-3-3 and binding detected by autoradiography. As shown in Figure 3.38 wild type (WT) *h*Par14 binds to GST-14-3-3. Single mutation in one of the predicted residues did not influence binding to GST-14-3-3, however double mutation completely abolish interaction with GST-14-3-3.

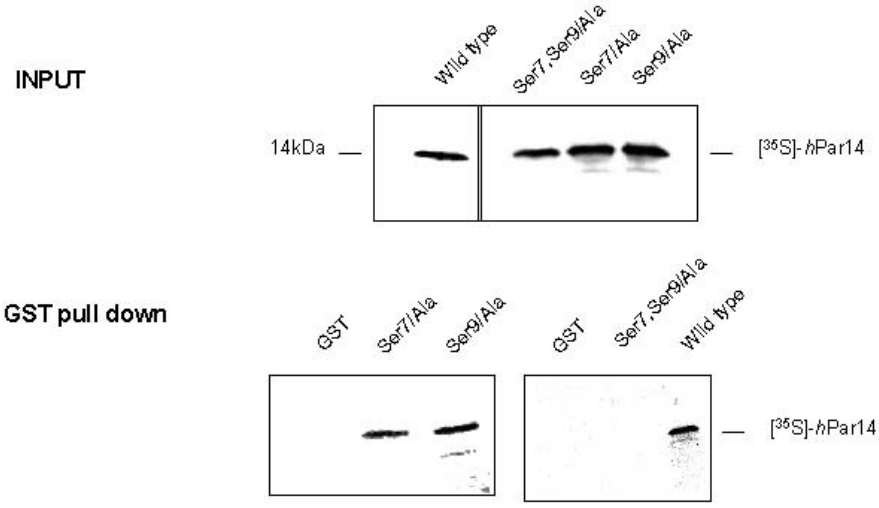

Figure 3-38 Binding of *in vitro* translated *h*Par14 WT and its mutants to GST-14-3-3. [^{35}S] methionine-labeled wild type *h*Par14 and mutants Ser7/Ala *h*Par14, Ser9/Ala *h*Par14 and Ser7,Ser9/Ala *h*Par14 were incubated with GST, GST-14-3-3 and GSH beads. Beads were washed and boiled in sample buffer. Bound proteins were separated by SDS-PAGE and detected by autoradiography.

3.4.5 Co-expression of *h*Par14 and 14-3-3 co-localize proteins in cytoplasm

14-3-3 proteins are reported to localize in the cytoplasm, however, recent data suggest that they can also transit to the nucleus and participate in dynamic nucleocytoplasmic transport (Brunet, et al., 2002). The effect of co-expression HA-14-3-3 with His-*h*Par14 on the subcellular protein localization was investigated. At first, localization of 14-3-3 expressed in HeLa cells was tested. The protein is localized in the cytoplasm in agreement with previous reports (Figure 3.39).

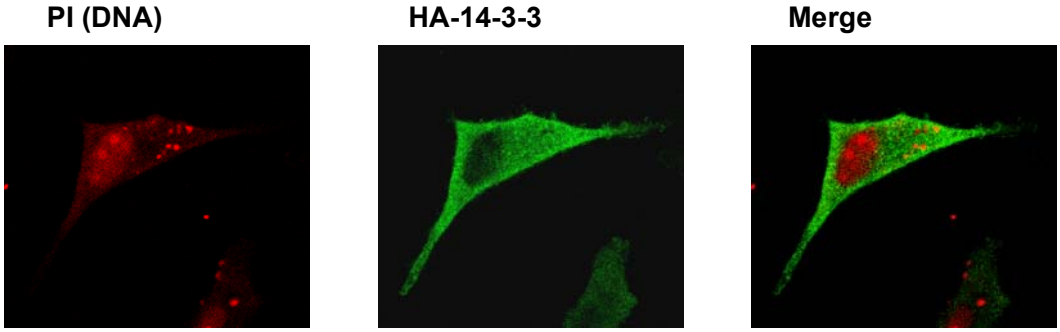

Figure 3.39 Localization of 14-3-3γ in HeLa cells. Transfected cells with 14-3-3γ construct were fixed and incubated with anti-HA antibody. Followed incubation with secondary goat anti-rabbit FITC coupled

antibody, cells were analysed by confocal fluorescence microscopy. Scale bar, 10μm. The nucleus was visualized with propidium iodide (PI).

Next, the effect of co-expression of HA 14-3-3γ with His-*h*Par14 wild type or mutant His-Ser7,Ser9/Ala *h*Par14 was tested (Figure 3.40 A). The double immunofluorescence staining of transfected cells revealed that co-expression of HA 14-3-3 with His-*h*Par14 significantly increased the cytoplasmic localization of His-*h*Par14 wild type, however, co-expression of HA 14-3-3 had no effect on the predominantly nuclear localization of the His-Ser7,Ser9 *h*Par14 mutant (Figure 3.40 B).

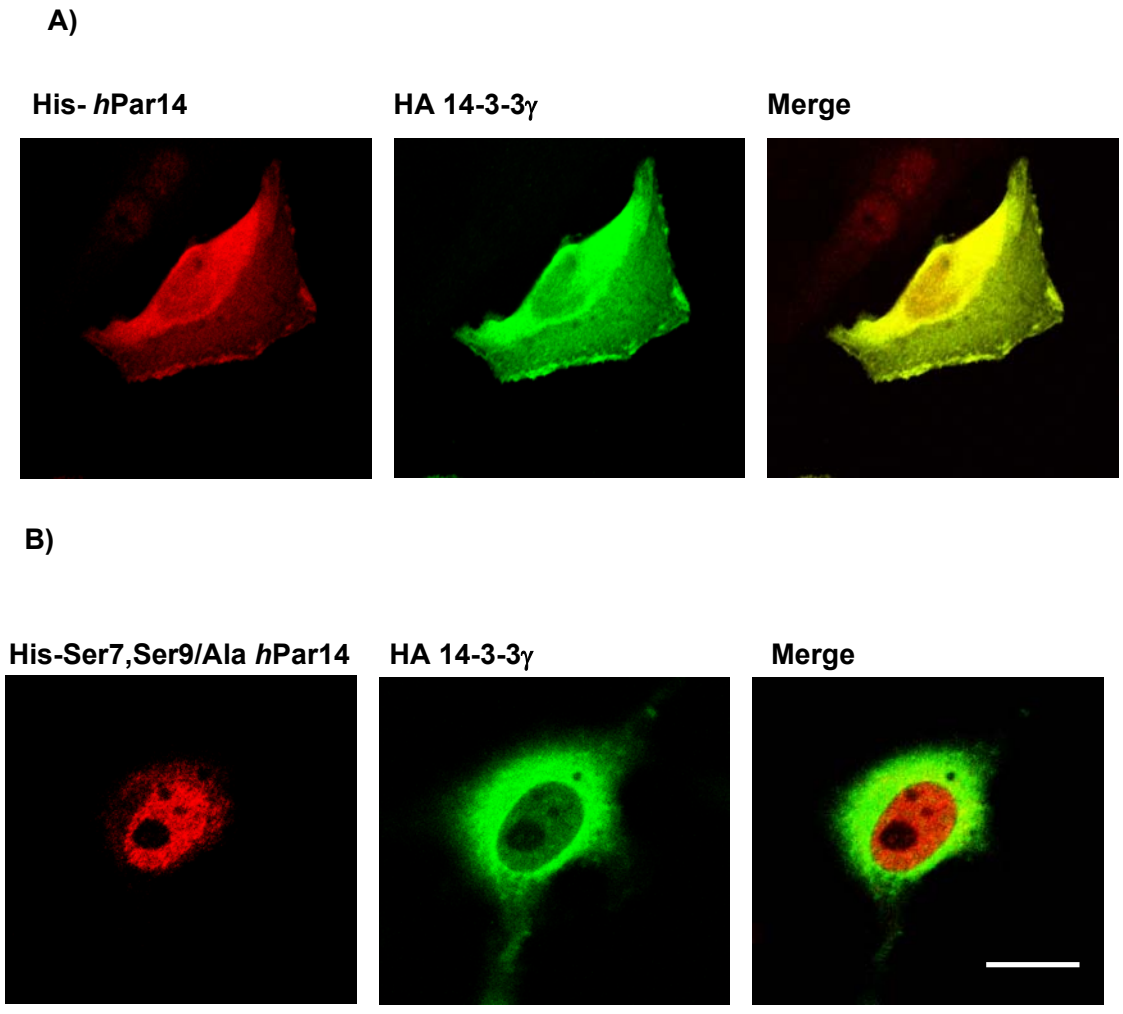

Figure 3.40 Co-localization of His-*h*Par14 wild type, mutant Ser7,Ser9/Ala His-*h*Par14 with HA 14-3-3γ. **A)** cells transfected with wild type His-*h*Par14/HA 14-3-3γ and **B)** with mutant His-Ser7,Ser9 *h*Par14/HA 14-3-3γ were fixed, permeabilized and incubated with anti-His and anti-HA antibodies. Followed

incubation with secondary FITC and TRITC coupled antibodies, cells were analysed at objective C-Apochromat 63x/1.2 W corr by using confocal fluorescence microscopy. Bar scale, 10μm.

Cells co-expressing *h*Par14/14-3-3 showed three different cellular localizations of *h*Par14, namely, predominantly nuclear, predominantly cytoplasmic and nuclear-cytoplasmic (Figure 3.41A). In cells expressing high levels of His-*h*Par14 with HA-14-3-3, around 75 % showed cytoplasm-dominant staining indicating accumulation of *h*Par14 in the cytoplasm. Less then 25 % of the cells demonstrated nuclear-cytoplasmic localization (Figure 3.41 C). The wild type *h*Par14 expressed in cells showed strict nuclear localization in around 60 % of counted cells (figure 3.41 B). Our results suggest that binding of 14-3-3 promotes the cytoplasmic retention and /or nuclear exclusion of His-*h*Par14.

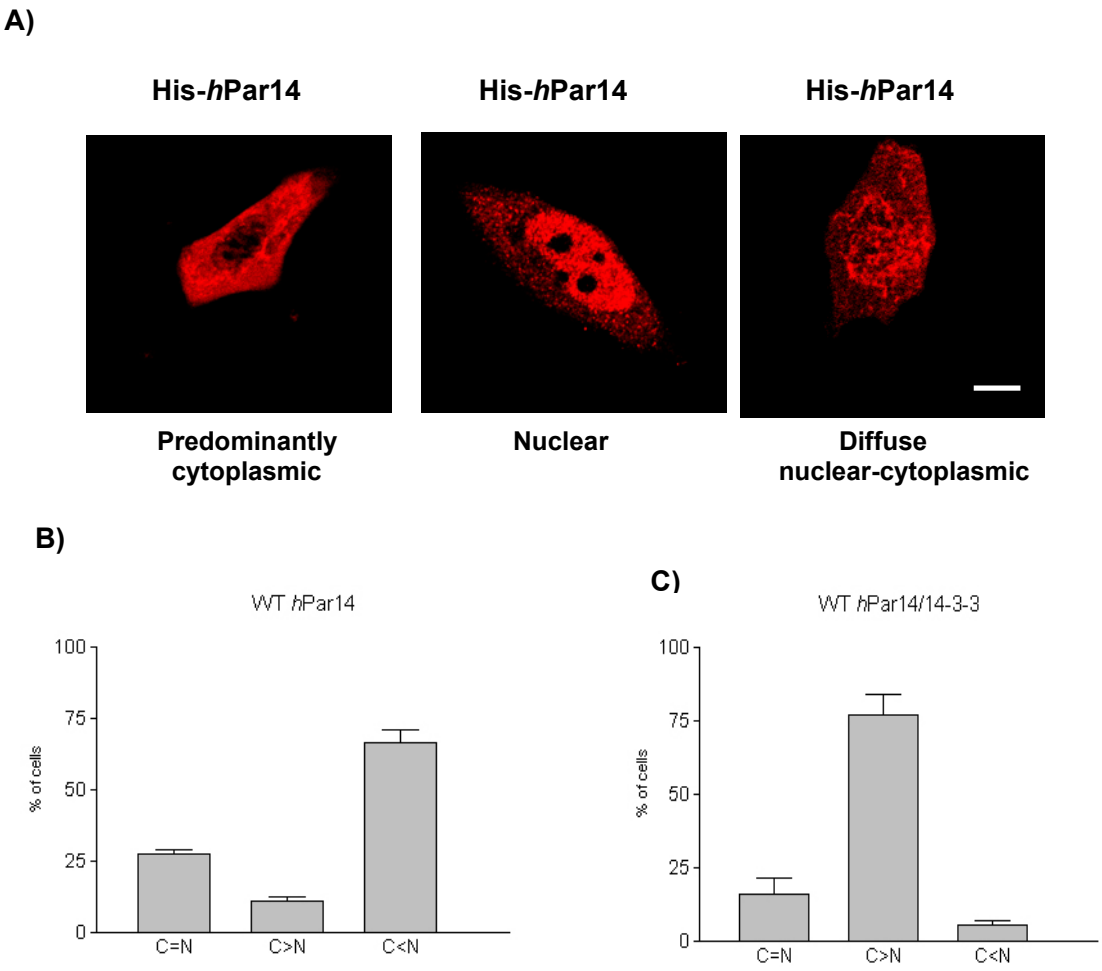

Figure 3.41 Co-localization of wild type *h*Par14 and 14-3-3γ in HeLa cells. **A)** localization of *h*Par14 in co-transfected cells with 14-3-3. The transfected cells were analysed by confocal fluorescence microscopy. Bar scale, 10μm. **B)** quantitative analysis of subcellular distribution of wild type *h*Par14 and

C) *h*Par14 co-expressed with 14-3-3. Cellular localization of *h*Par14 was scored according to whether it was higher in the nucleus (C<N), evenly distributed between nucleus and cytoplasm (C=N) or higher in cytoplasm (C>N). Around 300 cells were counted. Black lines indicate mean error.

3.4.6 Mapping the site on 14-3-3 responsible for binding to *h*Par14

Current reports demonstrated the importance of Lys49 located in helix αI of 14-3-3 protein for binding negatively charged ligands. The mutant that has Lys49 replaced by Glu (Lys49/Glu) has the same conformation as wild type 14-3-3 and is able to form homo-and heterodimers *in vitro* and *in vivo* (Zhang, et al., 1997, Brunet, et al., 2002) but is unable to bind to numerous 14-3-3 binding proteins including Raf (Zhang, et al 1997). The X-ray crystallographic studies revealed that Lys49 forms part of a positively-charged substrate-binding pocket in the central binding groove of 14-3-3 (Figure 3.42), where it directly coordinates the phosphoserine phosphate of 14-3-3 binding peptides (Yaffe, et al., 1997; Rittinger, et al., 1999). These structural observations on peptides suggested that the Lys49 mutation would be generally deficient in binding to phosphorylated protein ligands.

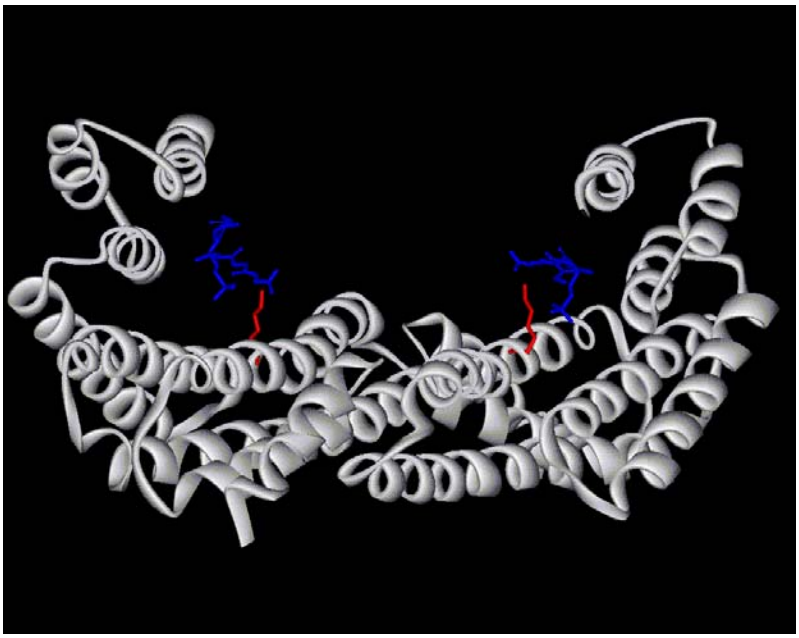

Figure 3.42 The 14-3-3 zeta dimer complexed with a phosphoserine-containing peptide derived from Raf (pdb-code: 1A37). Monomers (white) consist of nine α-helices. The red sticks represent amino acid Lys49 in the phosphoserine-binding pocket and blue sticks are peptide substrate.

3.4.6.1 Expression and purification of wild type and mutant Lys49/Glu 14-3-3 protein

The recombinant His-Lys49/Glu 14-3-3 was expressed and purified using Ni-NTA affinity chromatography. The purified protein fractions were analysed on SDS-PAGE and stained with Coomassie blue (Figure 3.43).

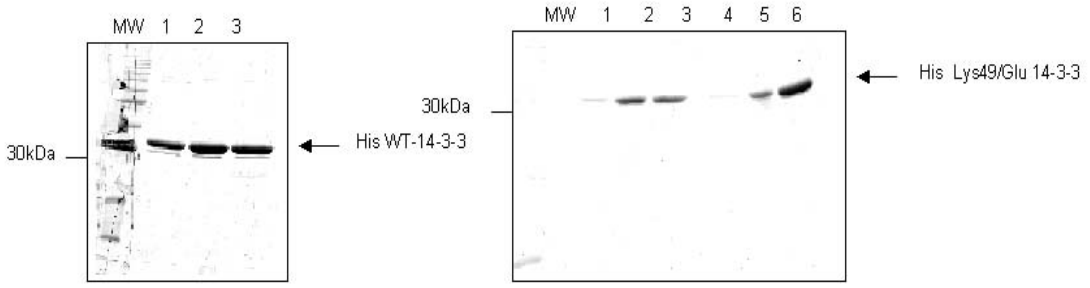

Figure 3.43 Purification of recombinant His WT14-3-3 and His Lys49/Glu 14-3-3. Recombinant proteins wild type and mutant 14-3-3 were expressed in *E. coli* and purified using affinity chromatography with Ni-NTA. The fractions were separated by 15 % SDS-PAGE or 10 % SDS-PAGE and proteins stained with Coomassie blue.

3.4.6.2 Lysine 49 in helix αI of 14-3-3 protein is important for binding *h*Par14

To investigate whether *h*Par14 binding occurs through the central binding groove of the 14-3-3 dimer, the binding assay with non-tagged *h*Par14 wild type and mutant His Lys49/Glu 14-3-3ε was performed. Equal amounts of [^{35}S] labelled wild type *h*Par14 (non-tagged) were incubated with Ni-NTA agarose tagged with His 14-3-3 wild type and mutant His-Lys49/Glu 14-3-3ε. Bound proteins were subjected to SDS-PAGE and detected by autoradiography. As shown in Figure 3-44, *h*Par14 binds only to wild type His 14-3-3 (line 1) and does not bind to the mutant His Lys49/Glu 14-3-3ε (lane 2). As a control, we used Ni-NTA beads alone incubated with labeled *h*Par14 (lane 3) or only with His Lys49/Glu 14-3-3.

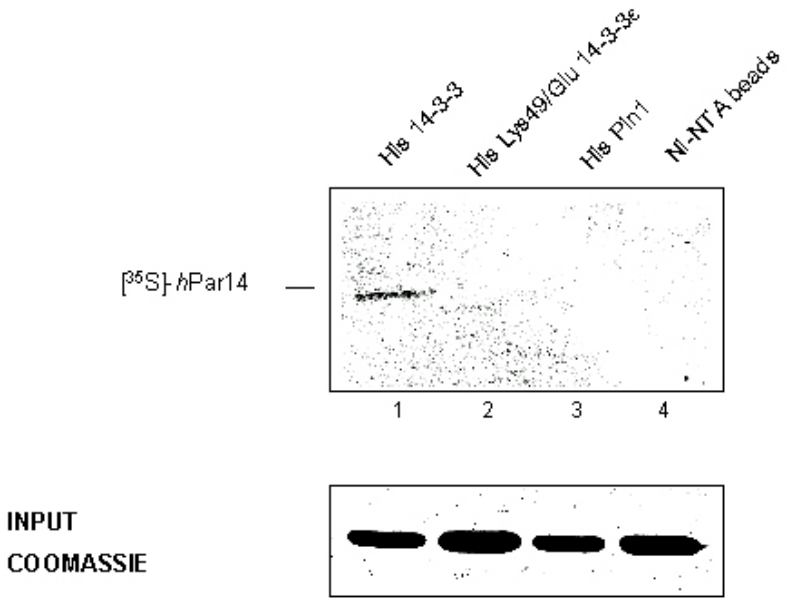

Figure 3.44 Mapping *h*Par14 binding site on 14-3-3. Translated *in vitro* ^{35}S-labelled non tagged *h*Par14 was incubated with 5 μg of recombinant proteins: His 14-3-3ζ/δ wild type, His Lys49/Glu 14-3-3 and His-Pin1 in the presence of Ni-NTA beads. Beads were washed and boiled in a sample buffer. Eluted proteins were separated by SDS-PAGE and detected by autoradiography. Lanes indicate: 1- His 14-3-3 wild type, 2- His Lys49/Glu 14-3-3ε , 3-His-Pin1 and 4- control (Ni-NTA beads).

It was previously shown that ligand binding defective mutant Lys49/Glu 14-3-3ε does not associate with phosphorylated substrates *in vitro* and *in vivo*. The mutant 14-3-3 is localized in the nucleus (Brunet et al., 2002). If the helix αI of 14-3-3 function as a true ligand binding site, co-expression of mutant 14-3-3 with *h*Par14 should localize *h*Par14 exclusively in the nucleus. The immunolocalization study showed that both proteins localize in the nucleus, supporting the hypothesis that lysine 49 is truly involved in *h*Par14 binding (Figure 3.45).

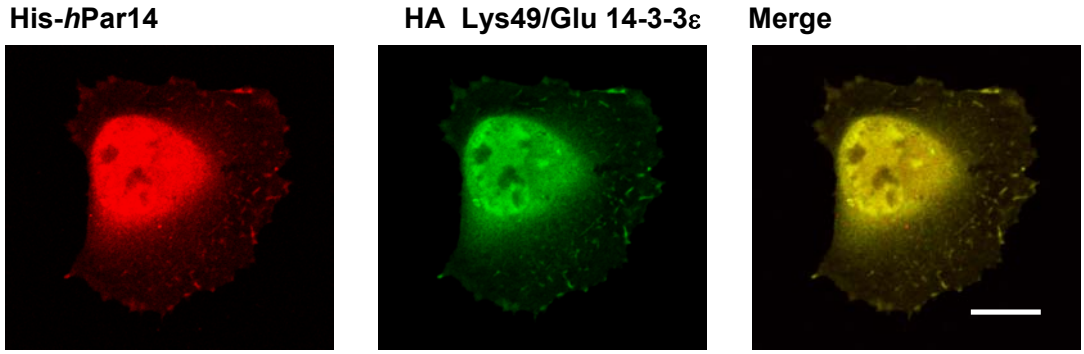

Figure 3.45 Nuclear co-localization of mutant 14-3-3ε with His-*h*Par14 wild type. Transfected cells with His-*h*Par14/HA Lys49/Glu 14-3-3ε mutant were fixed, permeabilized and incubated with anti-HA and

anti-His antibodies. Followed incubation with secondary FITC or TRITC coupled antibodies, cells were analysed at objective C-Apochromat 63x/1.2 W corr by using confocal fluorescence microscopy. Bar scale, 10μm.

3.4.7 Leptomycin B inhibits cytoplasmic co-localization of *h*Par14 with 14-3-3

It is now clearly establish that 14-3-3 proteins, in cooperation with Crm1 (an export protein), are involved in active export of substrate proteins from the nucleus (Muslin, et al., 2001; Rittinger, et al., 2001; Brunet, et al., 2002). Binding of 14-3-3 to their ligands represents a critical step in this process. To test whether Crm1 mediates nuclear export of *h*Par14, we transfected HeLa cells with His-*h*Par14 construct and incubated with leptomycin B (LMB). Leptomycin B was originally discovered as a potent anti-fungal antibiotic from *Streptomyces sp.* (Hamamoto, et al., 1983). Later, it has been shown that leptomycin B is a potent inhibitor of Crm1 mediated nuclear export (Kudo, et al., 1999). Treatment with LMB did not influence localization of *h*Par14 as shown in Figure 3.46.

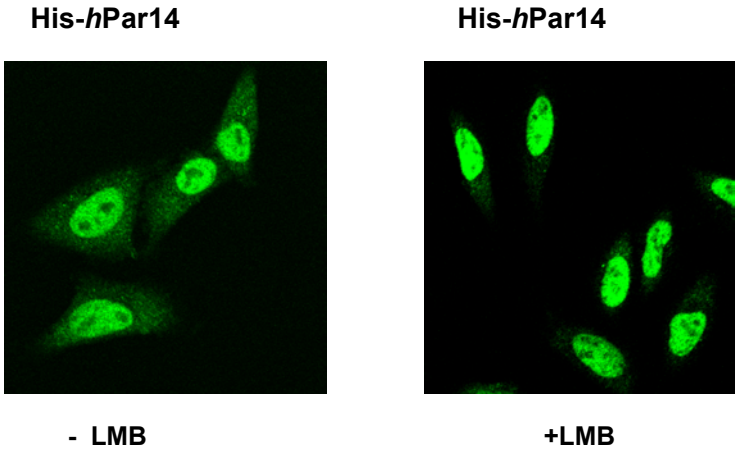

Figure 3.46 Treatment with LMB does not change localization of *h*Par14. Transfected HeLa cells with His-*h*Par14 were starved in 0.1 % serum for 24 h, treated with LMB (5 ng/ml) for 2 h and restimulated with serum. Cells were fixed, incubated with anti-His followed secondary goat anti-mouse FITC coupled antibodies and analysed at objective Plan Apochromat 40x by using confocal fluorescence microscopy.

To investigate whether cytoplasmic retention of *h*Par14 in co-expression with 14-3-3 is due to the active export from the nucleus, we performed the same experiment with HeLa cells co-transfected with His-*h*Par14 and HA 14-3-3γ constructs. The cells were maintained in 0.1% serum for 24 h and then incubated with leptomycin for two hours. After that time, cells were re-stimulated with 10 % serum. Immunofluorescence analysis revealed that in majority of cells

treated with LMB, *h*Par14 and 14-3-3 localize exclusively in the nucleus (Figure 3.47). This findings support the idea that binding of 14-3-3 promotes export of *h*Par14 to the cytoplasm.

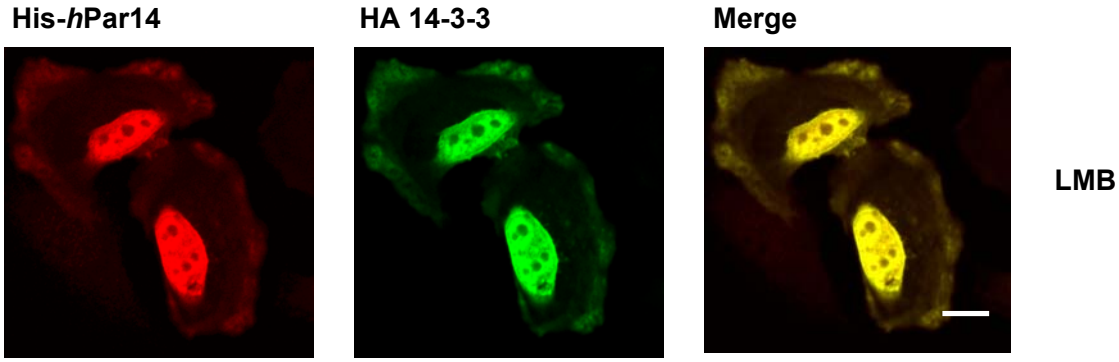

Figure 3.47 Nuclear co-localization of *h*Par14 and 14-3-3γ in cells treated with leptomycin B. Transfected cells with His-*h*Par14/HA 14-3-3γ were serum starved for 24h, treated with LMB (5 ng/ml) for 2h and restimulated with serum. Cells were fixed, incubated with anti-HA and anti-His antibodies followed staining with FITC or TRITC coupled secondary antibodies and analysed at objective C-Apochromat 63x/1.2 W corr by using confocal fluorescence microscopy. Bar scale, 10μm.

4. Discussion

Parvulins represent one of the three families of enzymes sharing peptidyl-prolyl *cis-trans* isomerase activity. They are ubiquitously expressed proteins in living organisms. While eukaryotic human parvulin Pin1 and prokaryotic parvulins have been studied in details, little is known about the function of a second human parvulin, *h*Par14.

4.1 The N-terminal basic domain of hPar14 is responsible for the entry to the nucleus and high affinity DNA-binding

In this study we demonstrated that the peptidyl prolyl *cis/trans* isomerase *h*Par14 is unevenly distributed in HeLa cells. It is present in a two fold greater amount in nucleus then in cytoplasm. Amino acid residues Ser7 to Lys14 are necessary for the targeting to the nucleus. The protein binds preferentially to bent A-tract sequences in the nanomolar range, as revealed by fluorescence titration experiments and electromobility shift assay. NMR studies showed that the binding interface on the PPIase domain of *h*Par14 is limited to a hydrophobic wedge consisting of 11 amino acids residues and is flanked by four polar residues. Additionally, six residues from the flexible N-terminal basic domain are directly involved in binding to double-stranded DNA and are necessary for high-affinity binding.

The nuclear localization of *h*Par14 suggests that the protein is involved in processes like transcription, chromatin architecture or cell cycle regulation. This is supported by the fact that *h*Pin1/Ess1, the closest relatives of *h*Par14 in human and yeast, are required for cell cycle regulation in HeLa cells and transcription regulation in yeast. In contrast to its homologues, which are found exclusively in the nucleus, *h*Par14 is shuttled between nucleus and cytoplasm. The sequence necessary for targeting *h*Par14 to the nucleus is restricted to a short stretch of eight residues, which does not exhibit a classical NLS sequence. This sequence contains two serine residues, which are putative targets for phosphorylation according to a NetPhos 2.0 prediction. Phosphorylation and dephosphorylation are potential signals to shuttle proteins between cytoplasm and nucleus (e.g. β-catenin) when triggered by a signal transduction cascade.

Our experiments suggest that *h*Par14 might be associated with double-stranded DNA in the nucleus. Although this has to be proven *in vivo*, the preference of the protein to bind tightly bent DNA might indicate a function in chromatin remodeling. This hypothesis is supported by the work of Wu et al.,2000 and Arevalo-Rodriguez, et al.,2000 who suggest that the effect of parvulins from higher organisms on the cell cycle is due to the control of cell-cycle genes. According to their studies, parvulins antagonize the histone deacetylation activity, thereby

participating in chromatin remodeling and in the transcription of genes required for mitosis. Chromatin remodeling is the mechanism of action of HMGN proteins. The presence of HMGN2 (HMGN-17) affects the rate of acetylation of the N termini of nucleosomal histones *in vitro*. The region AEGDAFGDKAKV of HMGN2, which is required for specific acetylation (Herera, et al., 1999), mimicks the sequence motif KxxG(G/A)Kx(notG)xK, that is acetylated in H3 (Kuo, et al., 1996). *h*Par14 contains the motif KSGSGKAGKGGA, which could serve as a putative competitor for the acetylation site of HMGN or histone proteins. The N-terminal sequence of *h*Par14 shows a striking similarity of 46 % to the flanking sequences of the CHUD domain of HMGN2 (Figure 3.6). Gly8, Lys14 and Ala18 of the *h*Par14, which are conserved between both proteins, are involved in direct binding to DNA. This indicates that the N terminus of HMGN2 and the N terminus of *h*Par14 share a common binding mode. As the N terminus of *h*Par14 and the N terminus of the CHUD domain of HMGN2 are prerequisites for high-affinity binding to tightly bent DNA, both proteins might target very similar substrate motifs at the chromatin scaffold.

NMR titration experiments of *h*Par14 with DNA suggest that the N terminus of the protein is involved in direct DNA binding and the PPIase domain should make contacts to DNA (Surmacz, et al.,2002). Interestingly, there are structural features in the PPIase domain of hPar14 that can be found in other DNA-binding proteins, the so-called HMGB domains.

HMGB motifs occur in sequence specific transcription factors like SRY and Lef-1 and the chromosomal associated vertebrate HMG1 and HMG2 proteins, which bind with low sequence specificity to DNA (Travers, 2000). The DNA-binding site presents a hydrophobic patch that conforms to the minor groove. At the center of the interface side chains of various residues insert deeply into the minor groove of the bent DNA. Among the family of HMGB domains, the components of the hydrophobic wedge are conserved, comprising residues 9, 12, 13 and 43. In the Lef-1/DNA complex (Love, et al., 1995), one residue of the protein (Met13) partially intercalates between two adenine bases. Lef-1 facilitates its DNA interaction by Leu9, Phe12, Met13, Met16 and Arg43.

*h*Par14 shows a homologous motif occurring in its first α-helix, where His48 in *h*Par14 substitutes Leu9 of Lef-1 and Phe12, Met13 and Met16 in Lef-1 are homologous or identical to residues Ile51, Met52 and Met55 of the PPIase (Figure 4.1). The latter residues of *h*Par14 show chemical shift changes when the free protein is complexed to DNA.

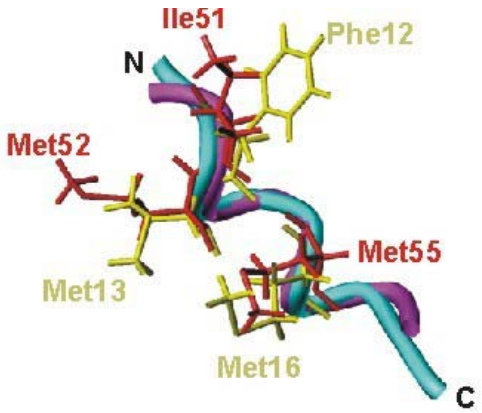

LEF-1	-	A	F	M	L	Y	M	K	E	M -
hPar14	-	K	I	M	E	A	M	K	L	K -

Figure 4.1 Sequence and structural homology of *h*Par14 and Lef-1. *Upper picture*, ribbon-and-stick representation of an overlay of residues Ala11 to Met19 of the DNA-binding motif of Lef-1 within the structural homologous motif of *h*Par14 Lys50 to Lys58. *Lower picture*, sequence alignment of the corresponding regions. According to Surmacz, et al., 2002

The C-terminal basic domain of Lef-1 is located in the compressed major groove opposite the more widened minor groove and stabilizes the bending of DNA by charge neutralization.

It might be a valid model that the basic N-terminal domain of *h*Par14, with some of its resonances shifting on addition of DNA might have an identical function in DNA-binding and that *h*Par14 facilitates complex formation in the similar way as Lef-1. Thus, binding of *h*Par14 to nucleic acids might involve similar structural motifs as found in the HMGN/HMGB family of proteins. Although our short constructs might not completely substitute longer *in vivo* binding partners of *h*Par14, their corresponding K_d values are of the order of 10^{-7} at 27°C (Surmacz, et al., 2002). Dissociation constants of 10^{-7} have been observed for the binding of HMGN proteins to nucleosomal particles (Postnikov, et al., 1994) and for HMGB proteins (10^{-7} up to 10^{-12}) depending on their nucleic acid binding partners (Gillard & Strauss, 2000).

The nuclear localization, the DNA binding capability to nucleosomal-like DNA and sequence and structural homology to chromatin-associated proteins suggest that *h*Par14 is involved in chromatin architecture and/or chromatin remodeling. Shuttling the protein between cytoplasm and nucleus might be the regulating element to switch its action on and off. Our hypothesis is, that *h*Par14, when bound to DNA catalyses prolyl isomerization of proteins that regulate the dynamic organization of the chromatin structure. The latter would mean that *h*Par14 could play

a role in regulating entry or offset of M-phase transition or transcription of genes. Thus, the function of *h*Par14 might be closely related to that of *h*Pin1.

4.2 Phosphorylation of *h*Par14 by CK2

The investigation of the subcellular localization of protein components that are part of signal transduction pathways has become an important tool for elucidating the mechanisms by which these pathways are regulated. This study demonstrates that *h*Par14 is phosphorylated *in vitro* and *in vivo*. The protein is a specific substrate for CK2. Additionally, *h*Par14 interacts with CK2α and CK2β subunits *in vivo*, as revealed by co-immunoprecipitation and co-localization analyses. The Ser19 residue of *h*Par14 is an important *in vitro* CK2 phosphorylation site. When this phosphorylation site is mutated from an amino acid with a phosphate-acceptor group to an alanine the nuclear import of the protein variant is completely abolished. Additionally, the Ser19Ala mutant of *h*Par14 looses its ability to bind DNA as revealed by electromobility shift assay (Figure 3.30).

The phosphorylation of *h*Par14 by CK2 is inhibited by a CK2 specific kinase inhibitor DRB and interestingly, not by heparin. Heparin is CK2 inhibitor and the critical inhibitory concentration of this compound can vary depending on the acidic nature of the specific substrate (O'Farrell, et al., 1999). The possible explanation for the lack of inhibition observed for heparin is that a short cluster of acidic amino acids in *h*Par14 competes with the kinase for heparin interaction. This unusual effect of the resistance of CK2 enzymatic activity to heparin is not a unique observation. The phosphorylation of nucleoplasmin by CK2 was reported by Taylor and collaborators to be resistant to heparin (Taylor, et al., 1987). In this study, an additional effect of heparin on the phosphorylation of *h*Par14 was observed. Apparently, using of heparin to inhibit phosphorylation of *h*Par14 resulted in an increased phosphorylation level. Moreover, the heparin was able to inhibit autophosphorylation of both subunits of CK2 but failed to inhibit phosphorylation of the substrate protein. The increased effect of *h*Par14 phosphorylation in the presence of heparin may be due to internal changes in the structure of *h*Par14, since the protein has a binding affinity to heparin (Uchida, et al., 1999). The binding of heparin could induce conformational changes in *h*Par14 structure and expose a second putative CK2 phosphorylation site at the Ser104 residue.

A common feature of CK2 recognition motif is the presence of highly acidic phosphoacceptor sites within a consensus sequence, S/T-*x*-*x*-E/D, which generally includes several additional negatively, charged side chains (either carboxylic or phosphorylated side chains) (Meggio, et al., 1994). The position *n* + 3 from a potential phosphate acceptor site is crucial for kinase

recognition. The requirement of acidic clusters in this position for optimal phosphorylation efficiency has been clearly outlined by systematic studies with peptide substrates (Sarno, et al., 1996).

The Ser19 residue embedded within the sequence AASGSDSA of the N-terminal extension of *h*Par14 is located at the position -3 relative to the aspartic acid residue. This motif resembles a consensus sequence of CK2, suggesting the relevance of CK2 phosphorylation. This is also supported by kinetic data obtained for CK2. The enzymatic activity of kinase (k_{cat}/K_M) in the presence of *h*Par14 as a substrate is equal to 0.25 μM^{-1} s^{-1}. It is difficult to compare our data to known values obtained for CK2, since all kinetic analysis was done with peptide substrates. The constant obtained with peptide substrate RRRADDSDDDDD for CK2 is xx μM^{-1} s^{-1} (Sarno, et al., 1996).

The CK2 motif within *h*Par14 like protein seems to be conserved. Several *h*Par14-related parvulins show a similar consensus pattern (Figure 4.2).

```
hPar14          ----MPPKGKS----GSGKAGKGGAASGSDSADKKAQGPKGGGNA----------37
M.mus           ----MPPKGKS----GSGKGGKGGAASGSDSADKKSQGPKGGGNA----------37
X.lae           ----MPPKGK-----G-GKGAKGGAASG-EAADKKAQTPKGG-NA----------33
L.jap           ---------------KGKGKQ---AASGSDENASKGKGKGAKGGDGLG-------30
A.tha           ------MGKDAK---AGGKGKGKQ-ASGSEEAPSKGKGKAGKAADGLGTCTY---42
                                        *.     ::::..        : :  *..
```

Figure 4.2 Sequence alignment of the N-terminal basic extension of *h*Par14 to related parvulins from various species. Red, the conserved serine residue within CK2 consensus motif; green- negatively charged amino acid at position +3 relative to serine.

However, the possibility of another, yet unidentified kinase phosphorylating the *h*Par14 on Ser19 may not be excluded. The number of predicted kinases from available sequence data of the human genome is above 500 (Kostich, et al., 2002). Only a small fraction of these kinases is expressed and characterized. So there is a high probability for other kinases with a very similar substrate specificity and architecture of the ATP-binding site, which would catalyse the phosphorylation of similar substrates as CK2 and be affected by similar inhibitors as DRB.

4.2.1 Subcellular localization of *h*Par14 is regulated by phosphorylation at Ser19 residue

Under normal conditions the main fraction of *h*Par14 is found in the nucleus of cells. The mutation of Ser19 to Ala of *h*Par14 changes this distribution pattern and the protein variant is found almost exclusively in the cytoplasm. The substitution of Ser/Thr residues by Glu or Asp is frequently used to mimic a phosphorylated residue resulting in mutants mimicking a

constitutively phosphorylated protein (Dean, et al., 1989; Ducommn, et al, 1991; Gould, et al., 1991; Reizer, et al., 1989; Huffine & Scholtz, 1996; Wagner, 1997; Dulhanty, et al., 1995)
Therefore, the role of Ser19Glu mutant of *h*Par14 on cellular distribution was investigated. Interestingly, the mutant is mainly enriched at the nuclear membrane and the nucleus, but does not retain in cytoplasm (Figure 3.28). Obviously the side chain structure and the single charge at the glutamic acid are able to mimic the dianionic phosphorylated serine in part, but not completely. However, it supports strongly the hypothesis that the phosphorylation state of Ser19 is crucial for guiding *h*Par14 to the nucleus.
How does the phosphorylation at Ser19 regulate the subcellular localization of *h*Par14? Proteins with small molecular mass like *h*Par14 may diffuse passively through the nuclear pore complex. However, small proteins like HMGN proteins are actively imported to the nucleus via their nuclear localization signal (Hock, et al., 1998). This process is due to the bi-partie nuclear localization signal of HMGN proteins which is localized within the N-terminal extension. The high similarity observed within the N-terminal extension of *h*Par14 to that of the HMGN proteins suggests that *h*Par14 could have a similar localization signal. Through truncation analysis, the nuclear localization of *h*Par14 was demonstrated to be control by a short stretch of eight amino acid residues (Ser7 to Lys 14). Ser19 was shown earlier to be a phosphorylation site within *h*Pa14 and is located near this NLS. Consequently, the phosphorylation at this serine residue may influence the recognition of the protein by the machinery of active nuclear import and thus switch cellular distribution. The subcellular localization of some proteins is switched by the phosphorylation in close neighbourhood to the NLS sequence (Rihs, et al., 1991; Kinzler, et al., 1996; Block, et al., 2001; Kaffman, et al., 1998). The SV-40 large T antigen is phosphorylated by CK2 within a motif in close neighbourhood to the nuclear localization signal. This phosphorylation increases the rate of nuclear import of SV-40 protein (Rihs, et al., 1991). The same regulation is observed in adenomatous polyposis coli (APC) and human ubiquitin-conjugating enzyme CDC34 proteins. The nuclear localization of adenomatous polyposis coli and human ubiquitin-conjugating enzyme CDC34 proteins was reported to be phosphorylation dependent. The APC is a tumour suppressor protein and its mutational inactivation may be rate-limiting for the initiation of tumour progression (Kinzler, et al., 1996). The subcellular regulation of APC protein is controlled by dual phosphorylation. The phosphorylation at the CK2 site within the first nuclear localization signal causes increased nuclear translocation, in contrast to the second nuclear localization site phosphorylated by PKA where decreased nuclear localization is observed (Zhang, et al., 2001). In the case of CDC34 that is localized to

the nucleus, mutations at serine residues within the CK2 recognition motif abolished phosphorylation of CDC34 and resulted in its cytoplasmic retention (Block, et al., 2001).

The phosphorylation of an individual amino acid residue can directly affect protein conformation (Kipping, et al., 2001). This conformational change may regulate the access of phosphorylated protein to the nuclear import machinery. As a result, an increased efficiency of nuclear import of *h*Par14 through a more stable interaction with an import protein would be possible.

Phosphorylation of some DNA binding proteins negatively regulates their interaction with DNA. Indeed, phosphorylation of Ser19 in the N-terminal extension of *h*Par14 weakens the binding of protein to DNA as revealed by electromobility shift assays. This effect is a direct consequence of the introduction of negative charges to the site of DNA interaction at Ser19 within *h*Par14. The neighbouring amino acids Gly8, Lys14 and Ala18 are directly involved in DNA binding.

Similar to the function of HMGN1 and HMGN2 proteins, *h*Par14 may decondense chromatin and thus, may enhance transcription form chromatin templates. For chromatin-binding proteins, it has been suggested that the phosphorylation displaces the transcriptional machinery and chromatin-modifying enzymes from chromatin and facilitates chromatin condensation. It is possible that in the nucleus the phosphorylation state of *h*Par14 is in a constant state of turnover and that the equilibrium is favouring greatly the dephosphorylated state. In effect, the phosphorylation of *h*Par14 negatively regulates binding of proteins to DNA. The negative regulation of DNA binding upon phosphorylation was reported as well for HMGN proteins (Lund & Berg, 1991; Spaulding, et al., 1991). However, the biological significance of this event in living cells has yet to be understood.

4.3 *h*Par14 interacts with 14-3-3 proteins

The list of identified nucleocytoplasmic shuttling proteins is still increasing including transport receptors and adaptors (Görlich & Kutay, 1999), transcription factors (Cartwright & Helin, 2000), cell cycle regulators (Yang & Kornbluth, 1999), and numerous RNA binding proteins (Shyu & Wilkinson, 2000). It is well established that shuttling proteins act not only as carriers of cargo in transit between the nucleus and the cytoplasm, but they also play an important role in relaying information between this two major cellular compartments. Studies on the nucleocytoplasmic shuttling of nucleolin led to the proposal that all nuclear proteins have the ability to be exported from the nucleus (Schmidt-Zachmann, et al., 1993).

*h*Par14 was identified in this work as a 14-3-3 binding partner. The binding of *h*Par14 to 14-3-3 proteins is largely dependent on a specific site within the N-terminal extension of *h*Par14 as confirmed by GST pull-down assay. The binding of *h*Par14 to 14-3-3 proteins occurs via a common ligand-binding site, which involves Lys49 residue of 14-3-3 located within helix αI. The general function of this helix is to participate directly in the binding to phosphorylated ligands (Brunet, et al., 2002). The elimination of Lys49 within helix αI of 14-3-3 disrupts the interaction to numerous phosphorylated protein ligands e.g. Raf-1 kinase or exoenzyme S (Fu, et al., 1997). The ligand-binding defective mutant 14-3-3 with substituted Lys49 to Glu did not interact with *h*Par14 and both proteins co-localized to the nucleus. Dephosphorylation and mutagenesis studies revealed that the interaction is largely dependent on the phosphorylation of *h*Par14. The 14-3-3 binding through Ser7 and Ser9 residues of *h*Par14 is one of mechanism that promotes cytoplasmic localization of *h*Par14.

Although an extensive range of studies investigating 14-3-3 proteins have been published, few papers characterize more than one isoforms as candidate interacting proteins. While the amino acid sequences of the seven identified 14-3-3 isoforms are highly conserved (Atiken, et al., 1992), the retention of multiple isoforms throughout evolution suggests that they may have evolved distinct, non-redundant functions. Some proteins, such as Raf1, may be promiscuous in their association with multiple 14-3-3 isoforms (Freed, et al., 1994; Fantl, et al., 1994). Similar to the example described above, *h*Par14 interacts with more than one isoform of 14-3-3 indicating various biological relevance of this interaction.

The general mechanism of action of 14-3-3 proteins involves the formation of complexes with target proteins. In many instances, such complexes depend on the phosphorylation of the 14-3-3 binding partner (Muslin, et al., 1996). The phosphorylation dependent 14-3-3 binding generally involves a conserved phosphoserine or phosphothreonine residue flanked by basic, aromatic, and aliphatic amino acids, along with additional serine or threonine residues. There are two classes of 14-3-3 binding consensus motifs, in which an arginine or lysine residue is preferred at either the –3 (type I) or –4 (type II) position relative to the phosphorylated residue, with nearby amino acids also being important (Yaffe, et al., 1997). The type I sites are the most common motifs, and have been found in most 14-3-3 targets (Table 4.1).

Table 4.1 The phosphorylated motifs of 14-3-3 binding proteins

Protein	Sequence	Motif	Reference
Raf-1	^{256}RST**S**TP	RSX**S**XP	Michaud, et al., 1995 Muslin, et al., 1996
Raf-1	^{618}RSA**S**EP	RSX**S**XP	Muslin, et al., 1996
BAD	^{107}RSRHS**S**YP	RXRXX**S**XP	Zha, et al., 1996
BAD	^{131}RGRSR**S**AP	RXRSX**S**XP	Zha, et al., 1996
Cdc25c	^{213}RSR**S**MP	RSX**S**XP	Peng, et al., 1997
PTPH1	^{356}RSL**S**VE and ^{832}RVD**S**EP	RXX**S**	Zhang, et al., 1997
Keratin 18	^{26}RPVSSAA**S**VY	RXXSSXX**S**X	Ku, et al., 1998
*h*Par14	^{4}KGK**S**G**S**GKAGK	KxK**S**x**S**	this work

The identified motif KGKSGSGK within *h*Par14 closely resembles the type I site described for 14-3-3 binding motifs with a positively charged lysine residue at position –3 to serine 7 and serine 9 residues of *h*Par14. Both amino acids within the predicted motif are potential targets for PKB kinase. Moreover, the phosphorylation of *h*Par14 by either PKB or PKC was confirmed *in vitro*. The double mutant *h*Par14 with substitution in both Ser7 and Ser9 failed to be phosphorylated *in vitro* by PKB and no binding of mutant *h*Par14 to 14-3-3 in a GST pull down assay was observed. Both kinase PKB and PKC have similar substrate recognition motif. Many other AGC-type kinases as PKA and Aurora show very similar substrate specificity as PKB and would be candidates for the *in vivo* phosphorylation of this motif in the N-terminus of *h*Par14.

The predicted phosphorylation sites Ser7 and Ser9 amino acids of *h*Par14 are localized between positively charged lysine residues. The reported minimum motif in a peptide enabling PKB phosphorylation is Arg-Xaa-Arg-Yaa-Zaa-Ser/Thr-Hyd, where Xaa is any amino acid, Yaa and Zaa are preferably small residues other than glycine, and Hyd is a bulky hydrophobic residue (phenylalanine or leucine) (Obata, et al., 2000). The amino acid arginine at position S-3 is an important residue within the recognition motif for PKB (Lawlor & Alessi, 2001). Mutation at this residue, even to Lys, severely decreased the ability of PKB to phosphorylate a peptide substrate (Lawlor & Alessi, 2001).

In the study case, two possible arguments may be proposed for the relevance of PKB phosphorylation in the interaction of *h*Par14 with 14-3-3. First, *h*Par14 was phosphorylated using PKB kinase prior to incubation with 14-3-3 proteins leading to a *h*Par14/14-3-3

interaction as revealed in a protein array experiments (Dr. M. Yaffe, personal communication). Second, *h*Par14 could be a substrate for PKB since both proteins have similar localization in the cytoplasm and the nucleus. So the kinase may phosphorylate either cytoplasmic or nuclear *h*Par14. Additionally, it has been reported that substrates for PKB also bind to 14-3-3 (Lawlor & Alessi, 2001). However, we cannot rule out that other kinase than PKB may phosphorylate indicated sites of *h*Par14 *in vivo*. As already mentioned in chapter 4.2 the knowledge about many human kinases is still very limited

It is also attractive to speculate that both cytoplasm and nuclear localized *h*Par14 is phosphorylated by PKB within its N-terminal extension after activation of the kinase by the growth factors. Since there is mounting evidence that insulin and many other growth factors activate PKB through a PI3K signalling pathway-dependent manner (Cross, et al., 1995). The activation of PKB leads to the phosphorylation of, e.g., forkhead transcriptional factor, FKHRL1, and its transition from the nucleus to the cytoplasm (Brunet, et al., 2002). The role of PKB phosphorylation in the *h*Par14 binding to 14-3-3, however, remains to be defined.

4.3.1 Binding of 14-3-3 to *h*Par14 guides the protein to the cytoplasm

It has been proposed that 14-3-3 proteins promote cytoplasmic localization of many proteins through masking of nuclear localization sequences (NLS) or unmasking of nuclear export signals (NES) (Muslin & Xing, 2000). Accessibility of nuclear import element within *h*Par14 could be influenced by 14-3-3 binding, especially since *h*Par14 amino acid sequence of that motif is close to the 14-3-3 binding site at Ser7, Ser9 residues. A detailed analysis of cells co-expressed wild type 14-3-3 with *h*Par14 revealed cytoplasmic localization of *h*Par14. In contrast, cells co-expressing double mutant Ser7/Ala and Ser9/Ala *h*Par14 with 14-3-3 showed strict nuclear localization of mutant protein. Additionally, cells expressing 14-3-3 and *h*Par14, treated with leptomycin B showed unexpected localization of both proteins to the nucleus. These results suggest that 14-3-3 proteins contribute to the relocalization of *h*Par14 to the cytoplasm. Two possible mechanism of regulation of the subcellular localization of *h*Par14 may be suggested.

First, 14-3-3 proteins promote cytoplasmic localization of many proteins through masking nuclear localization sequences (NLS) (Prymakowska-Bosak, et al., 2002) or unmasking of nuclear export signals (NES) (Muslin, et al., 2000). Accessibility of nuclear import or export elements within *h*Par14 can be influenced by 14-3-3 binding. The amino acids between Ser7 and Lys14 within the N-terminal extension of *h*Par14 are responsible for nuclear localization of

*h*Par14. Thus, binding of 14-3-3 may promote cytoplasmic accumulation of *h*Par14 by masking its nuclear localization signal and preventing nuclear import (Figure 4.3).

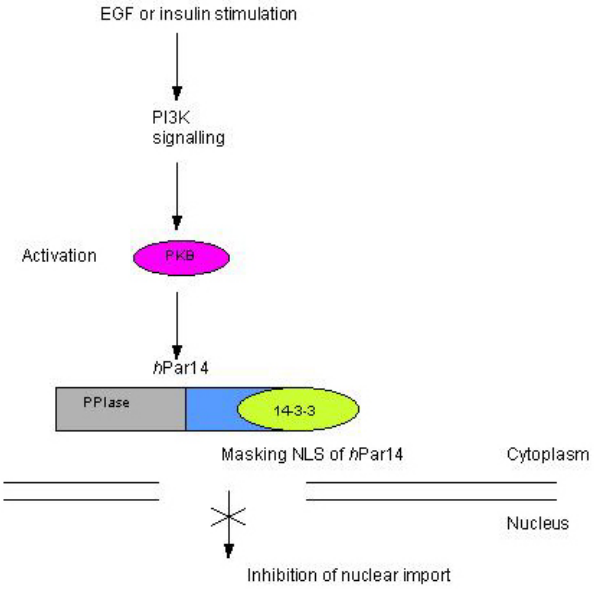

Figure 4.3 Schematic illustration of a model of *h*Par14 cytoplasmic retention mediated by 14-3-3. Growth factors or insulin binding to the tyrosine kinase receptor elicits recruitment and activation of PI 3-kinase (PI3K). Upon activation, PI 3-kinase transfer signal downstream leads to activation of PKB kinase and phosphorylation of Ser7 and Ser9 residues, located near to the nuclear localization signal (NLS) of *h*Par14). The N-terminal phosphorylated *h*Par14 binds to 14-3-3. Binding of 14-3-3 masks the NLS of *h*Par14, inhibits nuclear import and results in cytoplasmic localization of *h*Par14.

Second, 14-3-3 proteins are known to promote cytoplasmic localization of some important cell-cycle regulators such as Cdc25 and CDK2 (Graves, et al., 2001; Laronga, et al., 2000) upon export from the nucleus. Similar effect was observed for *h*Par14. The cytoplasmic localization of 14-3-3/*h*Par14 was inhibited by leptomycin B. Early, studies in *Schizosaccharomyces pombe* identified the cellular target of LMB as the CRM1 (chromosomal region maintenance)/exportin 1 protein (Nishi, et al., 1994), that is critical for the export of RNA and proteins containing a nuclear export sequences (NES). In the case of RNA export, CRM1 binds to ribonuclear proteins containing the NES motif. Based on the recently published data, showing interaction of *h*Par14 with pre-ribosomal and ribosomal proteins, *h*Par14 may action as a tag protein with chaperon function that binds to exported ribosomal proteins associated with Crm1. As a complex with 14-3-3, it may be exported from the nucleus in a CRM1

dependent way. This would promote the cytoplasmic localization of *h*Par14 (Figure 4.4). Binding of two proteins to each monomer of 14-3-3 individually, allow 14-3-3 to function as a molecular adaptor. A similar mechanism was observed for forkhead transcription factor, FKHRL1. Phosphorylation of FKHRL1 by PKB within the nucleus creates a binding site for 14-3-3 and export proteins from the nucleus via a NES of FKHRL1 (Brunet, et al., 2002). Binding of 14-3-3 near the NLS of FKHRL1 may disrupt subsequent nuclear re-import.

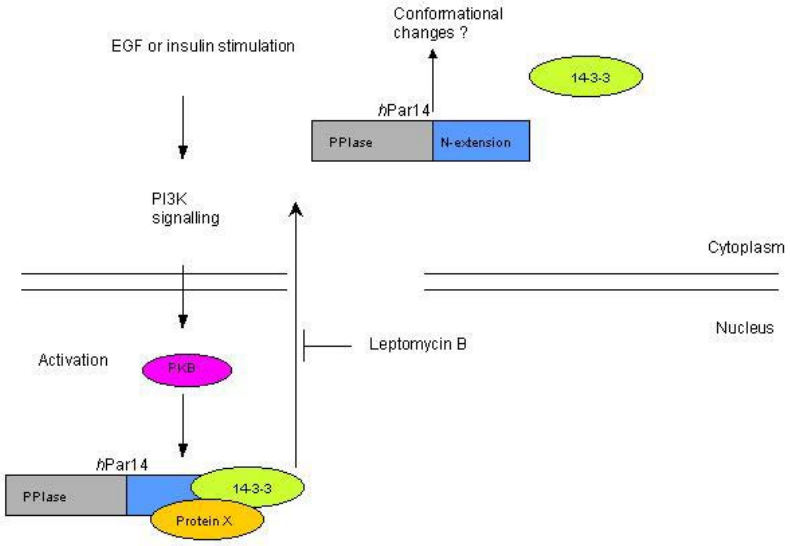

Figure 4.4 Schematic representation of a model of 14-3-3/*h*Par14 nuclear export. Binding of growth factors or insulin to the receptor recruits and activates PI 3-kinase. Upon activation, PI 3-kinase transfer signal downstream results in activation of PKB. Subsequently, activated PKB translocates to the nucleus and phosphorylates *h*Par14 at Ser7 and Ser9 residues. Phosphorylated *h*Par14 together with protein X (possessing NES element) bind to 14-3-3 and such protein complex is exported from the nucleus in a CRM1 dependent way. Binding of *h*Par14 to 14-3-3 results in conformational changes of *h*Par14 and may influence its enzymatic activity.

There are some hypotheses how of 14-3-3 mediates the *h*Par14 function. The N-terminal extension of *h*Par14 is essential for high affinity binding to bent DNA. The proposed function of *h*Par14 is chromatin remodeling and transcription. It is of note that the candidate 14-3-3 biding site falls in close neighbourhood to amino acids involved in binding of *h*Par14 to DNA. Hypothetically, the nuclear interaction between 14-3-3 and *h*Par14 may modulate the

subcellular localization of *h*Par14, either during phases of the cell cycle, or in response to specific stimuli and thereby modulating binding to DNA. On the other hand, the 14-3-3 interaction may influence the enzymatic activity of *h*Par14 like this was described for Raf protein (Roy, et al., 1998; Jaumot, et al., 1998). However, it remains unknown if binding of 14-3-3 induces the conformational protein structure of *h*Par14.

5. Conclusion

Peptidyl-prolyl *cis/trans* isomerases (PPIases) are a family of enzymes catalysing the *cis/trans* isomerization of peptidyl-prolyl bonds. Even though this enzyme family is ubiquitously distributed within living cells and it consists of many members the function of most of these members remains mainly unclear. Over the years evidences grew that PPIases are involved in many processes from the restructuring of the polypeptide chain to regulation of the cell cycle. Recently a new class of PPIases was discovered: the parvulins. One of their members, *h*Pin1 became a hot topic in research since it was shown to be involved in critical stages of cell cycle progression. A second member of the human parvulin family was identified only three years ago. Up to date little is known about the human parvulin 14 (*h*Par14). In this study, we could add some information to the picture of *h*Par14.

- The catalytic domain of *h*Par14 shows high sequence identity to its relative, *h*Pin1. However, while in *h*Pin1 there is a N-terminal WW domain present in *h*Par14 a N-terminal 35 amino acid extension is found which has no similarity to a WW domain but to a chromatin unfolding domain of HMG proteins.
- *h*Par14 is a DNA-binding protein with specificity for A-tract bend DNA structure. This type of structure often occurs in bent regions of DNA as populated in chromatin structures. So besides the sequence homology to HMG proteins, there seems to be also a functional similarity. These characteristics point towards an involvement of *h*Par14 in chromatin restructuring and activation of transcription.
- The protein is predominantly localized to the nucleus. The nuclear localization of *h*Par14 is driven by N-terminal extension that contains a putative nuclear localization sequence between Ser7and Lys11.
- An endogenous pool of cellular kinases obtained from cell extract and several recombinant kinases phosphorylates *h*Par14. The most effective phosphorylation of *h*Par14 was found for CK2 kinase and a major phosphorylation site was identified as Ser19. This residue is effectively phosphorylated by CK2 and the phosphorylation status mainly influences the subcellular localization. When this residue is mutated to alanine amino acid, *h*Par14 is no substrate for CK2 anymore and it is found solely in the cytoplasm.
- Two additional residues, Ser7 and Ser9 of *h*Par14 are phosphorylated by PKB and PKC. One of the active kinases was PKB, a kinase known to generate binding motifs for 14-3-3 proteins upon phosphorylation of its substrates.

- *h*Par14 interacts with 14-3-3 protein in a phosphorylation dependent manner. As an effect of this interaction *h*Par14 was re-localized to the cytoplasm. Both Ser7 and Ser9 residues of *h*Par14 are important for binding to 14-3-3. Mutation at this residues and co-localization revealed lack of interaction and nuclear localization of *h*Par14.
- The protein itself does not contain a nuclear export signal as showed in experiment with leptomycin B. However, the cytoplasmic localization of complex of *h*Par14 and 14-3-3 is inhibited by treatment with leptomycin B indicating a presence of a third protein that possess NES signal and drive nuclear export.

Despite the rapid progress in the area of the signal transduction field, many important questions remain to be answered, and this leads to considerations for possible future studies.

6. Summary

Studying the regulation and function of multiple signal transduction pathways is essential for understanding many biological processes. Mechanisms of regulation include protein-phosphorylation, shuttling of proteins between nucleus and cytoplasm, and DNA/protein interactions. The research in this dissertation has been focused on several important aspects of regulation of protein function and localization of the peptidyl-prolyl cis/trans isomerase, *h*Par14.

Our initial study was aimed at elucidating the function of *h*Par14. We first studied the cellular localization and the DNA-binding capability of this protein. The cellular expression pattern showed an uneven distribution of the protein between cytoplasm and nucleus. We determined the nuclear localization of *h*Par14 *in vivo* by fusing the protein to green fluorescent proteins and expressed in HeLa cells. Deletion mutants of *h*Par14 were used to determine the sequence, necessary for nuclear targeting to Ser7 –Lys14 of the N terminus of the protein.

We also showed by using DNA-cellulose affinity experiments that recombinant and endogenous *h*Par14, present in the nuclear fraction of HEK 293 cells, could bind to double-stranded native DNA *in vitro*. On the basis of homologies and similarities of *h*Par14 to members of the high-mobility group proteins, we developed double stranded DNA constructs and tested the *h*Par14 binding affinity in fluorescence titration and electromobility shift assays. The protein binds preferentially to bent A-tract sequences. The binding interface of the protein was determined by NMR studies of the complex of unlabeled DNA and uniformly ^{15}N-labeled *h*Par14$_{(1-131)}$. The unstructured N-terminal residues are necessary for high-affinity binding to DNA. Based on these findings in connection with sequence and structural homologies of *h*Par14 to members of the HMGB/HMGN protein family, we suggest a function of *h*Par14 in cell-cycle regulation or gene transcription.

The possible posttranslational modification of *h*Par14 was investigated. The phosphorylation of *h*Par14 was studied using a set of kinase assays. *h*Par14 is specifically phosphorylated by recombinant human casein kinase 2 (CK2) and CK2 kinase from HeLa nuclear/cytosol extracts. The phosphorylation of *h*Par14 is inhibited *in vitro* by 5,6 dichloro-1-β-*o*- ribofuranosyl benzimidazole (DRB), a specific inhibitor of CK2. Co-immunoprecipitation experiments showed that *h*Par14 interacts *in vivo* with endogenous CK2α and CK2β subunits. In co-localization studies, both proteins, the PPIase and catalytic subunit of CK2 were localized to the nuclear membrane. The serine 19 residue of *h*Par14 was identified as an *in vitro* CK2 phosphorylation site. Mutation at this residue to alanine abolishes the phosphorylation observed *in vitro* and *in vivo*. The expression of mutant His- Ser19/Ala *h*Par14 in HeLa cells leads to its accumulation

to the cytoplasm. In contrast to the expression of mutant His-Ser19/Glu *h*Par14 resulted in localization of protein to the nuclear membrane or to the nucleus.

The phosphorylation of *h*Par14 negatively regulates binding to DNA. Taken together, the subcellular localization of *h*Par14 is regulated by a complex pathway of phosphorylation/dephosphorylation reactions at residue within N-terminal, unstructured domain of *h*Par14.

Additionally to the effect described above, the phosphorylation at Ser7 and Ser9 of *h*Par14 creates a binding site for 14-3-3 proteins. Both residues are located within a novel 14-3-3 consensus motif. The interaction between *h*Par14 and 14-3-3 is phosphorylation dependent as showed by mutagenesis and GST pull-down assay. Association of *h*Par14 with 14-3-3 proteins is via a common ligand-binding site described for 14-3-3. The Lys49 of 14-3-3 seems to participate directly in the interaction with phosphorylated residues of *h*Par14. The subcellular localization of *h*Par14 is regulated by 14-3-3 protein. The 14-3-3 promotes cytoplasmic distribution of wild type *h*Par14 and not a mutant Ser7, Ser9/Ala *h*Par14. The inhibition of protein export using leptomycin B resulted in nuclear accumulation of *h*Par14 and 14-3-3. Two possible scenarios can be proposed. First, binding of 14-3-3 to *h*Par14 masks nuclear localization signal and in consequence inhibits the nuclear import of *h*Par14. Second, 14-3-3 promotes cytoplasmic retention of *h*Par14 via active export from the nucleus. This will involve another, unknown protein partner with nuclear export signal that binds to 14-3-3/*h*Par14 and brings the protein complex out of the nucleus.

6.Zusammenfassung

Für das Verständnis vieler biologischer Prozesse ist es essentiell, die Regulation und Funktion der verschiedenen Signaltransduktionswege zu untersuchen und zu verstehen. Solche Regulationsmechanismen sind zum Beispiel die Phosphorylierung von Proteinen, der Transport von Proteinen zwischen Zellkern und Zytoplasma sowie Wechselwirkungen zwischen DNS und Proteinen. In dieser Arbeit wurden verschieden Aspekte der Regulation und Funktion der humanen Peptidyl-Prolyl *cis-trans* Isomerase *h*Par14 untersucht.

Das initiale Interesse galt der Funktion von *h*Par14. Zuerst wurden die zelluläre Verteilung und eine mögliche DNA bindende Funktion untersucht. Das Protein wird in unterschiedlichen Konzentrationen im Zellkern und dem Zytoplasma gefunden. Konstrukte aus der Proteinsequenz von *h*Par14 und dem grün fluoreszierenden Protein werden in Experimenten in HeLa Zellen bevorzugt im Zellkern gefunden. Deletionsmutanten von *h*Par14 ergaben den Hinweis, daß die Aminosäurereste Ser7 bis Lys14 notwendig für diese Lokalisierung sind.

Desweiteren konnte durch die Messung der Affinität zu DNA-Zellulose gezeigt werden, daß rekombinantes und endogenes *h*Par14 aus den Zellkernfraktionen von HEK 293 Zellen *in vitro* an doppelsträngige DNA bindet. Auf der Grundlage von Sequenzähnlichkeiten von *h*Par14 zu Proteinen aus der Gruppe der High-Mobility Proteine (HMG) wurden doppelsträngige DNA Konstrukte entwickelt. Deren Bindungsaffinität zu *h*Par14 wurde dann mittels Fluoreszenztitration und EMSA Messungen (electromobility shift assay) bewertet. *h*Par14 bindet bevorzugt geknickte, sogenannte A-tract Sequenzen. Die Bindungsstelle wurde mittels NMR Messungen an Mischungen von DNA und ^{15}N-markiertem *h*Par14$_{(1-131)}$ ermittelt. Für eine hochaffine Bindung der DNA sind die N-terminalen Aminosäuren im nicht-strukturierten Bereich des Proteins unabdingbar. Diese Erkenntnisse und die strukturellen und sequentiellen Ähnlichkeiten von *h*Par14 zu Vertretern der HMGB/HMGN Proteinfamilie legen eine Beteiligung von *h*Par14 in der Regulation des Zellzyklus bzw. der Gentranskription nahe.

Desweiteren wurden mögliche posttranslationale Modifikationen an *h*Par14 untersucht. Verschiedene Kinase Assays wurden dazu genutzt. *h*Par14 wird spezifisch durch rekombinante humane Casein Kinase 2 (CK2), sowie durch CK2 aus zytosolischen und nuklearen HeLa Zellextrakten phosphoryliert. Diese Reaktion wird *in vitro* durch den spezifischen CK2 Inhibitor 5,6 Dichlor-1-β-*o*-Ribofuranosylbenzimidazol (DRB) inhibiert. Durch Koimmunoprezipitation konnte gezeigt werden, daß *h*Par14 *in vivo* mit der α und β Untereinheit von CK2 interagiert. Durch Kolokalisierungsstudien konnte eine Anreicherung beider Proteine, der PPIase und der Kinase, im Bereich der Kernmembran nachgewiesen

werden. Ser19 von *h*Par14 konnte *in vitro* als Ort der Phosphorylierung durch CK2 bestimmt werden. Der Austausch dieser Aminosäure durch ein Alanin verhindert die Phosphorylierung durch CK2. Wenn diese Mutante von *h*Par14 in HeLa Zellen exprimiert wird, verbleibt das Protein im Zytoplasma. Im Gegensatz dazu wird eine Proteinvariante Ser19/Glu im Bereich der Kernmembran und des Zellkerns akkumuliert.

Die Phosphorylierung von *h*Par14 reguliert dessen DNA Bindungsaktivität negativ. Zusätzliche Phosphorylierungen an den Seitenketten von Ser7 und Ser9 generieren ein Bindungsmotif für 14-3-3 Proteine. Beide Aminosäuren befinden sich im Kontext eines neuen 14-3-3 Konsensusmotivs. Die Interaktion zwischen *h*Par14 und 14-3-3 ist abhängig vom Phosphorylierungsstatus des *h*Par14, wie durch Mutations- und GST-pull-down Experimente gezeigt werden konnte. *h*Par14 wird über eine bekannte Ligandenbindungsstelle in 14-3-3 komplexiert. Daran direkt beteiligt ist das Lys49 des 14-3-3. Auch 14-3-3 Proteine sind an der zellulären Lokalisierung von *h*Par14 beteiligt. 14-3-3 bewirkt eine zytoplasmatische Anreicherung von *h*Par14. Sind die Reste Ser7 und Ser9 zu Alanin mutiert, geht dieser Effekt verloren. Auch die Inhibition des Proteinexportes durch Leptomyzin führt zu einem Verbleiben des *h*Par14 im Zellkern. Daraus ergeben sich zwei mögliche Szenarien. Im Komplex zwischen *h*Par14 und 14-3-3 wird eine Signalsequenz zum nuklearen Import maskiert und somit der Eintritt des Proteins in den Zellkern verhindert. Eine andere Möglichkeit besteht in der Rückführung von *h*Par14 aus dem Zellkern in das Zytoplasma. Dazu müßte ein Komplex zwischen *h*Par14, 14-3-3 und einem noch unbekannten Bindungspartner gebildet werden, der über eine Signalsequenz zum Export aus dem Zellkern verfügt.

Zusammenfassend läßt sich sagen, daß die zelluläre Lokalisierung von *h*Par14 durch ein komplexes Muster aus Phosphorylierungs-/Dephosphorylierungsereignissen an verschiedenen Resten der unstrukturierten N-terminalen Extension von *h*Par14 reguliert wird.

Albert, A., Lavoie, S., and Vincent, M. (1999) A hyperphosphorylated form of RNA polymerase II is the major interphase antigen of the phosphoprotein antibody MPM-2 and interacts with the peptidyl-prolyl isomerase Pin1. *J. Cell. Sci* **112**, 2493-2500

Allende, J.E., and Allende, C.C. (1995) Protein kinases. 4. Protein kinase CK2: an enzyme with multiple substrates and a puzzling regulation. *FASEB J.* **9**, 313-323

Arevalo-Rodriguez, M., Cardenas, M.E., Wu, X., Hanes, S.D., and Heitman, J. (2000) Cyclophilin A and Ess1 interact with and regulate silencing by the Sin3-Rpd3 histone deacetylase. *EMBO J.* **19**, 3739-3749

Aitken, A., Collinge, D.B., van Heusden, B.P., Isobe, T., Roseboom, P.H., Rosenfeld, G., and Soll, J. (1992) 14-3-3 proteins: a highly conserved, widespread family of eukaryotic proteins. *Trends Biochem. Sci.* **17**, 498-501

Atiken, A. (1996) 14-3-3 and its possible role in co-ordinating multiple signalling pathways. *Trends Cell Biol.* **6**, 341-347

Behrens, S., Maier, R., de Cock, H., Schmidt, F.X., and Gross, C.A. (2001) The SurA periplasmic PPIase lacking its parvulin domains function in vivo and has chaperon activity. *EMBO J.* **20**, 285-294

Bellacosa, A., Testa, J.R., Staal, S.P., and Tsichlis, P.N. (1991) A retroviral Oncogene, akt, encoding a serine-threonine kinase containing an SH2-like region. *Science* **254**, 274-277

Bihn, E.A., Paul, A.L., Wang, S.W., Erdos, G.W., and Ferl, R.J. (1997) Localization of 14-3-3 proteins in the nuclei of arabidopsis and maize. *Plant J* **12**,1439-1445

Block, K., Boyer, T.G., and Yew, P.R. (2001) Phosphorylation of the human ubiquitin-conjugating enzyme, CDC34, by casein kinase 2. *J. Biol. Chem*. **276**, 41049-41058

Brunet A, Greenberg, M.E. (1999) Akt promotes cell survival by phosphorylating and inhibiting a Forkhead transcription factor. *Cell* **96**, 857-868

Brunet, A., Kanai, F., Stehn, J., Xu, J., Sarbassova, D., Frangioni, J.V., Dalal, S.N., DeCaprion, J.A., Greenberg, E., Yaffe, M.B. (2002) 14-3-3 transits to the nucleus and participates in dynamic nucleocytoplasmic transport. *J. Cell. Biol.* **156**, 817-828

Bustin, M. (2001) Chromatin unfoldig and activation by HMGN (*) chromosomal proteins. *Trends. Biochem. Sci.* **26**, 431-437

Chang, L., and Karin, M. (2001) Mammalian MAP kinase signalling cascades. *Nature* **410**, 37-40

Cartwright, P., and Helin, K. (2000) Nucleocytoplasmic shuttling of transcription factors. *Cell. Mol. Life Sci*. **57**, 1193-1206

Crenshaw, D.G., Yang, J., Means, A.R., and Kornbluth, S. (1998) The mitotic peptidyl-prolyl isomerase, Pin1, interacts with Cdc25 and Plx1. *EMBO J.* **17**, 1315-1327

Dartigalongue, C., and Raina, S. (1998) A new heat-shock gene, ppiD, encodes a pepetidyl-prolyl isomerase required for folding of outer membrane proteins in *Escherichia coli*. *EMBO J*. **17**, 3968-3980

Dean, A.M., Lee, M.H., and Koshland, D.E. Jr. (1989) Phosphorylation inactivates Escherichia coli isocitrate dehydrogenase by preventing isocitrate binding. *J. Biol. Chem.* **264**, 20482-20486

Devasahayam, G., Chaturvedi, V., and Hanes, S.D. (2002) The Ess1 prolyl isomerase is required for growth and morphogenetic switching in *Candida albicans*. *Genetics* **160**, 37-48

Drouault, S., Anba, J., Bonneau, S., Bolotin, A., Ehrlich, S.D., and Renault, P. (2002) The peptidyl-prolyl isomerase motif is lacking in PmpA, the PrsA-like protein involved in the secretion machinery of Lactococcus lactis. *Appl. Environ. Microbiol.* **68,** 3932-3942

Ducommun, B., Brambilla, P., Felix, M.A., Franza, B.R., Jr, Karsenti, E., and Draetta, G. (1991) Cdc2 phosphorylation is required for its interaction with cyclin. *EMBO J.* **10**, 3311-3319

Dulhanty, A.M., Chang, X.B., and Riordan, J.R. (1995) Mutation of potential phosphorylation sites in the recombinant R domain of the cystic fibrosis transmembrane conductance regulator has significant effects on domain conformation. *Biochem. Biophys. Res. Commun.* **206**, 207-214

Fantl, W.J., Muslin, A.J., Kikuchi, A., Martin, J.A., MacNicol, A.M., Gross, R.W., and Williams, L.T. (1994) Activation of Raf-1 by 14-3-3 proteins. *Nature* **371**, 612-614

Faust, M., and Montenarh, M. (2000) Subcellular localization of protein kinase CK2. A key to its function? *Cell. Tissue Res*. **301**, 329-340

Ferrari, D.M., and Soling, H.D. (1999) The protein disulphide-isomerase family: unraveling a string of folds. *Biochem. J.* **339**, 1-10

Fischer, G., Bang, and H., Mech, C. (1984) Determination of enzymatic catalysis for the cis-trans-isomerization of peptide binding in proline-containing peptides. *Biomed. Biochim. Acta* **43**, 1101- 1111

Fischer, G., Wittmann-Liebold, B., Lang, K., Kiefhaber, T., and Schmidt, F.X. (1989) Cyclophilin and peptidyl-prolyl cis-trans isomerase are probably identical proteins. *Nature* **337**, 471-478

Ford, J.C., al-Khodairy, F., Fotou, E., Sheldrick, K.S., Griffiths, D.J., and Carr, A.M. (1994) 14-3-3 protein homologs required for the DNA damage checkpoint in fission yeast. *Science* **265**, 533-535

Freed, E., Symons, M., Macdonald, S.G., McCormick, F., and Ruggieri, R. (1994) Binding of 14-3-3 proteins to the protein kinase Raf and effects on its activation. *Science* **265**, 1713-1716

Fu, H., Subramanian, R.R., and Masters, S.C. (2000) 14-3-3 proteins: structure, function and regulation. *Annu. Rev. Pharmacol. Toxicol.* **40**, 617-647

Fujimori, F., Gunji, W., Kikuch, J., Mogi, T., Ohashi, Y., Makino, T., Oyama, A., Okuhara, K., Uchida, T., and Murakami, Y. (2001) Crosstalk of prolyl isomerases, Pin1/Ess1, and Cyclophilin A. *Biochem. Bioph. Res. Comm.* **289**, 181-190

Fujimori, F., Takahashi, K., Uchida, C., and Uchida, T. (1999) Mice lacking Pin1 develop normally but are defective in entering cell cycle from G_0 arrest. *Biochem. Biophys. Res. Commun.* **265**, 658-663

Fujiyama, S., Yanagida, M., Hayano, T., Miura, Y., Isobe, T., and Takahashi, N. (2002) Isolation and Proteomic Characterization of Human Parvulin-associating Preribosomal Ribonucleoprotein Complexes. *J. Biol. Chem.* **277**, 23773-23780

Gaiilard, C., and Strauss, F. (2000) High affinity binding of proteins HMG1 and HMG2 to semicatenated DNA loops. *BMC Mol. Biol.* **1**, 1-7

Galat, A. (1993) Peptidylproline cis-trans-isomerases: immunophilins. *Eur J Biochem* **216**, 689-707

Gama-Carvalho, M., and Carmo-Fonseca, M. (2001) The rules and roles of nucleocytoplasmic shuttling protein. *FEBS Lett.* **498**, 157-163

Gelperin, D., Weigle, J., Nelson, K., Roseboom, P., Irie, K., Matsumoto, K., and Lemmon, S. (1995) 14-3-3 proteins: potential roles in vesicular transport and Ras signaling in Saccharomyces cerevisiae. *Proc. Natl. Acad. Sci. U. S. A.* **92**, 11539-11543

Gerez, L., Mohrmann, K., van Raak, M., Jongeneelen, M., Zhou, X.Z., Lu, K.P., and van Der Sluijs, P. (2000) Accumulation of rab4GTP in the cytoplasm and association with the peptidyl-prolyl isomerase pin1 during mitosis. *Mol. Biol. Cell* **11**, 2201-2211

Görlich, D., and Kutay, U. (1999) Transport between the cell nucleus and cytoplasm. *Annu. Rev. Cell Dev. Biol.* **15**, 607-660

Gothel, S.F., and Marahiel M.A. (1999) Peptidyl-prolyl cis-trans isomerases, as a superfamily of ubiquitous folding catalysts. *Cell Mol. Life Sci.* **55**, 423-436

Gould, K.L., Moreno, S., Owen, D.J., Sazer, S., and Nurse, P. (1991) Phosphorylation at Thr167 is required for Schizosaccharomyces pombe p34cdc2 function. *EMBO J.* **10**, 3297-3309

Graef, I.A., Chen, F., Chen, L., Kuo, A., and Crabtree, G.R. (2001) Signals transduced by Ca(2+)/calcineurin and NFATc3/c4 pattern the developing vasculature. *Cell* **105**, 863-875

Graves, P.R., Lovly, C.M., Uy, G.L., and Piwnica-Worms, H. (2001) Localization of human Cdc25C is regulated both by nuclear export and 14-3-3 protein binding. *Oncogene* **20**, 1839-1851

Haandrikman, A.J., Kok, J., and Venema, G. (1991) Lactococcal proteinase maturation protein PrtM is a lipoprotein. *J Bacteriol.* **173**, 4517-4525

Hamamoto, T., Gunji, S., Tsuji, H., and Beppu, T. (1983) Leptomycins A and B, new antifungal antibiotics. I. Taxonomy of the producing strain and their fermentation, purification and characterization. *J. Antibiot*. (Tokyo) **36**, 639-645

Hanes, S.D., Shank, P.R., and Bostian, K.A. (1989) Sequence and mutational analysis of ESS1, a gene essential for growth in *Saccharomyces cerevisiae*. *Yeast* **5**, 55-72

Hani, J., Schelbert, B., Bernhardt, A., Domdey, H., Fischer, G., Wiebauer, K., and Rahfeld, J.U. (1999) Mutations in a peptidyl prolyl cis/trans-isomerase gene lead to a defect in 3'-end formation of a pre-mRNA in *Saccharomyces cerevisiae*. *J. Biol. Chem.* **274**, 108-116

Hani, J., Stumpf, G., and Domdey, H. (1995) PTF1 encodes an essential protein in *Saccharomyces cerevisiae*, which shows strong homology with a new putative family of PPIases. *FEBS Lett.* **356**, 198-202

Hathaway, G.M., Lubben, T.H., Traugh, J.A. (1980) Inhibition of casein kinase 2 by heparin. *J. Biol. Chem.* **255**, 8038-8041

He, J., Lau, A.G., Yaffe, M.B., and Hall, R.A. (2001) Phosphorylation and cell cycle-dependent regulation of Na+/H+ exchanger regulatory factor-1 by Cdc2 kinase. *J. Biol. Chem.* **276**, 41559-41565

Hecht, A., and Kemler, R. (2000) Curbing the nuclear activities of beta-catenin. Control over Wnt target gene expression. *EMBO Rep.* **1**, 24-28

Henderson, B.R. (2000) Nuclear-cytoplasmic shuttling of APC regulates beta-catenin subcellular localization and turnover. *Nat. Cell Biol*. **2**, 653-660

Herera, J.E., Sakaguchi, S., Bergel, M., Trieschman, L., Nakatani, Y., and Bustin, M. (1999) Specific acetylation of chromosomal protein HMG-17 by PCAF alters its interaction with nucleosoms. *Mol. Cell Biol.* 19, 3466-3473

Hock, R., Scheer, U., and Bustin, M. (1998) Chromosomal proteins HMG-14 and HMG-17 are released from mitotic chromosomes and imported into the nucleus by active transport. *J. Cell. Biol.* **143**, 1427-1436

Hsu, T., McRackan D., Vincent T.S., and Gert de Couet H. (2001) *Drosophila* Pin1 prolyl isomerase Dodo is a MAP kinase signal responder during oogenesis. *Nat. Cell Biol.* **3**, 538-543

Huang, H.K., Forsburg, S.L., John, U.P., O'Connell, J., and Hunter, T. (2001) Isolation and characterization of the Pin1/Ess1p homologue in *Schizosaccharomyces pombe*. *J. Cell. Science* **114**, 3779-3788

Huffine, M.E., and Scholtz, J.M. (1996) Energetic implications for protein phosphorylation. Conformational stability of HPr variants that mimic phosphorylated forms. *J. Biol. Chem.* **271**, 28898-28902

Hunter, T., and Karin, M. (1992) The regulation of transcription by phosphorylation. *Cell* **70**,375-387

Imhof, A., and Wolffe, A.P. (1999) Purification and properties of the Xenopus Hat1 acetyltransferase: association with the 14-3-3 proteins in the oocyte nucleus. *Biochemistry* **38**, 13085-13093

Ivery, M.T.G. (2000) Immunophilins: Switched on Protein Binding Domains? 452-484

Jacobson, M.R., Brigle, K.E., Bennett, L.T., Settequist, R.A., Wilson, M.S., Cash, V.L., Beynon, J., Newton, W.E., and Dean, D.R. (1989) Physical and genetic map of the major nif gene cluster from *Azotobacter vinelandii*. *J. Bacteriol.* **171**, 1017-1027

Jans, D.A. (1995) The regulation of protein transport to the nucleus by phosphorylation. *Biochem J* **311**, 705-716

Jaumot, M., and Hancock, J.F. (2001) Protein phosphatases 1 and 2A promote Raf-1 activation by regulating 14-3-3 interactions. *Oncogene* **20**, 3949-3958

Jin, Y.J., and Burakoff, S.J. (1993) The 25-kDa FK506-binding protein is localized in the nucleus and associates with casein kinase II and nucleolin. *Proc. Natl. Acad. Sci. U. S. A.* **90**, 7769-7773

Kaffman, A., Rank, N.M., O'Neill, E.M., Huang, L.S., O'Shea, E.K. (1998) The receptor Msn5 exports the phosphorylated transcription factor Pho4 out of the nucleus. *Nature* **396**, 482-486

Kamimoto, T., Zama, T., Aoki, R., Muro, Y., and Hagiwara, M. (2001) Identification of a novel kinesin-related protein, KRMP1, as a target for mitotic peptidyl-prolyl isomerase Pin1. *J. Biol. Chem.* **276**, 37520-37528

Kamphausen, T. (2002) Charakterisierung von AtFKBP42 und weiteren Peptidyl-Prolyl-cis/trans-Isomerasen aus Arabidopsis thaliana. PhD Thesis

Kinzler, K.W., and Vogelstein, B. (1996) Lessons from hereditary colorectal cancer. *Cell* **87**, 159-170

Kipping, M., Zarnt, T., Kiessig, S., Reimer, U., Fischer, U., and Bayer, P. (2001) Increased backbone flexibility in threonine^{45}-phosohorylated hirudin upon pH change. *Biochemistry* **40**, 7957-7963.

Komuro, A., Saeki, M., and Kato, S. (1999) Npw38, a novel nuclear protein possessing a WW domain capable of activating basal transcription. *Nucleic Acids Res*. **2Z**, 1957-1965

Kontinen, V.P., Saris, P., and Sarvas, M. (1991) A gene (prsA) of *Bacillus subtilis* involved in a novel, late stage of protein export. *Mol. Microbiol*. **5**, 1273-1283

Kontinen, V.P., and Sarvas, M. (1993) The PrsA lipoprotein is essential for protein secretion in Bacillus subtilis and sets a limit for high-level secretion. *Mol. Microbiol.* **8**, 727-737

Kops, G.J. (1999) Direct control of the forkhead transcription factor AFX by protein kinase B. *Nature* **398**, 630-634

Kops, O., Eckerskorn, C., Hottenrott, S., Fischer, G., Mi, H., and Tropschung, M. (1998) Ssp1, a Site specific Parvulin homologue from *Neurospora crassa* active in protein folding. *J. Biol. Chem.* **273**, 31971-31976

Kops, O., Zhou, X.Z., and Lu, K.P. (2002) Pin1 modulates the dephosphorylation of the RNA polymerase II C-terminal domain by yeast Fcp1. *FEBS Lett* **513**, 305-311

Kostich, M., English, J., Madison, V., Gheyas, F., Wang, L., Qiu, P., Greene, J., and Laz, T.M. (2002) Human members of the eukaryotic protein kinase family. Genome Biol. 3, RESEARCH0043.1-RESEARCH0043.12

Ku, N.O., Liao, J., and Omary, M.B. (1998) Phosphorylation of human keratin 18 serine 33 regulates binding to 14-3-3 proteins. *EMBO J.* **17**, 1892-1906

Kudo, N., Matsumori, N., Taoka, H., Fujiwara, D., Schreiner, E.P., Wolff, B., Yoshida, M., and Horinouchi, S. (1999) Leptomycin B inactivates CRM1/exportin 1 by covalent modification at a cysteine residue in the central conserved region. *Proc. Natl. Acad. Sci. U. S. A*. **96**, 9112-9117

Kumagai, A., and Dunphy, W.G. (1999) Binding of 14-3-3 proteins and nuclear export control the intracellular localization of the mitotic inducer Cdc25. *Genes Dev.* **13**, 1067-1072

Kuo, M.H., Brownell, J.E., Sobel, R.E., Ranalli, T.A., Cook, R.G., Edmondson, D.G et al. (1996) Transcription-linked acetylation by Gcn5p of histone H3 and H4 specific lysines. *Nature* **383**, 269-272

Landrieu, L., Vezlder, D.L., Fruchart, J., Odaert, B., Casteels, P., Portetelle, D., Van Montague, M., Inze, D., and Lippens, G. (2000) The Arabidopsis thaliana Pin1 at gene encodes a single-domain phosphorylation dependent peptidyl prolyl cis-trans isomerase. *J. Biol. Chem.* **275**, 10577-10581

Laronga, C., Yang, H.Y., Neal, C., and Lee, M.H. (2000) Association of the cyclin-dependent kinases and 14-3-3 sigma negatively regulates cell cycle progression. *J. Biol. Chem*. **275**, 23106-23112

Lavoie, S.B., Albert, A.L., Handa, H., Vincent, M., and Bensaude, O. (2001) The peptidyl-prolyl isomerase Pin1 interacts with hSpt5 phosphorylated by Cdk9. *J. Mol. Biol.* **312**, 675-685

Lawlor, M.A., and Alessi, D.R. (2001) PKB/Akt: a key mediator of cell proliferation, survival and insulin response. *J. Cell. Sci.* **114**, 2903-2910

Lazar, S.W., and Kotler, R. (1996) Sur A assists the folding of *Escherichia coli* outer membrane proteins. *J. Bacteriol.* **178**, 1770-1773

Lei, S., Pulakat, L., and Gavini, N. (1999) Regulated expression of the nifM of Azotobacter vinelandii in response to molybdenum and vanadium supplements in Burk's nitrogen-free growth medium. *Biochem. Biophys. Res. Commun.* **264**, 186-190

Leskelä, S., Wahlström, E., Kontinen, V.P., and Sarvas M. (1999) Lipid modification of prelipoproteins is dispensable for growth but essential for efficient protein secretion in *Bacillus subtilis*: characterization of the lgt gene. *Mol. Microbiol*. **31**, 1075-1085

Liou, Y., Ryo, A., Huang, H., Lu, P., Bronson, R., Fujimori, F., Uchida, T., Hunter, T., and Lu, K.P. (2002) Loss of Pin1 function in the mouse causes phenotypes resembling cyclin D1-null phenotypes. *Proc. Natl. Acad. Sci. U.S.A.* **99**, 1335-1340

Liu, D., Bienkowska, J., Petsoa, C., Collier, R.J., Fu, H., and Liddington, R. (1995). Crystal structure of the zeta isoform of the 14-3-3 protein. *Nature* **376**, 191-194

Liu, W., Youn, H., Zhou, X.Z., Lu, K.P., and Liu, J.O. (2001) Binding of and regulation of the transcription factor NFAT by the peptidyl prolyl cis-trans isomerase Pin1. *FEBS Lett.* **496**, 105-108

Lopez-Girona, A., Furnari, B., Mondesert, O., and Russel, P. (1999) Nuclear localization of Cdc25 is regulated by DNA damage and a 14-3-3 protein. *Nature* **397**, 172-175

Love, J.J., Xiang, L., Case, D.A., Giese, K., Grosschedl, R., and Wright, P.E. (1995) Structural basis for DNA bending by the architectural transcription factor Lef-1. *Nature* **376**,791-795

Lu, K.P., Hanes, S.D., and Hunter, T. (1996) A human peptidyl-prolyl isomerase essential for regulation of mitosis. *Nature* **380**, 544-547

Lu, P.J., Wulf, G., Zhou, X.Z., Davies, P., and Lu, K.P. (1999) The prolyl isomerase Pin1 restores the function of Alzheimer-associated phosphorylated tau protein. *Nature* **399**, 784-788

Lu, P.J., Zhou, X.Z., Liou, Y.C., Noel, J.P., and Lu, K.P. (2002) Critical role of WW domain phosphorylation in regulating phosphoserine binding activity and Pin1 function. *J. Biol. Chem.* **277**, 2381-2384

Lu, P.J., Zhou, X.Z., Shen, M., and Lu, K.P. (1999) A function of WW domains as phosphoserine- or phosphothreonine-binding modules. *Science* **283**, 1325-1328

Lund, T., and Berg, K. (1991) Metaphase-specific phosphorylations weaken the association between chromosomal proteins HMG 14 and 17, and DNA. *FEBS Lett.* **289**, 113-116

MacCallum, D.E. and Hall, P.A. (2000) The biochemical characterization of the DNA binding activity of pKi67. *J. Pathol.* **191**, 286-298

MacDonald, D., Herbert, K., Zhang, X.L., Polgruto, T., and Lu, P. (2001) Solution structure of an A-tract DNA bend. *J. Mol. Biol.* **306**,1081-1098

Maleszka, R., Hanes, S.D., Hackett, R.L., de Couet, H.G., and Miklos, G.L. (1996) The Drosophila melanogaster dodo (dod) gene, conserved in humans, is functionally interchangeable with ESS1 cell division gene of *Saccharomyces cerevisiae. Proc. Natl. Acad. Sci. U.S.A.* **93**, 447-451

Marini, J.C., Levene, S.D., Crothers, D.M., and Englund, P.T. (1982) Bent helical structure in kinetoplast DNA. *Proc. Natl. Acad. Sci. U.S.A.* **76**, 7664-7668

Meggio, F., Marin, O., and Pinna, L.A. (1994) Substrate specificity of protein kinase CK2. *Cell. Mol. Biol. Res.* **40**, 401-409

Messenger, M.M., Saulnier, R.B., Gilchrist, A.D., Diamond, P., Gorbsky, G.J., and Litchfield, D.W. (2002) Interactions between protein kinase CK2 and Pin1: evidence for phosphorylation-dependent interactions. *J. Biol. Chem.* **25**, 23054-23064

Metzner, M., Stoller, G., Rucknagel, K.P., Lu, K.P., Fischer, G., Luckner, M., and Kullertz, G. (2001) Functional replacement of the essential ESS1 in yeast by the plant parvulin DlPar13. *J. Biol. Chem.* **17**,13524-13529

Michaud, N.R., Fabian, J.R., Mathes, K.D., and Morrison, D.K. (1995) 14-3-3 is not essential for Raf-1 function: identification of Raf-1 proteins that are biologically activated in a 14-3-3- and Ras-independent manner. *Mol. Cell. Biol*. **15**, 3390-3397

Misumi, S., Fuchigami, T., Takamune, N., Takahashi, I., Takama, M., and Shoji, S. (2002) Three isoforms of cyclophilin A associated with human immunodeficiency virus type 1 were found by proteomics by using two-dimensional gel electrophoresis and matrix-assisted laser desorption ionization-time of flight mass spectrometry. *J. Virol*. **76**, 10000-10008

Miyata, Y., Chambraud, B., Radanyi, C., Leclerc, J., Lebeau, M.C., Renoir, J.M., Shirai, R., Catelli, M.G., Yahara, I., and Baulieu, E.E. (1997) Phosphorylation of the immunosuppressant FK506-binding protein FKBP52 by casein kinase II: regulation of HSP90-binding activity of FKBP52. *Proc. Nat. Acad. Sci. U. S. A.* **94**, 14500-14505

Moore, B., and Perez, V.J. (1967) in: Physiological and Biochemical Aspects of Nervous Integration (Carlson, F.D., Ed.), pp. 343-359, Prentice-Halle, Englewood Cliffs, NJ.

Morris, D.P., Phatnani, H.P., and Greenleaf, A. L. (1999) Phospho-carboxyl-terminal domain binding and the role of a prolyl isomerase in pre-mRNA 3'-End formation. *J. Biol. Chem.* **274**, 31583-31587

Muslin, A.J., and Xing, H. (2000) 14-3-3 proteins: regulation of subcellular localization by molecular interference. *Cell. Signal.* **12**, 703-709

Muslin, A.J., Tanner, J.W., Allen, P.M., and Shaw, A.S. (1996) Interaction of 14-3-3 with signaling proteins is mediated by the recognition of phosphoserine. *Cell* **84**, 889-897

Nelson, J.S., Giver, L., Ellington, A.D., and Letsinger, R. (1996) Incorporation of non-nucleotide bridge into harpin oligonucleotides capable of high-affinity binding to the Rev protein of HIV. *Biochemistry* **35**, 5339-5344

Nigg, E.A. (1995) Cyclin-dependent protein kinases: key regulators of the eukaryote cell cycle. *BioEssays* **17**, 471-480

Nishi, K., Yoshida, M., Fujiwara, D., Nishikawa, M., Horinouchi, S., and Beppu, T. (1994) Leptomycin B targets a regulatory cascade of crm1, a fission yeast nuclear protein, involved in control of higher order chromosome structure and gene expression. *J. Biol. Chem*. **269**, 6320-6324

O'Farrell, F., Loog, M., Janson, I.M., Ek, P. (1999) Kinetic study of the inhibition of CK2 by heparin fragments of different length. *Biochem. Bioph. Acta* **1433**, 68-75

Obata, T., Yaffe, M.B., Leparc, G.G., Piro, E.T., Maegawa, H., Kashiwagi, A., Kikkawa, R., and Cantley, L.C. (2000) Peptide and protein library screening defines optimal substrate motifs for Akt/PKB. *J. Biol. Chem.* **275**, 36108-36115

Obsil, T., Ghirlando, R., Klein, D.C., Ganguly, S., and Dyda F. (2001) Crystal structure of the 14-3-3zeta:serotonin N-acetyltransferase complex. a role for scaffolding in enzyme regulation. *Cell* **105**, 257-267

Osmani, S.A., May, G.S., and Morris, N.R. (1987) Regulation of the mRNA levels of nimA, a gene required for the G2-M transition in Aspergillus nidulans. *J. Cell. Biol.* **104,** 1495-1504

Osmani, S.A., Pu, R.T., and Morris, N.R. (1988) Mitotic induction and maintenance by Overexpression of a G2-specific gene that encodes a potential protein kinase. *Cell* **53**, 237-244

Pathan, N., Aime-Sempe, C., Kitada, S., Basu, A., Haldar, S., and Reed, JC. (2001) Microtubule-targeting drugs induce bcl-2 phosphorylation and association with Pin1. *Neoplasia* **3**, 550-559

Peng, C.Y., Graves, P.R., Thoma, R.S., Wu, Z., Shaw, A.S., Piwnica-Worms, H. (19997) Mitotic and G2 checkpoint control: regulation of 14-3-3 protein binding by phosphorylation on Cdc25c on serine-216. *Science* **277**, 1501-1505

Petrova, N., Gigova, L., and Venkov, P. (2000) NifH and NifM proteins interact as demonstrated by the yeast two-hybrid system. *Biochem. Biophys. Res. Commun.* **270**, 863-867

Pinna, L.A. (1994) A historical view of protein kinase CK2. *Cell. Mol. Biol. Res*. **40**, 383-390

Postnikov, Y.V., Lehn, D.A., Robinson, R.C., Friedman, F.K., Shiloach, J., and Bustin, M. (1994) The cooperative binding of chromosomal protein HMG-14 to nucleosome cores is reduced by single point mutations in the nucleosomal binding domain. *Nucl. Acids Res.* **22**, 4520-4526

Prymakowska-Bosak, M., Hock, R., Catez, F., Lim, J.H., Birger, Y., Shirakawa, H., Lee, K., and Bustin, M. (2002) Mitotic phosphorylation of chromosomal protein HMGN1 inhibits nuclear import and promotes interaction with 14-3-3 proteins. *Mol. Cell. Biol.* **22**, 6809-6819

Rahfeld, J. U., Schierhorn, A., Mann, K., and Fischer, G. (1994a) A novel peptidyl-prolyl cis-trans isomerase from *Escherichia coli. FEBS Lett.* **343**, 65-69

Rahfeld, J.U., Rucknagel, K.P., Schelbert, B., Ludwig, B., Hacker, J., Mann, K., and Fischer, G. (1994b) Conformation of the existence of a third family among peptidyl-prolyl cis-trans isomerases: amino acid sequence and recombinant production of parvulin. *FEBS Lett.* **352**, 180-184

Ranganathan, R., Lu, K.P., Hunter, T., and Noel, J.P. (1997) Structural and functional analysis of the mitotic peptidyl-prolyl isomerase Pin1 suggests that substrate recognition is phosphorylation dependent. *Cell* **89**, 875-886

Reizer, J., Sutrina, S.L., Saier, M.H., Stewart, G.C., Peterkofsky, A., and Reddy, P. (1989) Mechanistic and physiological consequences of HPr(ser) phosphorylation on the activities of the phosphoenolpyruvate:sugar phosphotransferase system in gram-positive bacteria: studies with site-specific mutants of HPr. *EMBO J.* **8**, 2111-2120

Rihs, H.P., Jans, D.A., Fan, H., and Peters, R. (1991) The rate of nuclear cytoplasmic protein transport is determined by the casein kinase II site flanking the nuclear localization sequence of the SV40 T-antigen. *EMBO J.* **10**, 633-639

Rippmann, J.F., Hobbie, S., Daiber, C., Guilliard, B., Bauer, M., Birk, J., Nar, H., Garin-Chesa, P., Retting, W.J., and Schnapp, A. (2000) Phosphorylation-dependent proline isomerization catalyzed by Pin1 is essential for tumor cell survival and entry into mitosis. *Cell. Growth Differ.* **11**, 409-416

Rittinger, K., Budman, J., Xu, J., Volinia, S., Cantley, L.C., Smerdon, S.J., Gamblin, S.J., and Yaffe, M.B. (1999) Structural analysis of 14-3-3 phosphopeptide complexes identifies a dual role for the nuclear export signal of 14-3-3 in ligand binding. *Mol. Cell* **4**, 1-20

Rouviere, P.E., and Gross, C.A. (1996) SurA, a periplasmic protein with peptidyl-prolyl isomerase activity, participates in the assembly of outer membrane porins. *Genes Dev.* **10**, 3170-3182

Roy, S., McPherson, R.A., Apolloni, A., Yan, J., Lane, A., Clyde-Smith, J., and Hancock, J.F. (1998) 14-3-3 facilitates Ras-dependent Raf-1 activation in vitro and in vivo. *Mol. Cell. Biol.* **18**, 3947-3955

Rubinfeld, B., Albert, I., Porfiri, E., Fiol, C., Munemitsu, S., and Polakis, P. (1996) Binding of GSK3beta to the APC-beta-catenin complex and regulation of complex assembly. *Science* **272**, 1023-1026

Rudd, K.E., Sofia, H.J., Koonin, E.V., Plunket, G., Lazar, S., and Rouviere, P.E. (1995) A new family of peptidyl isomerases: evidence for general protein folding catalysts. *EMBO J.* **14**, 5494-5505

Rulten, S., Thorpe, J., and Kay, J. (1999) Identification of eukaryotic parvulin homologues: a new subfamily of peptidyl prolyl cis-trans isomerases. *Biochem. Biophys. Res. Commun*. **259**, 557-562

Ryo, A., Nakamura, M., Wulf, G., Liou, Y.Ch., Lu, K.P. (2001) Pin1 regulates turnover and subcellular localization of β-catenin by inhibiting its interaction with APC. *Nat. Cell Biol.* **3**, 793-801

Sambrook, J., Fisch, E.F., and Maniatis, T. (1989) Molecular cloning: A Laboratory manual, Second edition, Cold Spring Harbor Laboratory Press, Cold Spring Harbor, NY, USA

Sarno, S., Vaglio, P., Meggio, F., Issinger, O.G., and Pinna, L.A. (1996) Protein kinase CK2 mutants defective in substrate recognition. Purification and kinetic analysis. *J. Biol. Chem.* **271**, 10595-10601

Scheid, M.P., and Woodgett, J.R. (2001) PKB/Akt: functional insights from genetic models. *Nature* **2**, 760-768

Schiene-Fischer, and C., Yu, C. (2001) Receptor accessory folding helper enzymes: the functional role of peptidyl prolyl cis/trans isomerases. *FEBS Lett* **495**, 1-6

Schmidt-Zachmann, M.S., and Nigg, E.A. (1993) Protein localization to the nucleolus: a search for targeting domains in nucleolin. *J. Cell. Sci*. **105**, 799-806

Schreiber, S.L. (1991) Chemistry and biology of the immunophilins and their immunosuppressive ligands. *Science* **251**, 283-287

Schreiber, E., Matthias, P., Müller M.M., and Schaffner W. (1989) Rapid detection of octamer binding proteins with "mini-extracts", prepared from a small number of cells. *Nucl. Acids Res.* **17**, p. 6419

Schutkowski, M., Bernhardt, A., Zhou, X.Z., Shen, M., Reimer, U., Rahfeld, J.U., Lu, K.P., and Fischer, G. (1998) Role of phosphorylation in determining the backbone dynamics of the serine/threonine-proline motif and Pin1 substrate recognition. *Biochemistry* **37**, 5566-5575

Seimiya, H., Sawada, H., Muramatsu, Y., Shimizu, M., Ohko, K., Yamane, K., and Tsuruo, T. (2000) Involvement of 14-3-3 proteins in nuclear localization of telomerase. *EMBO J.* **19**, 2652-2661

Sekerina, E., Rahfeld, J.U., Muller, J., Fanghanel, J., Rascher, C., Fischer, G., and Bayer, P. (2000) NMR solution structure of *h*Par14 reveals similarity to the peptidyl prolyl cis/trans isomerase domain of the mitotic regulator *h*Pin1 but indicates a different functionality of the protein. *J. Mol. Biol.* **301**, 1003-1017

Shaw, P.E. (2002) Peptidyl-prolyl isomerases: a new twist to transcription. *EMBO Rep* **3**, 521-526

Shen, M., Stukenberg, P.T., Kirschner, M.W., and Lu, K.P. (1998) The essential mitotic peptidyl prolyl isomerase Pin1 binds and regulates mitosis-specific phosphoproteins. *Genes Dev.* **12**, 706-720

Shyu, A.B., and Wilkinson, M.F. (2000) The double lives of shuttling mRNA binding proteins. *Cell* **102**, 135-138

Spaulding S.W., Fucile N.W., Bofinger D.P., Shelfin L.G. (1991) Cyclic adenosine 3',5' monophosphatase-dependent phosphorylation of HMG 14 inhibits its interactions with nucleosomes. *Mol. Endocrinol.* **5**, 42-50

Steplewski, A., Ebel, W., Planey, S.L., Alnemri, E.S., Robertson, N.M., Litwack, G. (2000) Phosphorylation of the insect immunophilin FKBP46 by the Spodoptera frugiperda homolog of casein kinase II. *Gene* **246**, 169-178

Stukenberg, P.T., and Kirschner, M.W. (2001) Pin1 acts catalytically to promote a conformational change in Cdc25. *Mol. Cell.* **7**, 1071-1083

Sudol, M. (1996) Structure and function of the WW domain. *Prog. Biophys. Mol. Biol.* **65**, 113-132

Surmacz, T.A., Bayer, E., Rahfeld, J.U., Fischer, G., and Bayer, P. (2002) The N-terminal Basic Domain of Human Parvulin *h*Par14 is responsible for the Entry to the Nucleus and High-affinity DNA-Binding. *J. Mol. Biol.* **321**, 235-247

Taylor, A., Allende, C.C., Weinmann, R., and Allende, J.E. (1987) The phosphorylation of nucleoplasmin by casein kinase-2 is resistant to heparin inhibition. *FEBS Let.* **226**,109-114

Terada, T., Shirouzu, M., Fukumori, Y., Fujimori, J., Ito, Y., Kigawa, T., Yokoyama, S., and Uchida, T. (2001) Solution structure of the Human Parvulin-like Peptidyl Prolyl cis-trans isomerase, hPar14. *J. Mol. Biol.* **305**, 917-926

Thorpe, J.R., Rulten, S.L., and Kay, J.E. (1999) Binding of a putative and a known chaperone protein revealed by immunogold labeling transmission electron microscopy: a suggested use of chaperons as probes for the distribution of their target proteins. *J. Histochem. Cytochem.* **47**, 1633-1640

Tormo, A., Almiron, M., and Kolter, R. (1990) SurA, an *Escherichia coli* gene essential for survival in

Travers, A. (2000) Recognition of distorted DNA structures by HMG domains. *Curr. Opin. Struct. Biol.* **10**, 102-109

Trieschmann, L., Postnikov, Y.V., Rickers, A., and Bustin, M. (1995) Modular structure of chromosomal proteins HMG-14 and HMG-17 –definition of a transcriptional enhancement domain distinct from the nucleosomal binding domain. *Mol. Cell. Biol.* **15**, 6663-6669

Tzivion G., and Avruch J. (2002) 14-3-3 proteins: active cofactors in cellular regulation by serine/threonine phosphorylation. *J. Biol. Chem.* 277, 3061-3064

Uchida, T., Fujimori, F., Tradler, T., Fischer, G., and Rahfeld, J.U. (1999) Identification and characterization of a 14 kDa human protein as a novel parvulin-like peptidyl prolyl cis/trans isomerase. *FEBS Lett.* **446**, 278-282

Verdecia, M.A., Bowman, M.E, Lu, K.P., Hunter, T., and Noel, J.P. (2000) Structural basis for phosphoserine-proline recognition by group IV WW domains. *Nat. Struct. Biol* **7**, 639-643

Vos, P., van Assenldonk, M., van Jeveren, F., Siezen, R., Simons, G., de Vos, W.M. (1989) A maturation protein is essential for production of active forms of Lactococcus lactis SK11 serine proteinase located in or secreted from the cell envelope. *J. Bacteriol.* **171**, 2795-2802

Wagner, P. (1997) Phosphorylation mutants of p53 show differential complex formation with putative dehydrogenase Tms1 of fission yeast. *Eur. J. Biochem*. **248**, 441-444

Widom, J. (2001) Role of DNA sequence in nucleosome stability and dynamics. *Quart. Rev. Biophys.* **34**, 269-324

Winkler, K.E., Swenson, K. I., Kornbluth, S., and Means, A. R. (2000) Requirement of the prolyl isomerase Pin1 for the replication checkpoint. *Science* **287**, 1644-1647

Wu, X., Wilcox, C.B., Devasahayam, G., Hackett, R.L., Arevalon-Rodriguez, M., Cardenas, M.E., Heitman, J., and Hanes, S.D. (2000) The Ess1 prolyl isomerase is linked to chromatin remodeling complexes and the general transcription machinery. *EMBO J.* **19**, 3727-3738

Wulf, G.M., Ryo, A., Wulf, G.G., Lee, S.W., Niu, T., Petkova, V., and Lu, K.P. (2001) Pin1 is overexpressed in breast cancer and cooperates with Ras signalling in increasing the transcriptional activity of c-Jun towards cyclin D1. *EMBO J*. **13**, 3459-3472

Wulf, G.M., Liou, Y.C., Ryo, A., Lee, S.W., and Lu, K.P. (2002) Role of Pin1 in the Regulation of p53 Stability and p21 Transactivation, and Cell Cycle Checkpoints in Response to DNA Damage. *J. Biol. Chem.* **277**, 47976-47979

Xiao, B., Smerdon, S.J., Jones, D.H., Dodson, G.G., Soneji, Y., Atiken, A., and Gamblin, S.J. (1995) Structure of a 14-3-3 protein and implications for coordination of multiple signalling pathways. *Nature* **376**, 188-191

Yaffe, M.B. (2002) How do 14-3-3 proteins work?- Gatekeeper phosphorylation and the molecular anvil hypothesis. *FEBS Lett.* **513**, 53-57

Yaffe, M.B., Rittinger, K., Volinia, S., Caron, P.R., Atiken, A., Leffers, H., Gamblin, S.J., Smerdon, S.J., Cantley, L.C. (1997) The structural basis for 14-3-3: phosphopeptide binding specificity. *Cell* **91**, 961-971

Yaffe, M.B., Schutkowski, M., Shen, M., Zhou, X.Z., Stukenberg, P.T., Rahfeld, J.U., Xu, J., Kuang, J., Kirschner, M.W., Fischer, G., Cantley, L.C., and Lu, K.P. (1997) Sequence-specific and phosphorylation-dependent proline isomerization: a potential mitotic regulatory mechanism. *Science* **278**, 1957-1960

Yang, J., and Kornbluth, S. (1999) All aboard the cyclin train: subcellular trafficking of cyclins and their CDK partners. *Trends Cell Biol.* **9**, 207-210

Yang, J., Winkler, K., Yoshida, M., Kornbluth, S. (1999) Maintenance of G2 arrest in the Xenopus oocyte: a role for 14-3-3 mediated inhibition of Cdc25 nuclear import. *EMBO J.* **18**, 2174-2183

Zacchi, P., Gostissa, M., Uchida, T., Salvagno, C., Avolio, F., Volinia, S., Ronai, Z., Blandino, G., Schneider, C., and Del Sal, G. (2002) The prolyl isomerase Pin1 reveals a mechanism to control p53 functions after genotoxic insults. *Nature* **419**, 853-857

Zandomeni, R., and Weinmann, R. (1984) Inhibitory effect of 5,6-dichloro-1-beta-D-ribofuranosylbenzimidazole on a protein kinase. *J. Biol. Chem.* **259**, 14804-14811

Zeng, Y., Forbes, K.C., Wu, Z., Moreno, S., Piwnica-Worms, H., and Enoch, T. (1998) Replication check point requires phosphorylation on the phosphatase Cdc25 by Cds1 or Chk1. *Nature* **395**, 507-510

Zha, J., Harada, H., Yang, E., Jockel, J., and Korsmeyer, S.J. (1996) Serine phosphorylation of death agonist BAD in response to survival factor results in binding to 14-3-3 not BCL-X(L). *Cell* **87**, 619-628

Zhang, F., White, R.L., and Neufeld, K.L. (2001) Cell density and phosphorylation control the subcellular localization of adenomatous polyposis coli protein. *Mol. Cell. Biol*. **21**, 8143-8156

Zhang, L., Wang, H., Liu, D., Liddington, R., and Fu, H. (1997) Raf-1 kinase and exoenzyme S interact with 14-3-3ζ through a common site involving lysine 49. *J. Biol. Chem.* **272**, 13717-13724

Zhang, S.H., Kobayashi, R., Graves, P.R., Piwnica-Worms, H., and Tonks, N.K. (1997) Serine phosphorylation-dependent association of the band 4.1-related protein-tyrosine phosphatase PTPH1 with 14-3-3beta protein. *J. Biol. Chem*. **272**, 27281-27287

Zheng, H., You, H., Zhou, X.Z., Murray, S.A., Uchida, T., Wulf, G., Gu, L., Tang, X., Lu, K.P., and Xiao ZX. (2002) The prolyl isomerase Pin1 is a regulator of p53 in genotoxic response. *Nature* **419**, 849-853

Zhou, Z.Z., Kops, O., Werner, A., Lu, P.J., Shen, M., Stoller, G., Kullertz, G., and Lu, K.P. (2000) Pin1-dependent prolyl isomerization regulates dephosphorylation of Cdc25C and Tau proteins. *Mol. Cell* **6**, 873-883

Eidesstattliche Erklärung

Hiermit erkläre ich, dass die vorliegende Arbeit von mir selbständig und nur unter Verwendung der angegeben Hilfsmittel angefertigt wurde. Ich versichere weiterhin, dass alle wörtlich oder inhaltlich entnommenen Stellen als solche gekennzeichnet sind.
Diese Arbeit wurde bisher an keiner anderen Universität vorgelegt.

Halle/Saale, im 3.2. 2003

Tatiana Reimer

Acknowledgments

I express my deepest gratitude to Prof. Gunter Fischer for providing me with the opportunity of developing this project and for his supervision, which more than often brought fruitful suggestions to this work.

I would like to thank Dr. Peter Bayer for our fruitful collaboration, interesting suggestions and stimulating discussion.

I am equally grateful for the invaluable contribution given by the following colleagues:
Dr. Matthias Weiwad who has done the *in vitro* kinase assay; Dr. Angelika Schierhorn for measuring mass spectra, and for determining the phosphorylation site; Dr. Peter Rücknagel for protein sequencing; Dr. Birte Hernandez-Alvarez and Dr. Jens-Ulrich Rahfeld, whose advices often have brought solutions to troublesome experiments, critical discussion and correction of my thesis; Dr. Gunnar Schotta for helping and supervising the confocal microscopy; Dr. Yxing Zhang, Chao Yu, Carolyn Vargas, and Frank Edlich for the nice and stimulating atmosphere in the group and for scientific help and friendship; Ms. Beate Rappsilber for the excellent technical assistance. And, above all, to all those colleagues, including the once above mentioned and many others, whose friendship and support have created a delightful working atmosphere- thank you.

I am especially indebted to Dr. Holger Bang for initiating the project and supervision in first few moths, Dr. Christine Rascher-Bang for welcome atmosphere at lab, Dr. M. Yaffe, Dr. A.J. Muslin, Dr. H. Fu and Dr. D. Litchfield for providing me with 14-3-3 and CK2 cDNAs.

I would like to thank Magda Rakwalska, Dr. Elena Bayer, Dr. Iza Szafraniak, Jurek Grabowski, and Prof. Marek Przybylski for their friendship, support and great time that we had together.

Finally, I thank to my parents and especially to my husband for never ending support. It would have been impossible to accomplish this work without their help.

Curriculum vitae

Personal Data

Family name	Reimer
Given name	Tatiana, Anna
Citizenship	Polish
Place of birth	2 June 1974 in Leszno, Poland
Maiden name	Surmacz

Education

1981-1989	Primary School No.1, Oborniki Wkp, Poland
1989-1993	Private SS Ursuline Secondary School, Poznan, Poland
1993-1998	Adam Mickiewicz University, Department of Biology, Poznan, Poland
1995-1998	Polish Academy of Science, Institute of Human Genetics, Poznan, Poland; undergraduate research work Master of Science Degree Scientific supervisor: Prof. J. Jaruzelska Research subject: Molecular investigation of male infertility
1998-1999	Case Western Reserve University, Cleveland, Ohio, USA Research Scholar Scientific supervisor: Prof. C. Merched (formerly Whitacre) Research subject: cancer biology
12.1999-2.2003	Max Planck Research Unit for Enzymology of Protein Folding, Halle/Saale, Germany Scientific supervisor: Prof. G. Fischer Research subject: The cellular function and localization of *h*Par14

Publications and Presentations

Published

Surmacz, T.A., Bayer, E., Rahfeld, J.U., Fischer, G., and Bayer, P. (2002) The N-terminal basic domain of human parvulin *h*Par14 is responsible for the entry to the nucleus and high-affinity DNA-binding. *J. Mol. Biol.* **321**, 235-247

Bayer P., and Surmacz TA. (2001) Living in cytosol. *TRENDS in Biochem. Sci.* **12**, 702

Jaruzelska. J., Korcz. A., Wojda. A., Jedrzejczak. P., Bierla. J., Surmacz. T., Pawelczyk. L., Page. D.C., and Kotecki. M. (2001) Mosaicism for 45,X cell line may accentuate the severity of spermatogenic defects in men with AZFc deletion. *J. Med. Genet.* **38**, 798-802

Surmacz, T.A., Weiwad, M., Schierhorn, A., Ruecknagel K.P., Rahfeld, J.U., Bayer, P., and Fischer G. Cellular localization of *cis/trans* isomerase human Parvulin 14 is regulated by CK2 phosphorylation. *in press*

Posters

Surmacz, T., Matuszak, R., Jedrzejczak, P., Jaruzelska, J. (1997) Analysis of the DAZ gene in patients with azoospermia. 29th Annual Meeting of the European Society of Human Genetics, Genova Italy;

Surmacz, T., Weiwad, M., Schierhorn, A., Rucknagel, P., Rahfeld, J.U., Fischer, G. (2002) "Phosphorylation of the *h*Par14 by casein kinase 2 and identification serine 19 as the *in vitro* phosphorylation site". Protein Phosphorylation and Mechanisms of Cellular Regulation, Keystone Meeting, Taos, New Mexico